Rotating Frame Relaxation Times for Off-Resonant MRI Pulses

M. M. Vermeulen

Technische Universiteit Delft

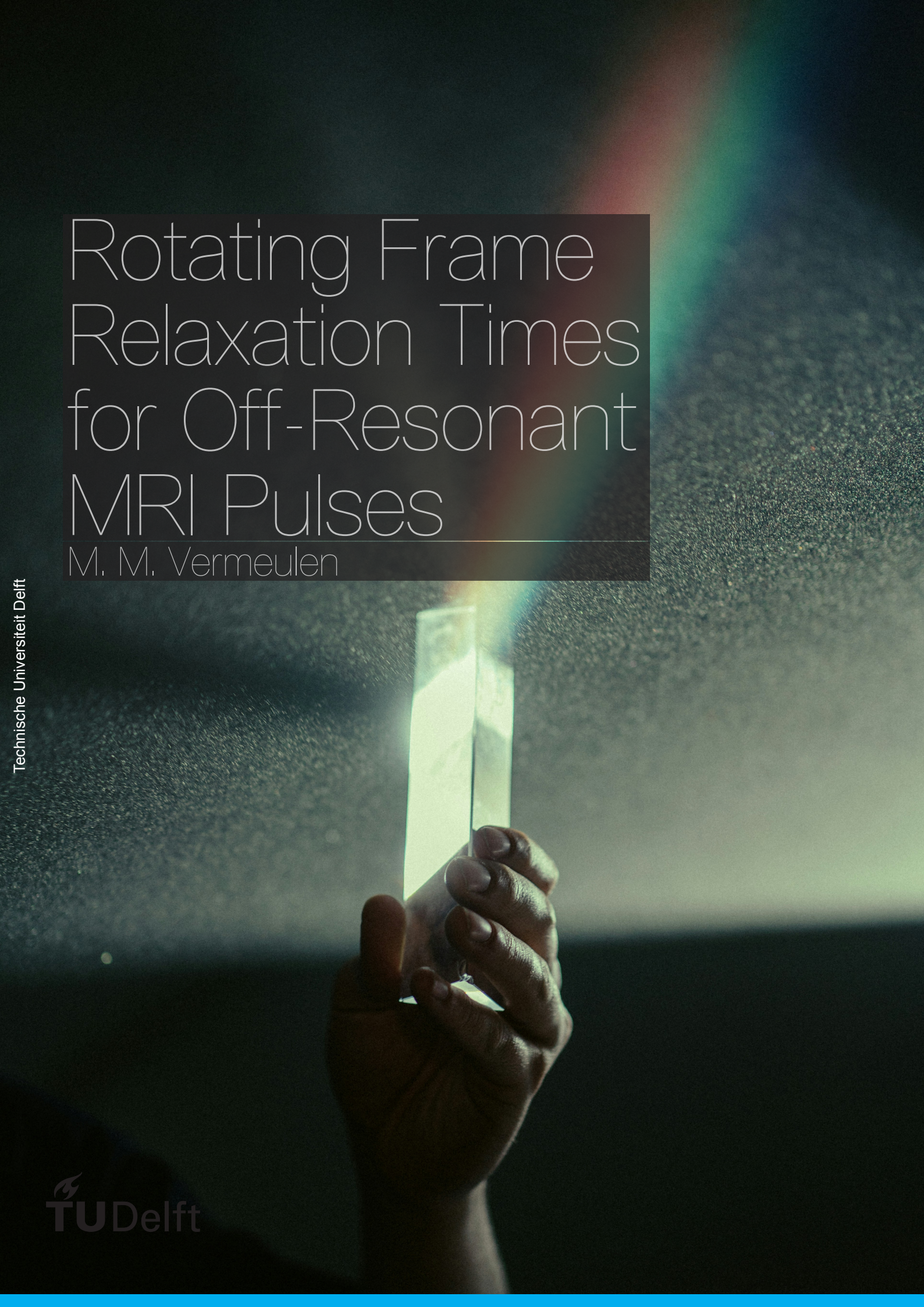

TU Delft

Rotating Frame Relaxation Times for Off-Resonant MRI Pulses

by

Mark Maarten Vermeulen

to obtain the degree of Master of Science

at the Delft University of Technology,

to be defended publicly on Friday March 15th, 2024 at 14:00.

Student number:	4867327	
Project duration:	11th July, 2023 – March 15th, 2024	
Supervision:	C. Coletti, MSc.	TU Delft
	S. Weingärtner, PhD.	TU Delft
Thesis committee:	S. Weingärtner, PhD.	TU Delft, supervisor
	F. Vos, PhD.	TU Delft
	M. Menzel, PhD.	TU Delft
	C. Coletti, MSc.	TU Delft, supervisor

Cover picture: A hand holding a prism (an example frequency-dependent behaviour of light) by Braxton Apana (retrieved from: https://unsplash.com/photos/person-holding-white-box-with-rainbow-light-VuNNRTFdrME)

An electronic version of this thesis is available at http://repository.tudelft.nl/.

TU Delft Mars Lab

Contents

Abstract

Rotating frame relaxation ($T_{1\rho}$) measurement is a promising technique for magnetic resonance imaging of, for example, articular cartilage and the heart. This technique is very sensitive to inhomogeneities in the main and excitation magnetic field, which causes the image to locally lose contrast. Adiabatic pulses are able to perform similar measurements ($T_{1\rho,\mathrm{adiab}}$) while being resistant to these inhomogeneities. For these pulses it is important to find the correct pulse parameters. Current optimization methods for these parameters rely on Bloch simulations, that ignore $T_{1\rho}$ relaxation during the pulse application. The Redfield method uses a semi-classical model that allows for the incorporation of these relaxation times. The goal of this project is to find an optimization method, based on Redfield theory, that can take $T_{1\rho}$ relaxation during the pulse application into account.

Redfield theory was first used to derive the relaxation times during continuous spin-lock pulses. These were in agreement to limits found in the literature. Next, the derivation was extended to also consider main field inhomogeneity, which results in off-resonant pulses. In the limit these agreed with our on-resonance derivation, and they also agreed with similar derivations found in the literature. Finally this derivation was extended to amplitude- and frequency-modulated pulses by means of finite-difference time simulations. For these simulations, it was assumed that the AM and FM modulation functions were constant during each time step: the *quasistatic assumption*.

Two parameters of the hyperbolic secant pulses were optimized: the peak sharpness β and the frequency modulation amplitude A. This optimization was based on an equal weighting of two scores. The first is the deviation in $T_{1\rho}$, predicted by the Redfield calculations, for off-resonance values of $0, 50, 100, \ldots, 200$ Hz. These represent the variations in the main magnetic field. The second is the final magnetization along the longitudinal axis, found using conventional Bloch simulations. As a comparison, state-of-the art optimization was performed using the final magnetization score only. It was observed that incorporating the $T_{1\rho}$ deviation into the optimization resulted in in a 83%, 83%, 88% improved resilience to off-resonance for $\tau_c = 0.01$, 0.1, 1 ns correlation times.

Experimental validation of the Redfield calculations encountered difficulties due to artefacts in the acquired MRI scans. These are assumed to be related to dephasing, and further research could avoid them by adding refocusing to their pulses. The qualitative behaviour acquired from this data matches with the calculations, but the actual values do not match theoretical predictions.

In conclusion, adding Redfield calculations to the pulse optimization method allows for the selection of parameters that are optimally resistant to magnetic field inhomogeneities. Further research is needed to obtain results that can improve MR imaging in practice.

Abbreviations and Symbols

MR(I) Magnetic Resonance (Imaging)

AM Amplitude Modulation

FM Frequency Modulation

RF Radio-Frequency / excitation pulse

$\boldsymbol{T_1}$ Relaxation time along the main magnetic field, no RF field present

$\boldsymbol{T_2}$ Relaxation time perpendicular to the main magnetic field, no RF field present

$\boldsymbol{T_{1\rho}}$ Relaxation time along the effective field, in the presence of an RF field

$\boldsymbol{T_{2\rho}}$ Relaxation time perpendicular to the effective field, in the presence of an RF field

$\boldsymbol{T_{1\rho,adiab}}$ Relaxation time along the effective field, in the presence of an adiabatic RF field

$\boldsymbol{B_0}$ Main magnetic field strength

$\boldsymbol{B_1}$ Radio-frequency field strength

RMS Root-Mean-Square

AHP Adiabatic Half-Passage, an adiabatic pulse that rotates the magnetization into the transverse plane

$\hat{I}_a$ Quantum mechanical spin operator in the a direction.

$\hat{\hat{R}}_{\theta\hat{I}_a}$ Operator for the rotation of spin Hamiltonians by θ degrees around the a axis.

1

Introduction

Magnetic Resonance Imaging (MRI) is an important imaging modality since it can create high-resolution cross-sectional images of the human body [1]. In MRI scanners, the nuclear spin magnetization is excited using radio-frequency pulses. Images are created based on the time evolution of this magnetization [2]. This evolution is caused by multiple effects, which can be characterized by time constants (T_1, T_2, $T_{1\rho}$, ...). These time constants change from tissue to tissue, and for healthy and diseased tissues. Measuring these relaxation properties with specific MRI sequences can provide important diagnostic information. Unfortunately, most MRI measurements are strongly patient-, scanner- and pulse sequence dependent [3]. This hinders monitoring patient progress between scans, and the creation of quantitative diagnastic criteria for diseases.

Rotating frame relaxation measurements are concerned with finding the $T_{1\rho}$ and $T_{2\rho}$ time constants. They are a promising technique that allow the use of MRI to assess slow molecular interactions in tissue. This assessment can find rich clinical applications, for example detection of arthritis in the articular cartilage of the knee [4] or assessment of scar tissue following myocardial infarction, without contrast agent injection [5]. Rotating frame relaxation measurements require continuous application of a electromagnetic excitation field. Local variations in both the main scanner field and this excitation field can cause contrast loss, which degrades image quality [6]. Furthermore, they hinder the quantitative comparison of measurements between patients [7]. Adiabatic pulses, whose orientation changes slowly in time, are resistant to the effect of these variations. Their effectiveness, however, is largely dependent on their pulse parameters [8]. Conventional methods to optimize these parameters are based on Bloch simulations, and thus neglect the influence of the excitation field on the relaxation. This makes these methods less suitable for rotating frame relaxation measurements.

A paper by Garwood et al. has demonstrated optimization of pulse parameters while neglecting relaxation [8]. A paper by Sorce et al. has examined the relaxation behaviour during adiabatic pulses, but has not investigated specifically the effect of pulse parameters [9]. There is thus still a need to investigate pulse optimization while considering rotating frame relaxation times.

In this project, we will use Redfield theory to create a pulse optimization framework that can take this relaxation behaviour into account. Redfield theory describes a semi-classical model, in which the spin system itself is treated quantum mechanically, while the interactions with its environment are described by classical thermodynamics. We will first use this model to derive the influence of local magnetic field variations on relaxation times. Then we will extend this calculation to amplitude- and frequency-modulated pulses. This is done by a finite-difference time simulation, where the assumption is made that these fields are constant in each timestep (a quasistatic assumption). We will apply these results to a pulse optimization algorithm. Finally, experimental measurements are made using pulses that emulate magnetic field variations. These measurements are used to our theoretical results of their influence on $T_{1\rho}$.

Chapter 2 describes the experimental methods used in this project, both for the mathematical derivations and the physical measurements. Chapter 3 contains the theoretical and experimental results.

Chapter 4 discusses the limitations and implications of these results, and further work. Chapter 5 provides the final conclusions. The part of this project that investigates the use of Redfield theory in pulse optimization has also been submitted to the 2024 EMBC conference.

1.1. Theoretical Background

This section contains a summary of the theoretical knowledge that is used in this report. First, MRI relaxation is examined as a classical phenomenon. Afterwards this description is extended using Redfield theory, that also takes into account the quantum mechanical nature of MRI relaxation.

1.1.1. Magnetic Resonance Imaging and Relaxation

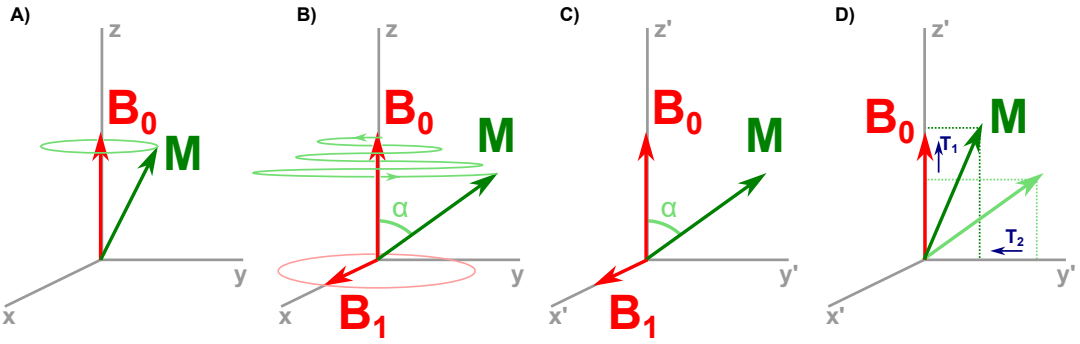

Figure 1.1: Figures showing the evolution of the magnetization (M, in green) during various stages of a classical MRI experiment. The excitation is assumed to be on-resonance. A) the main field B_0 magnetizes the tissue. The magnetization precesses around the main field. B) An radio-frequency pulse is applied to the tissue. This causes a rotating magnetic field B_1 to appear. B_1 causes the magnetization to tilt towards the transverse plane. C) The same as B), but now in the first rotating frame (x', y', z'), rotating at the same speed as the magnetization. D) After the RF pulse is switched off, the magnetization returns to its equilibrium position by relaxation. The longitudinal relaxation recovers with a time constant $1/T_1$, while the transverse relaxation disappears with a time constant $1/T_2$.

MRI scanners contain a big permanent magnet, generating a field with field strength in the order of 0.1 to 10 T. This main magnetic field B_0 is so strong that it magnetizes regions of the patient's tissue. Each of these regions acts like a magnetic dipole with strength μ, experiencing a torque $\tau = \boldsymbol{\mu} \times \boldsymbol{B}$ in an external magnetic field B. If the magnetization is not completely parallel to the magnetic field, this torque causes it to rotate around the magnetic field. This is called *precession*, and is shown in figure 1.1a. The speed of the precession depends on the strength of the magnetic field. The constant of proportionality is γ, the gyromagnetic ratio. Its value is around 42.58 MHz T^{-1} , so a standard MRI scanner with $B_0 = 3$T would have a precession frequency of $\omega_0 = \gamma B_0 = 804 \cdot 10^6$ rad/s ≈ 128 MHz. This is such a common calculation in MRI physics, that it is sometimes ignored altogether: it is common to talk about a pulse having a field strength of 50 Hz , which corresponds to 1.17 μT. The precession frequency in the main magnetic field is also called the *Larmor frequency*.

The magnetization component in the transverse plane acts like a rotating dipole, and thus emits electromagnetic waves. However, when only the main magnetic field is present, the magnetization is aligned to the z-axis and there is no detectable transverse component. To create a detectable signal, the magnetization must be tipped into the transverse plane. This is accomplished by using electromagnets to transmit a radio-frequency (RF) wave towards the patient.

In a classical MRI experiment a short, circularly polarized RF pulse is used. This pulse causes a rotating magnetic field B_1 to appear in the transverse (x, y) plane. Ideally, this rotation is also at the Larmor frequency, so that B_1 and the magnetization do not rotate with respect to each other. This is called on-resonance excitation. In that case, the torque due to this pulse simply rotates the magnetization around the B_1 field as shown in figure 1.1b. Since both B_1 and M are rotating at the Larmor frequency, it is convenient to consider a reference frame that also rotates at this frequency. This is called the *first rotating frame*, and is shown in figure 1.1c. In this frame, the only movement is the magnetization precessing around the B_1 field, tilting into the transverse plane. B_0 only causes the magnetization to precess, so it has no effect on the magnetization in this rotating frame. Therefore the effective field in this frame is $B_{\text{eff}} = B_1 \hat{x}'$

After this excitation, the RF pulse is switched off. The magnetization relaxes back to equilibrium through two processes: T_1 relaxation describes the return of the longitudinal magnetization to its original value. T_2 relaxation describes the decay of the transverse magnetization to zero. This relaxation can be seen in figure 1.1d. This relaxation is often modelled as an exponential function with time constant $1/T_1$ and $1/T_2$, respectively. The relaxation times T_1 and T_2 depend on the local environment of the protons. For example, fatty tissue tends to have a shorter T_1 than tissues with a higher water content. The magnetization is allowed to relax for a short period of time before imaging. This turns the relaxation time difference into a difference in magnetization, which is detectable through the electromagnetic waves emitted by the rotating magnetization.

More complex imaging methods will use additional RF-pulses to get a maximum signal from either T_1 or T_2 decay. Furthermore, they use additional so-called gradient fields to resolve the position of each magnetization. This project focuses on MR relaxation, but the details of these steps can be found in references [2] and [1].

The precession and relaxation phenomena are described in the *Bloch equations*:

$$\begin{aligned}\frac{dM_x}{dt} &= \gamma\left(\boldsymbol{M}\times\boldsymbol{B}\right)_x - \frac{M_x(t)}{T_2}\\ \frac{dM_y}{dt} &= \gamma\left(\boldsymbol{M}\times\boldsymbol{B}\right)_y - \frac{M_y(t)}{T_2}\\ \frac{dM_z}{dt} &= \gamma\left(\boldsymbol{M}\times\boldsymbol{B}\right)_z - \frac{M_z(t)-M_0}{T_1}\end{aligned} \tag{1.1}$$

Here $\boldsymbol{M}$ is the magnetization, $\boldsymbol{B}$ the magnetic field, γ the gyromagnetic ratio and M_0 the equilibrium magnetization (assumed to be along the z-axis).

These equations are a very popular way of modelling MRI, but they require T_1 and T_2 to be known in advance. This is not trivial, as multiple different processes contribute to both types of relaxation. In practice, the T_1 and T_2 values for tissues are measured experimentally, or found in the literature. This is also problematic, as measured relaxation times depend on the imaging method used [3].

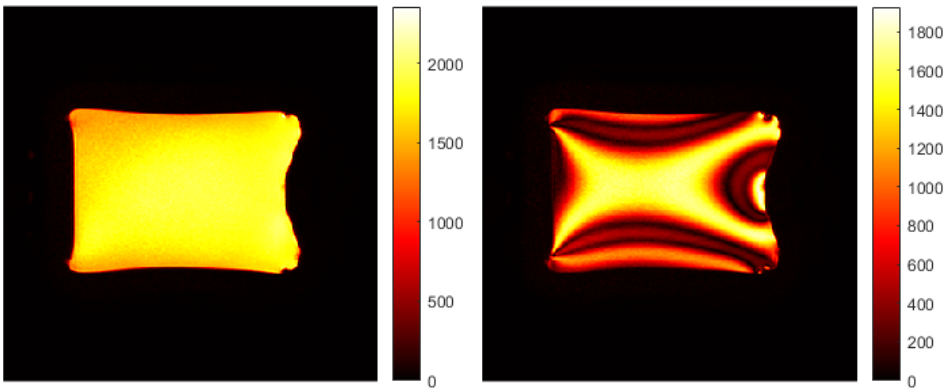

(a) On-resonance (b) Off-resonance

Figure 1.2: Two MRI images of the same bottle. The colour of each pixel represents the intensity of radio signals received by the scanner. B) shows strong off-resonance artefacts near the edges, due to the difference in susceptibility between the bottle and the surrounding air. A) does not show these artefacts, because a different preparation pulse was used.

If the RF pulse does not rotate at the Larmor frequency, we say that the RF pulse is *off-resonant*. In that case, both B_1 and the first rotating frame rotate at a frequency $\omega_{\mathrm{rf}} \neq \omega_0$. The magnetization, however, still precesses at a frequency ω_0. In this situation, a more careful approach is required to find the effective field. The calculation, shown in appendix A, shows that $B_{\mathrm{eff}} = B_1\hat{x'} - \Omega\hat{z'}$, where $\Omega = \omega_0 - \omega_{\mathrm{rf}}$ is called the off-resonance. The magnetization will precess around this effective field, and will thus not experience the same rotation as in the on-resonance case. The actual transverse component of the magnetization depends on the duration of the RF pulse, and the amount of off-resonance. In general, off-resonance is caused by inhomogeneities in the B_0 field, which are in turn caused by the different

magnetic susceptibilities in the tissue [10]. In practice, off-resonance artefacts tend to show up as ripples in regions were the MRI signal should be homogeneous. An example of this is shown in figure 1.2.

A rotating frame relaxation experiment is similar to a classical MRI experiment, except for that the RF pulse is not switched off during the relaxation. In a spin-lock experiment, the magnetization is first tipped into the transverse plane, and then the RF pulse is applied in phase to the magnetization. For an adiabatic[1] pulse experiment, the RF-pulse is transmitted so that it is aligned with the magnetization. In both cases, the magnetization precesses around the effective field. By varying the amplitude and frequency of the RF pulse, the effective field moves into the transverse plane. As long as this change is slow enough (i.e. the pulse is adiabatic) the magnetization will follow. A big advantage of adiabatic pulses is that the magnetization will follow the pulse, even if originally it is originally aligned differently due to off-resonance. In contrast, a normal block pulse will tip the magnetization by a fixed angle, no matter its original orientation.

In the next section, we show that there is not simply T_1 and T_2 relaxation during these rotating frame experiments. Instead, we must consider the relaxation parallel to the effective field, which is called $T_{1\rho}$, and perpendicular to this field, which is called $T_{2\rho}$. It is convenient to consider the *second rotating frame* (x'', y'', z''), where the effective field B_{eff} is aligned to the z''-axis, and which rotates with a frequency $\omega_{\text{eff}} = \sqrt{\omega_1^2 + \Omega^2}$ around this axis. In this frame, $T_{1\rho}$ and $T_{2\rho}$ relaxation are just the relaxation along the z''-axis and in the transverse plane, respectively.

During an adiabatic pulse, the apparent relaxation times additionally strongly depend on the parameters of the pulse that is being transmitted. Therefore, the relaxation times during these experiments are called $T_{1\rho,adiab}$ and $T_{2\rho,adiab}$ to distinguish them from $T_{1\rho}$ and $T_{2\rho}$.

1.1.2. Redfield Theory

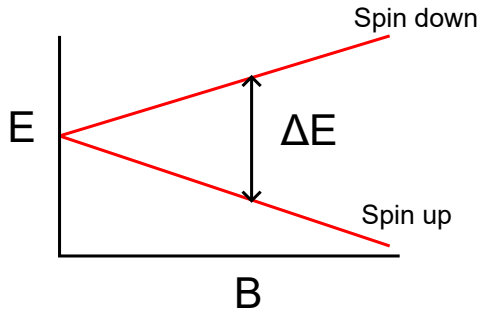

Figure 1.3: An illustration of the Zeeman effect. As the magnetic field B increases, the energy difference between the spin-up and spin-down eigenstates grows.

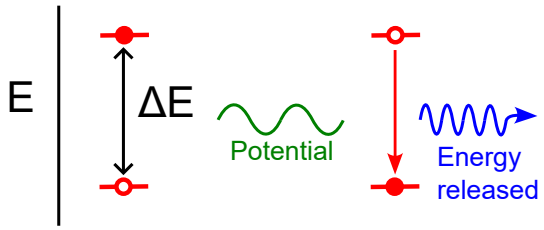

Figure 1.4: An illustration of stimulated emission. The proton (filled red dot) needs to release energy to move to the lower-energy state (hollow dot). This emission is only possible after an external potential interacts with the particle.

The relaxation times in the Bloch equations are phenomenological: they are observed, but do not correspond to a single physical process. Dipole-dipole relaxation, chemical shift anisotropy and J-coupling

[1] The pulse is adiabatic in the sense that it cause the effective field to slowly change orientation. There is still energy transfer from the pulse into the tissue.

are some of the relaxation mechanisms. In clinical MRI, where the signal is mostly due to proton spin, dipole-dipole interaction is often the biggest contributor, and we will focus on this phenomenon in the remainder of the work.

At a microscopic level, the spins are characterized by a *Hamiltonian*, that describes its energy as a function of external magnetic fields. This Hamiltonian has two energy eigenstates: the spin-up state, which is aligned parallel to the magnetic field, and the spin-down state that is aligned antiparallel. In practice the spins can be aligned in any direction by a superposition of these two states. The *Zeeman effect*, shown in figure 1.3, causes an energy difference between the spin-up and spin-down state. Similarly to classical behaviour, there is less potential energy when the magnetization is aligned to the magnetic field.

The Hamiltonian consists of two parts. The first part is H_0. It is time-independent, and caused by the orientation of the spin in the external magnetic field. In equilibrium, these are aligned parallel to each other, and the energy is minimal. After excitation, however, the spin is rotated and this energy is no longer minimal. Because of the relatively small energy difference, the spin will not spontaneously reorient itself [11]. Instead, this relaxation is *stimulated* by a time-dependent perturbation part H_1. This Hamiltonian will cause the spin to evolve from its original state to a superposition, from where it can relax back to equilibrium. Stimulated emission is shown in figure 1.4.

On a macroscopic scale, the behaviour of a single particle is irrelevant. Many MRI effects can be understood entirely classically [12], but relaxation rates must be calculated from the behaviour of an ensemble of many quantum particles. Redfield theory allows for these calculations using the density matrix formulation. The density matrix ρ represents the state of a group of protons using a matrix ρ. For a particle in the spin-up state $|\uparrow\rangle$, the density matrix is $|\uparrow\rangle\langle\uparrow|$, and for a particle in the spin-down state it is $|\downarrow\rangle\langle\downarrow|$. The power of the density matrix is that a mixture of 50% spin-up and 50% spin-down particles simply has a density matrix of $0.5\,|\uparrow\rangle\langle\uparrow| + 0.5\,|\downarrow\rangle\langle\downarrow|$. A more detailed description of the density matrix can be found in [13].

The evolution of the density matrix due to a Hamiltonian $\hat{\hat{H}}$ is given by the Liouville-von Neumann equation:

$$\frac{\partial}{\partial t}\hat{\rho} = -i\hat{\hat{H}}\hat{\rho} \tag{1.2}$$

Redfield theory mainly focuses on rewriting this into a master equation:

$$\frac{\partial}{\partial t}\hat{\rho} = -i\hat{\hat{H}}_0\hat{\rho} - \hat{\hat{\Gamma}}\hat{\rho}$$

Where $\hat{H}_0$ is the Hamiltonian due to the static main magnetic field, and $\hat{\hat{\Gamma}}$ is the *relaxation matrix* describing the effect of the B_1 field, and of relaxation interactions. It is possible to find the relaxation times by taking inner products of the spin operators $\hat{I}_{x,y,z}$ with this relaxation matrix. For example:

$$\frac{1}{T_1} = \frac{d\langle I_z\rangle}{dt} = \langle\hat{I}_z|\,\hat{\hat{\Gamma}}\,|\hat{I}_z\rangle$$

Redfield theory is described in more detail in [14] and [15].

2

Methods

2.1. Redfield Theory

2.1.1. On-Resonance

First, we calculate the $T_{1\rho}$ and $T_{2\rho}$ relaxation times for an on-resonance RF pulse. This is useful to find limiting cases for the off-resonance derivation and to be able to see the general properties of rotating frame relaxation. In all our Redfield derivations, it is assumed that the perturbation Hamiltonian comes from a randomly fluctuating field ΔB, which has a Lorentzian power spectrum. This is a good model for dipole-dipole relaxation, which is one of the main relaxation mechanism in clinical MRI, and the only relevant mechanism in homogeneous liquids. The final relaxation time is given as a function of the power spectrum of the ΔB fluctuations. This gives us an idea of the dependence of the relaxation times on molecular motion. A more detailed version of this derivation is shown in appendix B.

The magnetic fields in this case are B_0, the main magnetic field, B_1, the RF-pulse, and ΔB the randomly fluctuating field. These are given by:

$$\begin{aligned}\boldsymbol{B_0} &= B_0\hat{z}\\ \boldsymbol{B_1} &= B_1\left(\cos(\omega_0 t)\hat{x} - \sin(\omega_0 t)\hat{y}\right)\\ \boldsymbol{\Delta B} &= \Delta B_x(t)\hat{x} + \Delta B_y(t)\hat{y} + \Delta B_z(t)\hat{z}\end{aligned}$$

Since protons are spin-half particles, they behave like magnetic dipoles with a dipole moment $\boldsymbol{\mu}$. In a magnetic field $\boldsymbol{B}(t)$, they have potential energy given by:

$$E = -\boldsymbol{\mu}\cdot\boldsymbol{B}(t)$$

The dipole moment is given by the spin operators $\hat{I}_x$, $\hat{I}_y$, $\hat{I}_z$:

$$\hat{\mu}_{x,y,z} = \gamma\hbar\hat{I}_{x,y,z}$$

Here γ is the gyromagnetic ratio, and $\hbar$ is the reduced Planck constant. This leads to the following Hamiltonian:

$$\begin{aligned}\hat{H} = \frac{\hat{E}}{\hbar} &= \frac{-\hat{\mu}_x B_x(t) - \hat{\mu}_y B_y(t) - \hat{\mu}_z B_z(t)}{\hbar}\\ &= \frac{-\gamma\hbar\left(\hat{I}_x B_x(t) + \hat{I}_y B_y(t) + \hat{I}_z B_z(t)\right)}{\hbar}\\ &= -\gamma\left(\hat{I}_x B_x(t) + \hat{I}_y B_y(t) + \hat{I}_z B_z(t)\right)\end{aligned} \tag{2.1}$$

Filling in our magnetic fields gives:

$$\hat{H} = -\gamma B_0\hat{I}_z - \gamma B_1\left(\cos(\omega_0 t)\hat{I}_x - \sin(\omega_0 t)\hat{I}_y\right) - \gamma\Delta B_z(t)\hat{I}_z - \gamma\Delta B_x(t)\hat{I}_x - \gamma\Delta B_y(t)\hat{I}_y$$

Rearranging terms, and using the Larmor frequencies $\omega_0 = \gamma B_0$, $\omega_1 = \gamma B_1$:

$$\hat{H} = -\omega_0 \hat{I}_z - \omega_1 \left(\cos(\omega_0 t)\hat{I}_x - \sin(\omega_0 t)\hat{I}_y\right) - \gamma \Delta B_z(t)\hat{I}_z - \gamma \Delta B_x(t)\hat{I}_x - \gamma \Delta B_y(t)\hat{I}_y \tag{2.2}$$

In order to calculate the rotating frame relaxation time, this Hamiltonian must be transformed to the second rotating frame.

First, it is rotated $\omega_0 t$ around the z-axis, so that it is in the first rotating frame. Using the derivation in appendix A, it can be seen that this can be done by adding fictitious term, and applying a rotation operator to the Hamiltonian:

$$\hat{H}_{\text{eff}} = \omega_0 \hat{I}_z + \hat{\hat{R}}_{-\omega_0 t \hat{I}_z} \hat{H} \tag{2.3}$$

The rotations of the spin operators are:

$$\begin{aligned}
\hat{\hat{R}}_{-\omega_0 t \hat{I}_z} \hat{I}_x &= e^{-i\omega_0 t \hat{I}_z} \hat{I}_x e^{i\omega_0 t \hat{I}_z} = \hat{I}_{x'} \cos(\omega_0 t) + \hat{I}_{y'} \sin(\omega_0 t) \\
\hat{\hat{R}}_{-\omega_0 t \hat{I}_z} \hat{I}_y &= e^{-i\omega_0 t \hat{I}_z} \hat{I}_y e^{i\omega_0 t \hat{I}_z} = \hat{I}_{y'} \cos(\omega_0 t) - \hat{I}_{x'} \sin(\omega_0 t) \\
\hat{\hat{R}}_{-\omega_0 t \hat{I}_z} \hat{I}_z &= e^{-i\omega_0 t \hat{I}_z} \hat{I}_z e^{i\omega_0 t \hat{I}_z} = \hat{I}_{z'}
\end{aligned} \tag{2.4}$$

So that finally filling in the Hamiltonian gives the first rotating frame expression:

$$\hat{H}_{\text{eff}} = -\gamma \Delta B_z(t)\hat{I}_{z'} - \omega_1 \hat{I}_{x'} - \gamma \hat{\hat{R}}_{-\omega_0 t \hat{I}_z} \left(\Delta B_x(t)\hat{I}_x + \Delta B_y(t)\hat{I}_y\right)$$

In order to simplify the last term, we make use of the spin-raising and lowering operators:

$$\hat{I}_+ = \hat{I}_x + i\hat{I}_y \quad \text{and} \quad \hat{I}_- = \hat{I}_x - i\hat{I}_y$$

These are the eigenoperators of this rotation:

$$\begin{aligned}
\hat{\hat{R}}_{-\omega_0 t \hat{I}_z} \hat{I}_+ &= e^{-i\omega_0 t \hat{I}_z} \hat{I}_+ e^{i\omega_0 t \hat{I}_z} = e^{-i\omega_0 t} \hat{I}_+ \\
\hat{\hat{R}}_{-\omega_0 t \hat{I}_z} \hat{I}_- &= e^{-i\omega_0 t \hat{I}_z} \hat{I}_- e^{i\omega_0 t \hat{I}_z} = e^{i\omega_0 t} \hat{I}_-
\end{aligned}$$

Hence we can finally write this as:

$$\hat{H}_{\text{eff}} = -\gamma \Delta B_z(t)\hat{I}_{z'} - \omega_1 \hat{I}_{x'} - \frac{\gamma}{2} e^{-i\omega_0 t} \hat{I}_+ \left(\Delta B_x(t) - i\Delta B_y(t)\right) - \frac{\gamma}{2} e^{i\omega_0 t} \hat{I}_- \left(\Delta B_x(t) + i\Delta B_y(t)\right)$$

Note that now the only term that is constant in time is $\hat{H}_0' = -\omega_1 \hat{I}_{x'}$. This is the Hamiltonian due to the effective field. We can thus move to the second rotating frame, rotating with angular velocity $-\omega_1$ around the $\hat{x}'$ axis. To find these rotations, it is convenient to do a coordinate substitution:

$$\tilde{x} = y' \qquad \tilde{y} = z' \qquad \tilde{z} = x'$$

Applying this substitution, and calculating the rotations, eventually gives:

$$\begin{aligned}
\hat{H}'_{\text{eff}} = &-\frac{\gamma}{2} \hat{I}_{\tilde{z}} \left(\left(\Delta B_x(t) - i\Delta B_y(t)\right) e^{-i\omega_0 t} + \left(\Delta B_x(t) + i\Delta B_y(t)\right) e^{i\omega_0 t}\right) \\
&+ \frac{i\gamma}{2} \hat{I}_{\mp} \left(\Delta B_z(t) e^{-i\omega_1 t} - \frac{1}{2}\left(\Delta B_x(t) - i\Delta B_y(t)\right) e^{-i(\omega_0 + \omega_1)t} + \frac{1}{2}\left(\Delta B_x(t) + i\Delta B_y(t)\right) e^{-i(-\omega_0 + \omega_1)t}\right) \\
&- \frac{i\gamma}{2} \hat{I}_{\simeq} \left(\Delta B_z(t) e^{i\omega_1 t} + \frac{1}{2}\left(\Delta B_x(t) - i\Delta B_y(t)\right) e^{-i(\omega_0 - \omega_1)t} - \frac{1}{2}\left(\Delta B_x(t) + i\Delta B_y(t)\right) e^{-i(-\omega_0 - \omega_1)t}\right) \\
= &\, F'_0(t)\hat{I}_{\tilde{z}} + F'_1(t)\hat{I}_{\mp} + F'_{-1}(t)\hat{I}_{\simeq}
\end{aligned}$$

Where in the last equation the Hamiltonian was split into terms of each of the eigenoperators of $\hat{\hat{H}}_0'$. The relaxation operator $\hat{\hat{\Gamma}}$ can be found by calculating the power spectra of these values:

$$\hat{\hat{\Gamma}} = \sum_q J_q \hat{\hat{A}}_{-q} \hat{\hat{A}}_q$$

with:

$$J_q = \int_0^\infty G_q(\tau)d\tau = \int_0^\infty \overline{F_{-q}(t)F_q(t-\tau)}d\tau$$

We assume our fluctuations follow:

$$\left\langle \Delta B_p(t)\Delta B_q(t-\tau)\right\rangle = \begin{cases} 0 & p \neq q \\ G(\tau) = \left\langle B^2\right\rangle e^{-|\tau|/\tau_c} & p = q \end{cases} \tag{2.5}$$

With a power spectrum:

$$J(\omega) = \frac{1}{\langle B^2\rangle}\int_0^\infty G(\tau)e^{-i\omega\tau}d\tau = \int_0^\infty e^{-|\tau|/\tau_c}e^{-i\omega\tau}d\tau = \frac{\tau_c}{1+\omega^2\tau_c^2} \tag{2.6}$$

Carrying out these calculations gives:

$$J_0 = \frac{\gamma^2}{2}\left(\left\langle B_x^2\right\rangle + \left\langle B_y^2\right\rangle\right)J(\omega_0) = \gamma^2\left\langle B^2\right\rangle J(\omega_0)$$

and

$$J_1 = J_{-1} = \frac{\gamma^2}{4}\left\langle B_z^2\right\rangle J(\omega_1) + \frac{\gamma^2}{16}\left\langle B_x^2\right\rangle (J(\omega_0-\omega_1)+J(\omega_0+\omega_1)) + \frac{\gamma^2}{16}\left\langle B_y^2\right\rangle (J(\omega_0-\omega_1)+J(\omega_0+\omega_1))$$

The relaxation times follow from inner products with the relaxation matrix:

$$\begin{aligned} \frac{1}{T_{1\rho}} &= \langle \hat{I}_{\tilde{z}}|\,\hat{\hat{\Gamma}}\,|\hat{I}_{\tilde{z}}\rangle = J_{-1}\langle \hat{I}_{\tilde{z}}|\,\hat{\hat{I}}_{\mp}\hat{\hat{I}}_{\simeq}\,|\hat{I}_{\tilde{z}}\rangle + J_1\langle \hat{I}_{\tilde{z}}|\,\hat{\hat{I}}_{\simeq}\hat{\hat{I}}_{\mp}\,|\hat{I}_{\tilde{z}}\rangle + J_0\langle \hat{I}_{\tilde{z}}|\,\hat{\hat{I}}_{\tilde{z}}\hat{\hat{I}}_{\tilde{z}}\,|\hat{I}_{\tilde{z}}\rangle \\ &= 2(J_{-1}+J_1) \\ &= 2\left(\frac{\gamma^2}{4}\left\langle B^2\right\rangle (J(\omega_1)+J(\omega_0)) + \frac{\gamma^2}{4}\left\langle B^2\right\rangle (J(\omega_1)+J(\omega_0))\right) \\ &= \gamma^2\left\langle B^2\right\rangle (J(\omega_1)+J(\omega_0)) \end{aligned} \tag{2.7}$$

and

$$\begin{aligned} \frac{1}{T_{2\rho}} &= \langle \hat{I}_{\tilde{x}}|\,\hat{\hat{\Gamma}}\,|\hat{I}_{\tilde{x}}\rangle = J_0\,\mathrm{Tr}\left(\hat{I}_{\tilde{x}}\hat{\hat{I}}_{\tilde{z}}\hat{\hat{I}}_{\tilde{z}}\hat{I}_{\tilde{x}}\right) + 2J_1\left(\mathrm{Tr}\left(\hat{I}_{\tilde{x}}\hat{\hat{I}}_{\tilde{x}}\hat{\hat{I}}_{\tilde{x}}\hat{I}_{\tilde{x}}\right) + \mathrm{Tr}\left(\hat{I}_{\tilde{x}}\hat{\hat{I}}_{\tilde{y}}\hat{\hat{I}}_{\tilde{y}}\hat{I}_{\tilde{x}}\right)\right) \\ &= J_0 + 2J_1 \\ &= \gamma^2\left\langle B^2\right\rangle J(\omega_0) + \frac{\gamma^2}{2}\left\langle B^2\right\rangle (J(\omega_1)+J(\omega_0)) \\ &= \frac{\gamma^2}{2}\left\langle B^2\right\rangle (J(\omega_1)+3J(\omega_0)) \end{aligned} \tag{2.8}$$

Where we also assumed equal fluctuation size in each direction ($\left\langle B_{x,y,z}^2\right\rangle = \left\langle B^2\right\rangle$).

2.1.2. Time-independent Off-Resonance

In this section, we consider the case that the RF-field rotates at a frequency $\omega_{\mathrm{rf}} \neq \omega_0$, but ω_{rf} does not depend on time. This can, for instance, happen when B_0 inhomogeneity causes different ω_0 for different spins. The derivation is mostly the same as in the on-resonance case shown above, until the second rotating frame. A more detailed version of this derivation is shown in appendix C.

We once again have B_0, the main magnetic field, B_1, the RF-pulse, and ΔB the randomly fluctuating field.

$$\begin{aligned} \boldsymbol{B_0} &= B_0\hat{z} \\ \boldsymbol{B_1} &= B_1\left(\cos(\omega_{\mathrm{rf}}t)\hat{x} - \sin(\omega_{\mathrm{rf}}t)\hat{y}\right) \\ \boldsymbol{\Delta B} &= \Delta B_x(t)\hat{x} + \Delta B_y(t)\hat{y} + \Delta B_z(t)\hat{z} \end{aligned}$$

The energy corresponding to a magnetic field is given by the Hamiltonian:

$$\hat{H} = -\gamma \left(\hat{I}_x B_x(t) + \hat{I}_y B_y(t) + \hat{I}_z B_z(t) \right)$$

Filling this in gives:

$$\hat{H} = -\gamma B_0 \hat{I}_z - \gamma B_1 \left(\cos(\omega_{\mathrm{rf}} t) \hat{I}_x - \sin(\omega_{\mathrm{rf}} t) \hat{I}_y \right) - \gamma \Delta B_z(t) \hat{I}_z - \gamma \Delta B_x(t) \hat{I}_x - \gamma \Delta B_y(t) \hat{I}_y$$

In order to get real $T_{1\rho}$ relaxation, we must transform to the second rotating frame. In the first rotating frame, a rotation of $\omega_{\mathrm{rf}} t$ around the z-axis, gives:

$$\hat{H}_{\mathrm{eff}} = -\Omega \hat{I}_{z'} - \gamma \Delta B_z(t) \hat{I}_{z'} - \omega_1 \hat{I}_{x'} - \frac{\gamma}{2} e^{-i\omega_{\mathrm{rf}} t} \hat{I}_+ \left(\Delta B_x(t) - i \Delta B_y(t) \right) - \frac{\gamma}{2} e^{i\omega_{\mathrm{rf}} t} \hat{I}_- \left(\Delta B_x(t) + i \Delta B_y(t) \right) \tag{2.9}$$

Moving to the second rotating frame requires a tilt so that B_{eff} is aligned to the z''-axis). This is shown

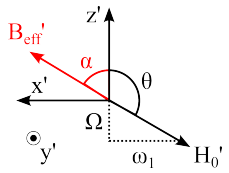

Figure 2.1: $\boldsymbol{B}'_{\mathrm{eff}}$ in the first rotating frame

as the angle α in figure 2.1. It also requires a rotation of $\omega_{\mathrm{eff}} t = \sqrt{\omega_1^2 + \Omega^2}\, t$ around the z''-axis. This gives:

$$\begin{aligned}
\hat{H}''_{\mathrm{eff}} \omega_{\mathrm{eff}} &= \hat{I}_{z''} \left(-\Omega \gamma \Delta B_z(t) - \frac{\omega_1 \gamma}{2} \Delta B_-(t) e^{-i\omega_{\mathrm{rf}} t} - \frac{\omega_1 \gamma}{2} \Delta B_+(t) e^{i\omega_{\mathrm{rf}} t} \right) \\
&\quad + \frac{1}{2} \hat{I}_{+''} \left(\omega_1 \gamma \Delta B_z(t) e^{-i\omega_{\mathrm{eff}} t} - \frac{\gamma}{2} (\Omega + \omega_{\mathrm{eff}}) \Delta B_-(t) e^{-i(\omega_{\mathrm{rf}} + \omega_{\mathrm{eff}}) t} - \frac{\gamma}{2} (\Omega - \omega_{\mathrm{eff}}) \Delta B_+(t) e^{i(\omega_{\mathrm{rf}} - \omega_{\mathrm{eff}}) t} \right) \\
&\quad + \frac{1}{2} \hat{I}_{-''} \left(\omega_1 \gamma \Delta B_z(t) e^{i\omega_{\mathrm{eff}} t} - \frac{\gamma}{2} (\Omega - \omega_{\mathrm{eff}}) \Delta B_-(t) e^{-i(\omega_{\mathrm{rf}} - \omega_{\mathrm{eff}}) t} - \frac{\gamma}{2} (\Omega + \omega_{\mathrm{eff}}) \Delta B_+(t) e^{i(\omega_{\mathrm{rf}} + \omega_{\mathrm{eff}}) t} \right) \\
&= F_0 \hat{I}_{z''} + F_1 \hat{I}_{+''} + + F_{-1} \hat{I}_{-''}
\end{aligned}$$

The relaxation operator $\hat{\Gamma}$ can be found by calculated in the same way as for the on-resonance case. This gives:

$$\begin{aligned}
J_0 &= \frac{\gamma^2 \Omega^2}{\omega_{\mathrm{eff}}^2} \langle B^2 \rangle J(0) + \frac{\gamma^2 \omega_1^2}{\omega_{\mathrm{eff}}^2} \langle B^2 \rangle J(\omega_{\mathrm{rf}}) \\
&= \frac{\gamma^2 \Omega^2}{\omega_1^2 + \Omega^2} \langle B^2 \rangle J(0) + \frac{\gamma^2 \omega_1^2}{\omega_1^2 + \Omega^2} \langle B^2 \rangle J(\omega_{\mathrm{rf}})
\end{aligned}$$

and

$$\begin{aligned}
J_1 &= \frac{\gamma^2 \omega_1^2}{4\omega_{\mathrm{eff}}^2} \langle B^2 \rangle J(\omega_{\mathrm{eff}}) + \frac{\gamma^2 (\Omega + \omega_{\mathrm{eff}})^2}{8\omega_{\mathrm{eff}}^2} \langle B^2 \rangle J(\omega_{\mathrm{rf}} + \omega_{\mathrm{eff}}) \\
&\quad + \frac{\gamma^2 (\Omega - \omega_{\mathrm{eff}})^2}{8\omega_{\mathrm{eff}}^2} \langle B^2 \rangle J(\omega_{\mathrm{rf}} - \omega_{\mathrm{eff}})
\end{aligned}$$

Finally, we can once again find our relaxation times using inner products with the relaxation matrix:

$$\begin{aligned}
\frac{1}{T_{1\rho}} &= \langle \hat{I}_{\tilde{z}} | \hat{\Gamma} | \hat{I}_{\tilde{z}} \rangle = J_{-1} \langle \hat{I}_{\tilde{z}} | \hat{I}_{\mp} \hat{I}_{\simeq} | \hat{I}_{\tilde{z}} \rangle + J_1 \langle \hat{I}_{\tilde{z}} | \hat{I}_{\simeq} \hat{I}_{\mp} | \hat{I}_{\tilde{z}} \rangle + J_0 \langle \hat{I}_{\tilde{z}} | \hat{I}_{\tilde{z}} \hat{I}_{\tilde{z}} | \hat{I}_{\tilde{z}} \rangle \\
&= 2J_{-1} \operatorname{Tr} \left(\hat{I}_{\tilde{z}} \hat{I}_{\tilde{z}} \right) + 2J_1 \operatorname{Tr} \left(\hat{I}_{\tilde{z}} \hat{I}_{\tilde{z}} \right) = 2(J_{-1} + J_1) \\
&= 4J_1 = \frac{\gamma^2 \omega_1^2}{\omega_{\mathrm{eff}}^2} \langle B_{\tilde{z}}^2 \rangle J(\omega_{\mathrm{eff}}) + \frac{\gamma^2}{4\omega_{\mathrm{eff}}^2} \left(\langle B_x^2 \rangle + \langle B_y^2 \rangle \right) \left((\Omega + \omega_{\mathrm{eff}})^2 J(\omega_{\mathrm{rf}} + \omega_{\mathrm{eff}}) + (\Omega - \omega_{\mathrm{eff}})^2 J(\omega_{\mathrm{rf}} - \omega_{\mathrm{eff}}) \right)
\end{aligned} \tag{2.10}$$

For equal fluctuation size in all directions, so $\langle B_{x,y,z}^2 \rangle = \langle B^2 \rangle$:

$$\frac{1}{T_{1\rho}} = \frac{\gamma^2\omega_1^2}{\omega_{\text{eff}}^2}\langle B^2\rangle J(\omega_{\text{eff}}) + \frac{\gamma^2}{2\omega_{\text{eff}}^2}\langle B^2\rangle\left((\Omega+\omega_{\text{eff}})^2 J(\omega_{\text{rf}}+\omega_{\text{eff}}) + (\Omega-\omega_{\text{eff}})^2 J(\omega_{\text{rf}}-\omega_{\text{eff}})\right)$$

Similarly, $T_{2\rho}$ can be found using another inner product:

$$\begin{aligned}\frac{1}{T_{2\rho}} = J_0 + 2J_1 = {} & \frac{\gamma^2\Omega^2}{\omega_{\text{eff}}^2}\langle B_z^2\rangle J(0) + \frac{\gamma^2\omega_1^2}{2\omega_{\text{eff}}^2}\left(\langle B_x^2\rangle + \langle B_y^2\rangle\right) J(\omega_{\text{rf}}) + \frac{\gamma^2\omega_1^2}{2\omega_{\text{eff}}^2}\langle B_z^2\rangle J(\omega_{\text{eff}}) \\ & + \frac{\gamma^2(\Omega+\omega_{\text{eff}})^2}{8\omega_{\text{eff}}^2}\left(\langle B_x^2\rangle + \langle B_y^2\rangle\right) J(\omega_{\text{rf}}+\omega_{\text{eff}}) + \frac{\gamma^2(\Omega-\omega_{\text{eff}})^2}{8\omega_{\text{eff}}^2}\left(\langle B_x^2\rangle + \langle B_y^2\rangle\right) J(\omega_{\text{rf}}-\omega_{\text{eff}})\end{aligned} \tag{2.11}$$

Once again taking equal fluctuation size in all directions:

$$\begin{aligned}\frac{1}{T_{2\rho}} = {} & \frac{\gamma^2\Omega^2}{\omega_{\text{eff}}^2}\langle B^2\rangle J(0) + \frac{\gamma^2\omega_1^2}{\omega_{\text{eff}}^2}\langle B^2\rangle J(\omega_{\text{rf}}) + \frac{\gamma^2\omega_1^2}{2\omega_{\text{eff}}^2}\langle B^2\rangle J(\omega_{\text{eff}}) \\ & + \frac{\gamma^2(\Omega+\omega_{\text{eff}})^2}{4\omega_{\text{eff}}^2}\langle B^2\rangle J(\omega_{\text{rf}}+\omega_{\text{eff}}) + \frac{\gamma^2(\Omega-\omega_{\text{eff}})^2}{4\omega_{\text{eff}}^2}\langle B^2\rangle J(\omega_{\text{rf}}-\omega_{\text{eff}})\end{aligned}$$

In order to characterize equations 27 and 28, it is necessary to find values for some parameters. Some are constants, such as $\gamma = 2.675 \cdot 10^8$ rad $s^{-1}T^{-1}$ or $B_0 = 3$ T due to the scanner type. Others can be chosen based on reasonable assumptions: $B_1 = 1\ \mu$T, fluctuation correlation time $\tau_c = 1$ ns (which are of the right order for spin-lock pulses and water). The biggest challenge is finding $\langle B^2 \rangle$, as this cannot be set or measured directly. Instead, the formula for T_1 due to random fluctuating fields can be used:

$$\frac{1}{T_1} = 2\gamma^2\langle B^2\rangle\frac{\tau_c}{1+\omega_0^2\tau_c^2} \Rightarrow \langle B^2\rangle = \frac{1+\omega_0^2\tau_c^2}{2\gamma^2\tau_c T_1} \tag{2.12}$$

Together with a reasonable assumption $T_1 = 1.5$s it is now possible to fill in all parameters in formulas 27 and 28.

2.1.3. Amplitude- and Frequency-Modulated Pulses

The relaxation times calculated in the previous section correspond to spin-lock experiments. Spin-lock measurements are useful, but they are very susceptible to inhomogeneities in the B_0 and B_1 fields. An alternative to these spin-lock pulses are *adiabatic pulses*. While spin-lock pulses are just block functions, switching on and off a constant amplitude, adiabatic pulses have an amplitude and frequency modulation. An adiabatic pulse with amplitude modulation $\omega_1(t)$ and frequency modulation $\omega_{\text{rf}}(t) - \omega_0$ gives a magnetic field:

$$\boldsymbol{B_1} = \frac{\omega_1(t)}{\gamma}\left(\cos(\omega_{\text{rf}}(t)\cdot t)\hat{x} - \sin(\omega_{\text{rf}}(t)\cdot t)\hat{y}\right)$$

Analytical calculation of the relaxation times during adiabatic pulses is complex, as it involves integrals of products of many time-dependent factors. Therefore, we take a finite-difference approach. We divide the pulse into very short discrete time-steps, and assume that during each time-step the amplitude and the frequency modulation function are constant. This is called the *quasistatic assumption*. In that case, we can simply use the results for the time-independent off-resonance at each timestep, substituting the AM function in ω_1 and the FM function in $-\Omega$. This minus sign is due to our convention of the definition of the off-resonance.

A common type of adiabatic pulse is the hyperbolic secant pulse. These have an amplitude and frequency modulation given by:[8]

$$\begin{aligned}\omega_1(t) &= \omega_1^{\max}\cdot\operatorname{sech}\left(\beta\left(\frac{2t}{T_p}-1\right)\right) \\ -\Omega(t) &= A\tanh\left(\beta\left(\frac{2t}{T_p}-1\right)\right)\end{aligned} \tag{2.13}$$

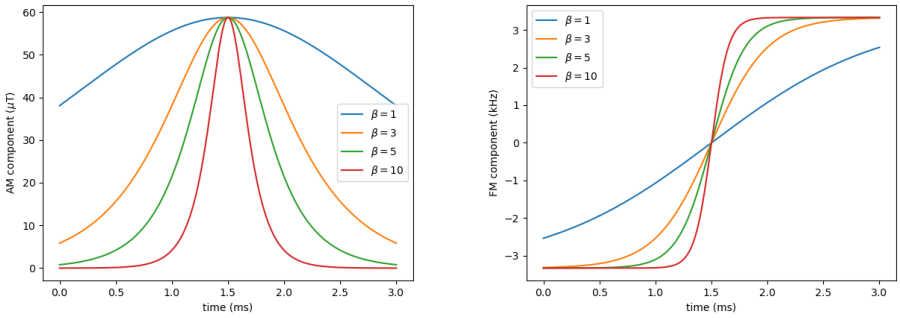

(a) Amplitude modulation

(b) Frequency modulation

Figure 2.2: Amplitude and frequency modulation functions for a hyperbolic secant pulse. The different colours represent different values for the parameter β.

Here β is a dimensionless parameter that influences the sharpness of the curve, $\omega_1^{\max}$ is the maximum amplitude of the pulse in rad/s. A is the maximum FM-modulation of the curve in rad/s, and T_p is the duration of the pulse in seconds. These modulation functions are also shown in figure 2.2. It can be seen that the higher β, the sharper the modulation functions.

Using the quasistatic assumption, the Redfield calculation gives a list $T_{1\rho,\text{adiab}}(t_i)$ of relaxation times for each time point t_i. To get the effect of the total pulse, the effective relaxation time can be found as a reciprocal sum:

$$\frac{1}{T_{1\rho,\text{adiab}}} = \frac{1}{T_p}\sum_i \frac{\Delta t}{T_{1\rho,\text{adiab}}(t_i)}$$

Where Δt is the time step, and T_p is the total pulse duration. The effective $T_{2\rho,\text{adiab}}$ can be found using an analogous formula

2.2. Applications

2.2.1. Pulse Optimization

The previous sections allow for the calculation of the relaxation times during a pulse in the presence of off-resonance. Our goal is to minize the the influence of the off-resonance on the final image in real MRI measurements. To this end, pulse parameters are found that exhibit the smallest difference in $T_{1\rho,\text{adiab}}$ in response to off-resonance.

The sharpness parameter β and the FM amplitude A were chosen as the independent variables for this optimization. A grid search was carried out on a 100 by 100 grid with $\beta \in \{0.1, 0.3, \ldots, 20\}$ and $A \in \{0, 50.4, \ldots, 5000\}$ Hz. For each combination (β, A) the pulse was initialized with a duration $T_p = 30$ ms. Next, the pulse was adjusted to satisfy two constraints. The first is that safety concerns require that the total power delivered to the patient is below a certain maximum. On the other hand, image contrast is improved by increasing the power. Concretely, this means that the root-means square B_1 must be ≤ 5.48 μT, and that the maximum B_1 must be ≤ 13.43 μT. The amplitude modulation function was scaled by a factor:

$$\alpha = \min\left(\frac{B_{1\max}^{\text{limit}}}{B_{1\max}}, \frac{B_{1\text{rms}}^{\text{limit}}}{B_{1\text{rms}}}\right) \tag{2.14}$$

The other constraint is that the relaxation should be mostly due to $T_{1\rho,\text{adiab}}$. Under some circumstances, e.g. when the RF pulse is a really sharp peak, T_1 relaxation occurs instead. To solve this, a constraint was put on the total decay fraction during the pulse, given by:

$$N = e^{-T_p/T_{1\rho,\text{adiab}}}$$

Where T_p is the total pulse duration, and $T_{1\rho,\text{eff}}$ is the effective relaxation rate of the pulse. In order to ensure $T_{1\rho,\text{adiab}}$ is the main contributor, the pulse duration is scaled until $N = 0.970 \pm 0.001$. This

guarantees that the pulse is long enough to cause at least some relaxation during the parts where the AM modulation is not zero.

After the pulse was rescaled to satisfy these constraints, the objective function of the optimization was calculated. First of all, the effective $T_{1\rho,\text{adiab}}$ was calculated for different off-resonance values Ω. The off-resonance was modelled by adding Ω to the frequency modulation part of the pulse. This was repeated for $\Omega \in \{0, 50, 100, \ldots, 200\}$ Hz. The root-mean-square (RMS) difference between the on-resonance and off-resonance relaxation times was taken as a measure of the off-resonance resiliency of the pulses.

Next, Bloch simulations were carried out on the same pulses. Bloch simulations are the conventional way to optimize pulses (e.g. in [5]) based on a finite-time discretization of the Bloch equations (equation 1.1). These Bloch simulations were used to find the final magnetization along the z-direction. In an adiabatic pulse, the magnetization will follow the effective field, and end up along the negative z-axis. However, if the effective field moves too rapidly, the pulse will not be adiabatic and the magnetization will not be inverted correctly. For this analysis it is not necessary to consider the (T_1 and T_2) relaxation, so these were neglected during the Bloch simulations.

Both these parameters were turned into a score from 0 to 1. The RMS difference ε in $T_{1\rho,\text{adiab}}$ due to off-resonance was scored as:

$$S_{\text{RMSdiff}}(\beta, A) = 1 - \frac{\varepsilon(\beta, A)}{\max_{\beta,A} \varepsilon(\beta, A)} \tag{2.15}$$

Therefore a score of 1 means no difference at all, while the biggest difference in the domain gets a score of 0. The Bloch simulations were scored according to the final z-magnetization M_z:

$$S_{\text{Bloch}}(\beta, A) = \frac{1 - M_z(\beta, A)}{2} \tag{2.16}$$

Therefore a complete inversion with $M_z = -1$ gets a score of 1, while no inversion at all gets a score of 0.

Two optimization methods were compared. The first made use of both the z-magentization score and the RMS deviation score. This method takes both the Redfield and Bloch simultions into account, and is the method that was in this paper. The second is the conventional optimization method, using only Bloch equations. For this optimization only the z-magnetization score was used. This second method therefore does not take rotating frame relaxation into account.

The optimization was repeated for both methods, for correlation times $\tau_c \in \{0.01, 0.1, 1.0\}$ ns, to simulate the effect of different samples. These are valid for liquids with molecular masses of $20, 200$ and 2000 Da.

2.3. Experimental Validation

2.3.1. Off-Resonance Behaviour

Equation 27 allows for the calculation of $T_{1\rho}$ in the presence of off-resonance. To validate these results, MRI scans were performed on phantoms, using a prepulse that simulates the effect of off-resonance. This prepulse is shown in figure 2.3. The first adiabatic half-passage (AHP) pulse rotates the magnetization into the transverse plane. During the second part, the AM and FM functions are held constant. This part functions like a spin-lock pulse, and the magnetization undergoes $T_{1\rho}$ relaxation. The final part is another AHP pulse, that aligns the magnetization again to the z-axis for measurement. Off-resonance is modelled by shifting the frequency modulation function by a constant. Since the true resonance frequency γB_0 remains constant, changing the frequency of this pulse has the same effect as off-resonance due to variations in B_0.

The AHP pulses were chosen because they can efficiently flip the magnetization even in the presence of off-resonance. If a block pulse was used, like in a normal experiment, the magnetization may not have been totally aligned to the z-axis at the end of the pulse. This would interfere with the measurement process of the magnetization. In this experiment, the AHP pulses had a hyperbolic secant shape (given in equation 2.13). The shape of the first AHP pulse is given by this equation for $0 \leq t \leq T_p/2$. The

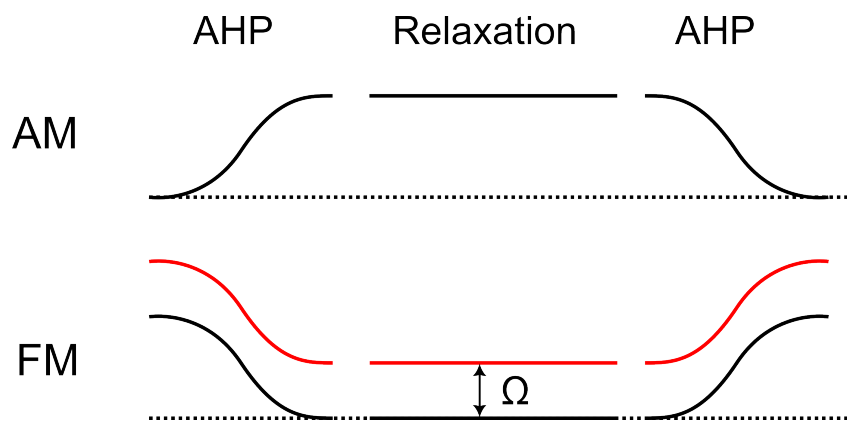

Figure 2.3: Sketch of the amplitude- and frequency modulation function of the prepulse used in the off-resonance experiment. The amplitude modulation function is the same for the on- and off-resonance version. The frequency modulation is different for the on- (black) and off-resonance case. The dotted line represents zero modulation.

shape of the second AHP follows from this equation for $T_p/2 \leq t \leq T_p$, and the FM part is flipped. This is because the magnetization should end up along the positive z-axis. Both pulses had $\beta = 4$ and an FM amplitude of 500 Hz.

The MRI scans were performed on a plastic jar, with filled with a mixture of water and nickel chloride. Nickel chloride was added to the water to lower its relaxation time, so that it exhibits more contrast in the MRI images. The scanner used was a 3T Philips Ingenia. First, the jar was positioned in the scanner, and a survey scan was performed to select a slice going lengthwise through the jar. Then a T_1 mapping sequence was performed. This allows for the calculation of T_1 values throughout the jar, which can be used to check if our assumptions for the $\langle B^2 \rangle$ calculation (equation 2.12) were valid. The T_1 mapping was based on the Modified Look-Locker Inversion Recovery method.

Next, the $T_{1\rho}$ measurements were performed. These consist of the pulse mentioned before, followed by a gradient echo sequence for imaging. This sequence was used as it can quickly image the longitudinal magnetization. A field of view of 150 by 150 mm was used, and a single 2D image was made of the selected slice. The echo time was set to be the shortest possible, and the pulse power was set to be as high as possible (in this case corresponding to a flip angle of 350 degrees). The scanner was set up to take 6 dynamic images. These dynamic images were taken after 0, 15, 20, 25 and 30 ms application of the prepulse. Of these time, 5 ms was for each of the AHP parts. The final image used a saturation prepulse, which is used to find the magnetization that would exist after a very long relaxation.

For each pixel an exponential fit was made to time evolution of the magnetization. This gives $T_{1\rho,\mathrm{adiab}}$ as one of the parameters. Additionally, the standard deviation of the measured signal from the exponential fit was calculated. This provides insight into the accuracy of the fit.

3

Results

3.1. Redfield Theory

3.1.1. Time-Independent Off-Resonance

On-resonance limit

To validate equations 27 and 28 for $T_{1\rho}$ and $T_{2\rho}$, various limits are taken and compared against the literature. Starting from the off-resonance derivation, and taking the limit $\Omega \to 0$, we obtain an expression for on-resonance excitation. This was both derived independently by us (in equation 2.7), and it is available in the literature [15]. Taking this limit gives $\omega_{\mathrm{rf}} \to \omega_0$ and $\omega_{\mathrm{eff}} \to \omega_1$. Applying this to equation 27 gives:

$$\frac{1}{T_{1\rho}} = \gamma^2 \langle B_z^2 \rangle J(\omega_1) + \frac{\gamma^2}{4} \left(\langle B_x^2 \rangle + \langle B_y^2 \rangle \right) \left(J(\omega_0 + \omega_1) + J(\omega_0 - \omega_1) \right)$$

Taking $\omega_0 \gg \omega_1$ (as $B_0 \gg B_1$):

$$\frac{1}{T_{1\rho}} = \gamma^2 \langle B_z^2 \rangle J(\omega_1) + \frac{\gamma^2}{2} \left(\langle B_x^2 \rangle + \langle B_y^2 \rangle \right) J(\omega_0)$$

Finally taking equal fluctuation magnitude in all directions ($\langle B_{x,y,z}^2 \rangle = \langle B^2 \rangle$):

$$\begin{aligned} \frac{1}{T_{1\rho}} &= \gamma^2 \langle B^2 \rangle J(\omega_1) + \gamma^2 \langle B^2 \rangle J(\omega_0) \\ &= \gamma^2 \langle B^2 \rangle \left(J(\omega_0) + J(\omega_1) \right) \end{aligned}$$

Which agrees with the theoretical limits mentioned above.

Similarly, taking the on-resonance limit of equation 28 gives:

$$\begin{aligned} \frac{1}{T_{2\rho}} = {} & \frac{\gamma^2}{2} \left(\langle B_x^2 \rangle + \langle B_y^2 \rangle \right) J(\omega_0) + \frac{\gamma^2}{2} \langle B_z^2 \rangle J(\omega_1) \\ & + \frac{\gamma^2}{8} \left(\langle B_x^2 \rangle + \langle B_y^2 \rangle \right) J(\omega_0 + \omega_1) + \frac{\gamma^2}{8} \left(\langle B_x^2 \rangle + \langle B_y^2 \rangle \right) J(\omega_0 - \omega_1) \end{aligned}$$

Taking $\omega_0 \gg \omega_1$:

$$\frac{1}{T_{2\rho}} = \frac{3\gamma^2}{4} \left(\langle B_x^2 \rangle + \langle B_y^2 \rangle \right) J(\omega_0) + \frac{\gamma^2}{2} \langle B_z^2 \rangle J(\omega_1)$$

And finally $\langle B_{x,y,z}^2 \rangle = \langle B^2 \rangle$:

$$\frac{1}{T_{2\rho}} = \frac{\gamma^2}{2} \langle B^2 \rangle \left(J(\omega_1) + 3J(\omega_0) \right)$$

Which agrees with our on-resonance result (equation 2.8).

ANZMAG limit

In June 2019, the Australian and New Zealand Society for Magnetic Resonance (ANZMAG) published a lecture series on NMR relaxation [16]. As a part of these lectures, they derived the $T_{1\rho}$ relaxation for time-independent off-resonance, but with only a fluctuation in the z-direction. Their result was:

$$\frac{1}{T_{1\rho}} = R_{1\rho} = 2J(\omega_{\text{eff}})$$

Furthermore, assuming (as we do) that the autocorrelation of the fluctuations decays exponentially with constant $k = \frac{1}{\tau_c}$:

$$\frac{1}{T_{1\rho}} = \frac{\sin^2(\alpha)\gamma^2 \left\langle B_z^2 \right\rangle \frac{1}{\tau_c}}{\frac{1}{\tau_c^2} + \omega_{\text{eff}}^2}$$

(adjusted to use our variable names, and pulling γ^2 out of their fluctuation amplitude)
Rewriting this gives:

$$\begin{aligned}\frac{1}{T_{1\rho}} &= \frac{\omega_1^2\gamma^2 \left\langle B_z^2 \right\rangle \tau_c}{\left(\omega_1^2 + \Omega^2\right)\left(1 + \omega_{\text{eff}}^2\tau_c^2\right)} \\ &= \frac{\omega_1^2\gamma^2 \left\langle B_z^2 \right\rangle \tau_c}{\left(\omega_1^2 + \Omega^2\right)\left(1 + \left(\omega_1^2 + \Omega^2\right)\tau_c^2\right)}\end{aligned}$$

If we set $\left\langle B_x^2 \right\rangle = \left\langle B_y^2 \right\rangle = 0$ in equation 27, we can also find $T_{1\rho}$ for fluctuations in the z-direction from our calculations. This gives:

$$\frac{1}{T_{1\rho}} = \frac{\gamma^2\omega_1^2}{\omega_{\text{eff}}^2} \left\langle B_z^2 \right\rangle J(\omega_{\text{eff}})$$

For the power spectrum of the fluctuations, we take a Lorentzian with correlation time τ_c:

$$J(\omega) = \frac{\tau_c}{1 + \omega^2\tau_c^2}$$

Filling this in gives:

$$\begin{aligned}\frac{1}{T_{1\rho}} &= \frac{\gamma^2\omega_1^2}{\omega_{\text{eff}}^2} \frac{\tau_c}{1 + \omega_{\text{eff}}^2\tau_c^2} \left\langle B_z^2 \right\rangle \\ &= \frac{\omega_1^2\gamma^2 \left\langle B_z^2 \right\rangle \tau_c}{\left(\Omega^2 + \omega_1^2\right)\left(1 + \left(\Omega^2 + \omega_1^2\right)\tau_c^2\right)}\end{aligned}$$

Which indeed agrees with the result from the ANZMAG lectures.

High-off-resonance limit

As the plots in the next section will show, the $T_{1\rho}$ and $T_{2\rho}$ relaxation times strongly approach a limit for large off-resonance values. To calculate these limits, we assume $\Omega \gg \omega_1$, which gives the following limits:

$$\omega_{\text{eff}} = \sqrt{\Omega^2 + \omega_1^2} = \Omega \qquad \frac{\Omega^2}{\omega_{\text{eff}}^2} = 1 \qquad \frac{\omega_1^2}{\omega_{\text{eff}}^2} = 0$$

$$\frac{\left(\Omega + \omega_{\text{eff}}\right)^2}{\omega_{\text{eff}}^2} = \frac{\left(\Omega + \Omega\right)^2}{\Omega^2} = 2^2 = 4 \qquad \frac{\left(\Omega - \omega_{\text{eff}}\right)^2}{\omega_{\text{eff}}^2} = \frac{\left(\Omega - \Omega\right)^2}{\Omega^2} = 0$$

Applying these to $T_{1\rho}$ gives:

$$\frac{1}{T_{1\rho}} = \frac{\gamma^2}{2} \left\langle B^2 \right\rangle 4J(\omega_{\text{rf}} + \omega_{\text{eff}}) = 2\gamma^2 \left\langle B^2 \right\rangle J(\omega_0 - \Omega + \Omega) = 2\gamma^2 \left\langle B^2 \right\rangle J(\omega_0) = \frac{1}{T_1}$$

Similarly for $T_{2\rho}$:

$$\frac{1}{T_{2\rho}} = \gamma^2 \langle B^2 \rangle J(0) + \frac{4\gamma^2}{4} \langle B^2 \rangle J(\omega_{\text{rf}} + \omega_{\text{eff}}) = \gamma^2 \langle B^2 \rangle J(0) + \gamma^2 \langle B^2 \rangle J(\omega_0 - \Omega + \Omega)$$
$$= \gamma^2 \langle B^2 \rangle (J(0) + J(\omega_0)) = \frac{1}{T_2}$$

Off-resonance plots

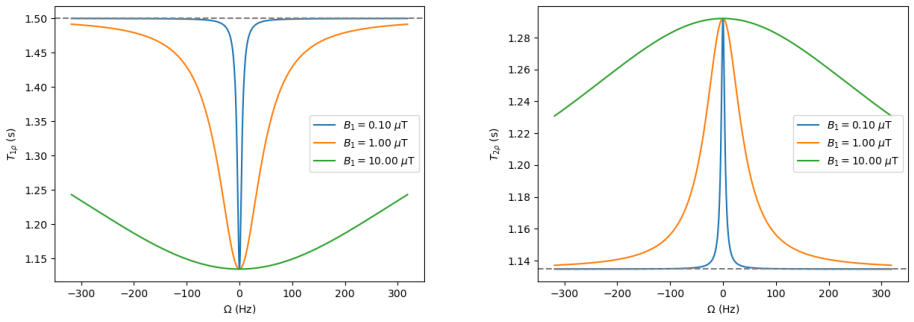

(a) $T_{1\rho}$ (b) $T_{2\rho}$

Figure 3.1: Plot of the $T_{1\rho}$ and $T_{2\rho}$ relaxation time versus the off-resonance Ω. The blue line represents a RF-field strength of $0.1\ \mu$T, the orange line $1\ \mu$T, and the green line $10\ \mu$T. The grey dashed line represents the limits of these values: T_1 for $T_{1\rho}$ and T_2 for $T_{2\rho}$.

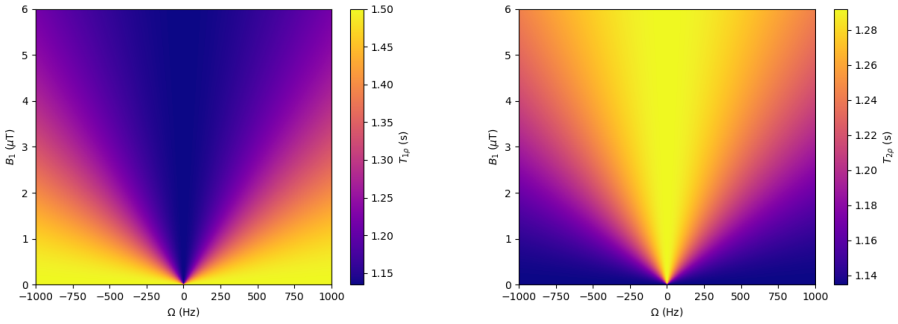

(a) $T_{1\rho}$ (b) $T_{2\rho}$

Figure 3.2: Plot of the $T_{1\rho}$ and $T_{2\rho}$ relaxation time versus the off-resonance Ω, and the RF-field strength B_1.

Figure 3.1 shows the relation between the off-resonance and the $T_{1\rho}$ relaxation time, for various RF amplitudes B_1. These plots are based on equation 27. $T_{1\rho}$ is minimal for on-resonance measurements, and increases to $T_1 = 1.5$ s for highly off-resonant measurements. The speed of this increase depends on B_1: the higher B_1, the less influence off-resonances have on the relaxation times. For the $T_{2\rho}$ relaxation time, from equation 28, something similar is observed. Instead of T_1, it approaches T_2 for high off-resonance. It also has a minimum instead of a maximum for on-resonance measurements.

Figure shows the $T_{1\rho}$ and $T_{2\rho}$ relaxation times for different combinations of off-resonance and B_1. It can still be seen that a higher B_1 leads to less influence due to off-resonance.

3.1.2. Amplitude- and Frequency Modulate pulses

Figure 3.3 shows the amplitude and frequency modulation functions of a hyperbolic secant pulse, given in equation 2.13. This pulse has parameters $\beta = 4$, a duration of 25 ms, an FM amplitude of 500 Hz, and an AM amplitude of $13.5\ \mu$T. The $T_{1\rho,\text{adiab}}$ relaxation times during this pulse are shown in figure 3.4. It was also assumed that the scanner had a main magnetic field $B_0 = 3$T and that the sample had

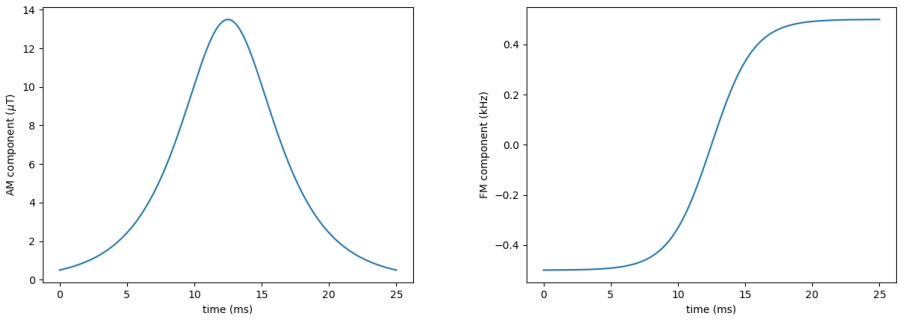

(a) Amplitude modulation (b) Frequency modulation

Figure 3.3: Plot of the shape of a hyperbolic secant pulse with $\beta = 4$, a duration of 25 ms, an FM amplitude of 500 Hz and an AM amplitude of 13.5 μT.

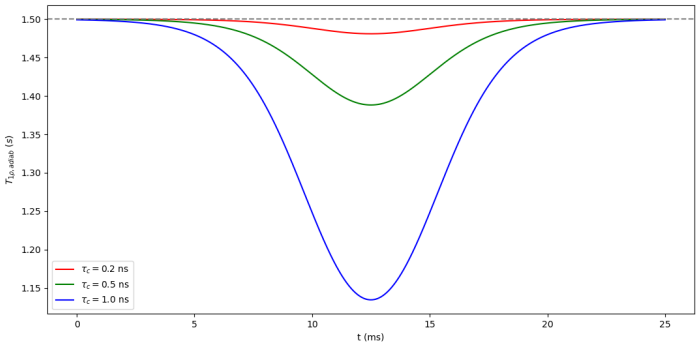

Figure 3.4: Figure showing the instantaneous relaxation times during the pulse shown in figure 3.3. A main field of 3 T and a T_1 relaxation time of 1.5ms was used. The red, green and blue lines correspond to a correlation time of 0.2, 0.5 and 1 ns respectively.

a relaxation time $T_1 = 1.5$s when no RF pulse was applied. This simulation was repeated for different random field correlation times τ_c, to simulate the effect of different samples being imaged.

3.2. Applications

3.2.1. Pulse Optimization

Figures 3.5a and b show the results of the Redfield and Bloch simulations for the different values of A and β. Interestingly, it can be seen that the RMS deviation due to off-resonance depends on the correlation time. The final z-magnetization does not depend on τ_c. This is because it was calculated using the Bloch equations, while τ_c is a parameter that is only present in the Redfield calculations.

The optimal solutions are shown in table 3.1. It can be seen that the addition of the Redfield method changes the pulse parameters significantly: β shifts by around 3.6, while A changes around 850 Hz.

			Redfield and Bloch		Bloch only	
τ_c (ns)	T_p (ms)	max B_1^+ (μT)	β_{opt} (a.u.)	A_{opt} (Hz)	β_{opt} (a.u.)	A_{opt} (Hz)
0.01	44.4	13.35	5.9	1472	9.5	615
0.1	44.4	13.35	5.9	1472	9.5	615
1.0	43.2	13.35	5.9	1522	9.3	564

Table 3.1: Optimal pulse parameters found by both methods. The pulse duration T_p and the maximum pulse amplitude B_1^+ were the result of the constraints on the optimization, and were the same for both methods. In all cases the optimization score was 1 (up to rounding error).

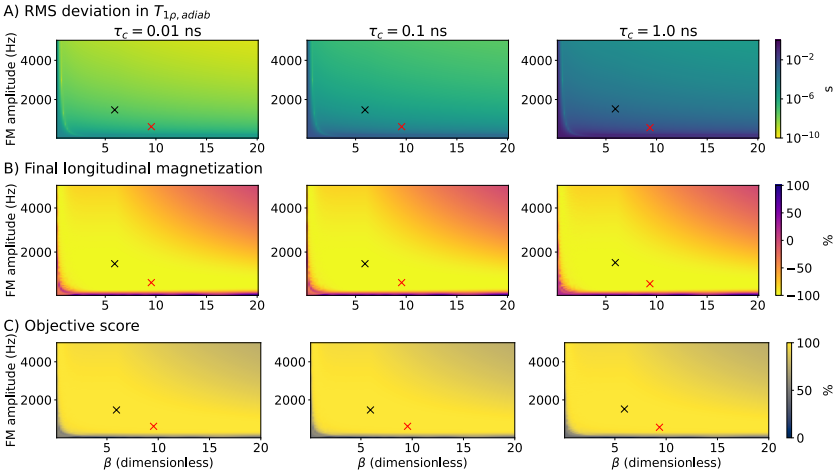

Figure 3.5: A collection of plots showing the different results used for the optimization. In all of these plots the black cross represents the optimal solution taking into account both criteria. The red cross is the optimal solution for Bloch simulations only. The columns show the results for different correlation times τ_c. A) Root-mean-square deviation of $T_{1\rho,\text{adiab}}$ for off-resonances $0, 50, \ldots, 200$ Hz. B) Final longitudinal magnetization after the Bloch simulations, given as a percentage of the original magnetization. C) Total objective score, normalized to give 100% at the highest score in this domain.

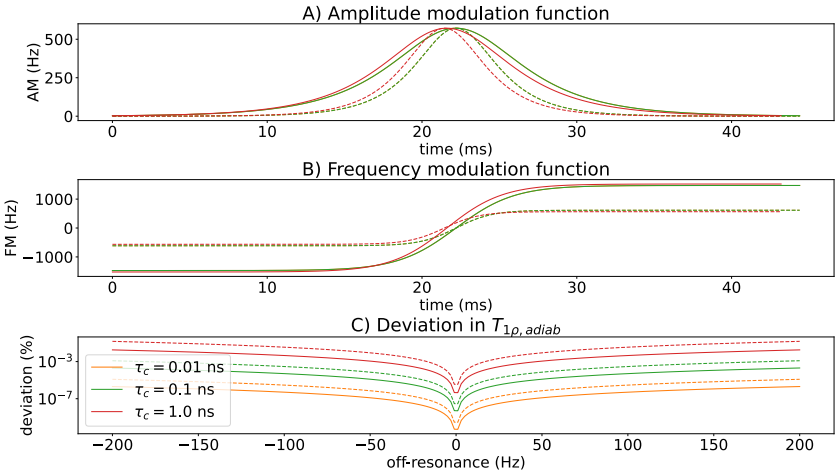

Figure 3.6: Plot of the optimal pulses found by the joint optimization (solid) and Bloch-only optimization (dotted lines). The orange, green and red lines represent correlation times of $0.01, 0.1$ and 1.0 ns. A) Amplitude modulation functions B) Frequency modulation functions C) Deviation in $T_{1\rho,\text{adiab}}$ for different off-resonance values.

All the pulses had a maximum B_1^+ amplitude of 13.35 μT, which was not the limit set in the constraint: $B_1^{max} \leq 13.43$ μT. Apparently the constraint on the root-mean-square B_1^+ was the limiting factor. Interestingly, $\tau_c = 0.01$ and 0.1 ns have identical results in this table, while $\tau_c = 1$ ns has different results for some parameters. Figure 3.6 show the pulses corresponding to these optimal values. The Bloch-only results (dotted lines) have a sharper peak in the AM function, and a smaller FM function than the result incorporating Redfield (solid line). The off-resonance always causes a larger deviation in the Bloch-only pulses than in the Bloch-and-Redfield pulses. The difference in RMS $T_{1\rho,\text{adiab}}$ deviation between the two optimization methods is 83% for $\tau_c = 0.01$ ns , 83% for $\tau_c = 0.1$ ns and 88% for $\tau_c = 1$ ns

Figure 3.7 shows a larger version of the final longitudinal magnetization on the optimization domain. Four different regions are marked, according to their (β, A) position, and their final magnetization. Representative magnetization evolutions in these regions are shown in figure 3.8. Region A is the adiabatic region: this has intermediate values for β and A, and a final magnetization that is around -1. In this region, the pulse moves slowly (in the first rotating frame) and the magnetization smoothly follows it. This is also shown in figure 3.8A: the magnetization changes smoothly and is fully inverted.

Region B corresponds to low FM amplitudes A, and a final magnetization that is higher than 0. Since

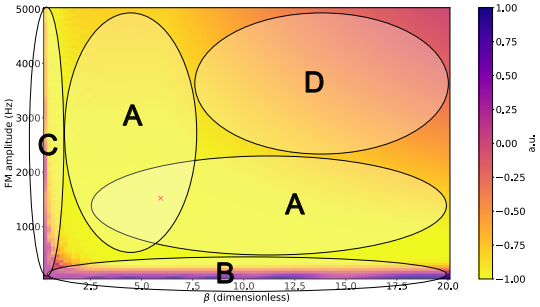

Figure 3.7: Final longitudinal magnetization on the optimization domain. The intial magnetization was 1. Four regions are marked: A) adiabatic, B) block-pulse-like, C) chirp-like and D) non-adiabatic.

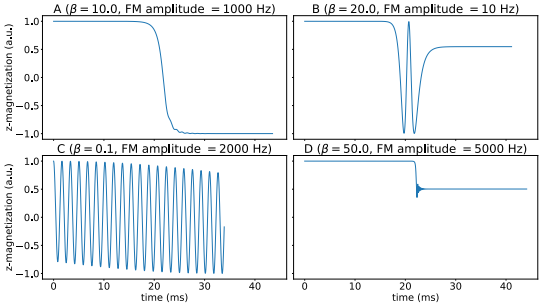

Figure 3.8: Representative examples of the longitudinal magnetization evolution for each of the domains in figure 3.7. The pulse durations differ between the figures due to the rescaling in the optimization algorithm.

the frequency modulation is so low, the B_1 field barely rotates around the z-axis. In that case the B_1 field behaves like the excitation pulse in a T_1 relaxation experiment: the field flips the magnetization by being perpendicularly oriented to it. This can also be seen in figure 3.8B: at $t = 20$ ms, the magnetization rotates quickly around the x-axis.

Region C corresponds to low β, so very broad pulses. Since the FM amplitude A is not empty, pulses in this region perform similarly to a chirp pulse. A chirp pulse has a constant AM function, and a linear FM function. These pulses cause the magnetization to oscillate rapidly [8]. This is also observed in figure 3.8C.

Finally, region D corresponds to high β, high A and a final magnetization that is between 0 and -0.75. Due to the high β, the AM function is a sharp peak, and the FM function also changes rapidly. The high A also causes the range of the FM function to be large. Combined, this means that the B_1 field due to this pulse moves rapidly, and the magnetization cannot follow it. This is also seen in figure 3.8D: at $t = 20$ms, the magnetization first follows the effective field. But this field moves too quickly, and the magnetization falls behind. This causes the final magnetization to not be fully inverted.

3.3. Experimental Validation

3.3.1. Off-Resonance Behaviour

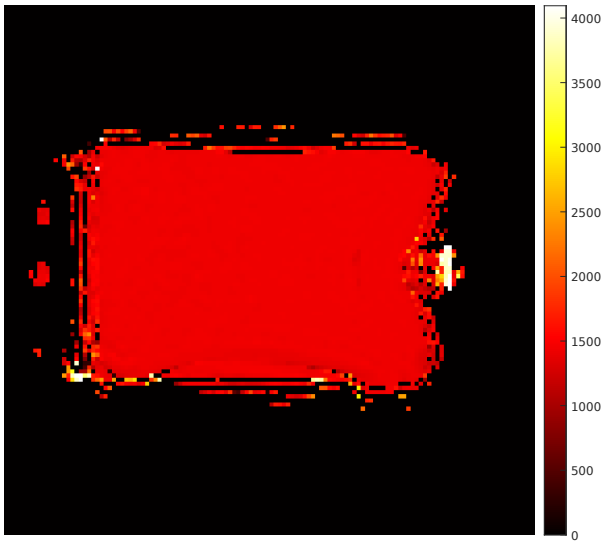

Figure 3.9: Map of the T_1 values inside the jar, reconstructed by the scanner. The scale is in milliseconds.

The T_1 map reconstructed by the scanner is shown in figure 3.9. The mean T_1 value inside the bottle is 1.464 s, with a standard deviation of 0.265 s. The results of our time-independent off-resonance

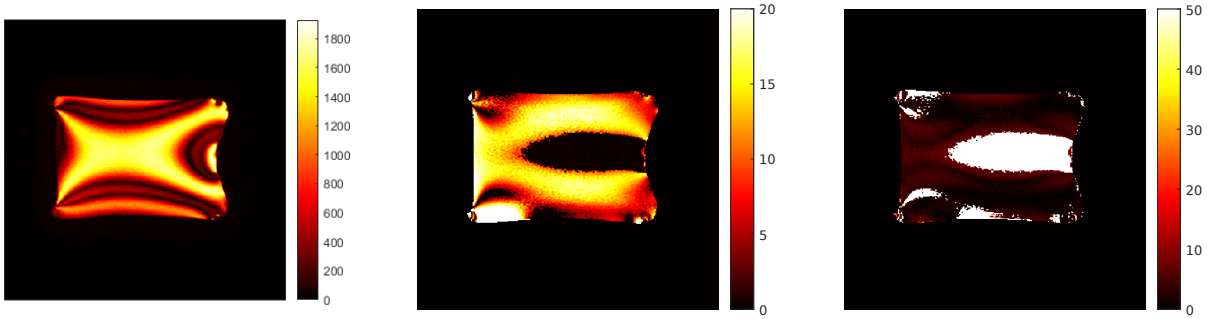

(a) Single image (b) $T_{1\rho}$ map (c) Standard deviation map (clipped at 50)

Figure 3.10: Examples of the artefacts seen during this experiment. A) shows the image obtained during a single dynamic scan. B) shows the calculated $T_{1\rho}$ map for the on-resonance scan. Values of $T_{1\rho}$ above 20 s were discarded, as these are physically infeasible. C) shows the standard deviation of the exponential fit (clipped at 50) for the on-resonance scan.

model, shown in figure 3.1, assumed $T_1 = 1.5$ s. They should therefore be a good fit for these experiments.

The individual images acquired during the $T_{1\rho}$ measurement show very strong artefacts. An example of this can be seen in figure 3.10a. Instead of an uniform signal throughout the bottle, strong "ripples" can be seen near the edges. Similar ripples can also be seen in the $T_{1\rho}$ maps (e.g. figure 3.10b). Furthermore, in the dark spots caused by these ripples, the standard deviation is high (as can be seen in figure 3.10c). Some pixels have values that are unphysical: relaxation times on the order of 10^5 s with standard deviations of up to 10^{61}. Normal relaxation times are of the order of microseconds to seconds. This could be the result of the artefacts changing the measured signal interfering with the exponential fit.

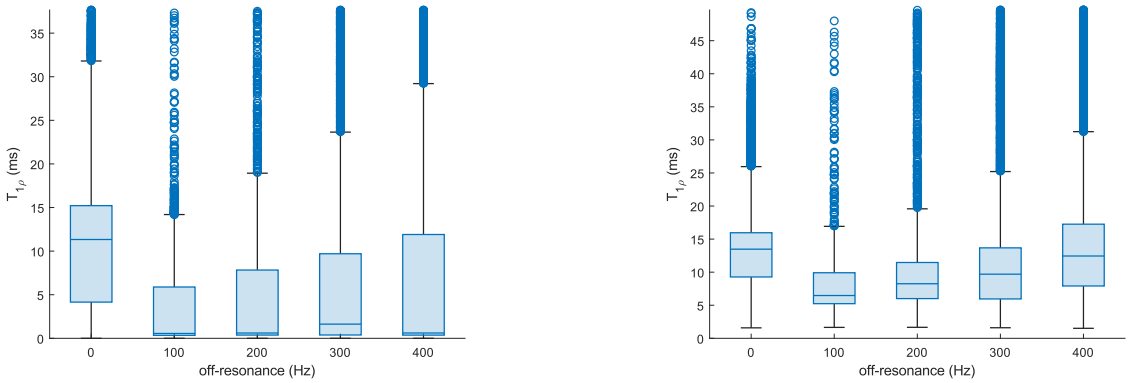

(a) Entire image (b) Pixels with fit STD < 10

Figure 3.11: Box plot of the $T_{1\rho}$ values found by the fitting, for different off-resonance frequencies. These plots are cropped to show the box and whiskers: not all outliers are visible. A) considers the entire image, while b) considers only the pixels where the fit had a standard deviation of < 100

Figure 3.11a shows a box plot of the distribution of $T_{1\rho}$ values throughout the maps, for each off-resonance frequency. It can be seen that the 0 Hz off-resonance values are significantly larger than those for the other measurements. The statistical mode of these $T_{1\rho}$ values is nearly constant, while the third quartile and higher values increase with the off-resonance. Outliers with $T_{1\rho}$ of up to 160 seconds are present in the data, but not shown in the plots as they would stretch the vertical axes too far.

Many pixels in the $T_{1\rho}$ maps had a very high standard deviation, which is an indication that the exponential fit was not accurate. Excluding the pixels with a standard deviation of 100 or more results in the box plot shown in figure 3.11b. In this figure, the 0 Hz off-resonance values are still larger than the other values. Additionally, there appears to be an upward trend of the $T_{1\rho}$ values with increasing off-resonance.

4

Discussion

The time-independent off-resonance Redfield calculations match earlier results. In the on-resonance limit, they agree with our on-resonance calculations. When the random field fluctuations are only aligned with the z-axis, they agree with the limits found in the ANZMAG lecture [16]. In the high off-resonance limit $\Omega \gg \omega_1$, we obtain $T_{1\rho} \to T_1$ and $T_{2\rho} \to T_2$. These results agree with our off-resonance plots (figure 3.1). They can also be explained by looking at the coordinate system (figure 2.1). If $\Omega \gg \omega_1$, then B'_{eff} is aligned with the z'-axis, and so our second rotating frame coincides with the first rotating frame.

The correlation time τ_c of the fluctuations can be a source of error. It is not directly measured in MRI experiments, so instead a reasonable estimate was used. These correlation times model the molecular motion of the sample, so they can be influenced by the molecular mass and the sample temperature.

For the Redfield calculations, it was assumed that relaxation is only the result of a randomly fluctuating field. This is an approximation: in reality the relaxation is the result of dipole-dipole interactions between protons. A more accurate model uses a Hamiltonian which directly models the dipole-dipole interaction. An example of such a model is given in section 4.4 of [14]. For imaging solid samples, such as actual patient tissues, chemical exchange also contributes to the relaxation. This can be modelled as an additional term in the Hamiltonian. These additions can lead to more accurate results, but also make the calculations involved much more complex.

The relaxation during amplitude- and frequency-modulated pulses was assumed to be quasistatic. This assumption allowed us to reuse the results for time-independent off-resonance. It does however neglect the effect that the time derivatives of the AM and FM functions could have on the relaxation. Since this project involves adiabatic pulses, where these derivatives are required to be small anyway, this assumption is valid. However this assumption could hinder the extension of our results to non-adiabatic pulses.

The size of the effects ignored by the quasi-static assumption could be estimated by a calculation. In this calculation Redfield theory is applied to an AM function that is linear with a slope α. The FM function is held constant. Comparing the exact Redfield result to the result obtained with the quasistatic approximation reveals the effect size. Alternatively, the effect could be estimated by comparing the qausi-static result with a real measurement on an MRI scanner. We recommend these investigations for further research.

Further research could also investigate the relaxation times for other pulse shapes. With the quasistatic assumption, these calculations can be done by substituting different AM and FM functions in the finite difference algorithm. No additional derivations are necessary.

In the pulse optimization results, it was seen that the RMS $T_{1\rho,\text{adiab}}$ deviation due to off-resonance strongly depended on the correlation times τ_c. This can be explained by the fact that the power spectrum $J(\omega)$ of the fluctuations (equation 25) depends on τ_c. The off-resonance causes a change in ω_{rf}

and ω_{eff}, which are substituted into $J(\omega)$ in equation 27.

The relative difference in RMS $T_{1\rho,\text{adiab}}$ deviation due to off-resonance is big $(83,83,88\%)$. In absolute value, however, the effect of off-resonance on $T_{1\rho}$ is very small. It is never more than 0.15% compared to on-resonance (for the optimal pulse found using only Bloch simulations, and $\tau_c = 1$ ns). For $\tau_c = 0.01$ ns, the effect is never larger than $1.2 \cdot 10^{-5}\%$. This can be explained by the fact that the hyperbolic secant pulses used for this optimization are designed to be resistant to off-resonance effects. They appear to retain this property even at suboptimal pulse parameters. Further research could investigate if this optimization provides more substantial gains in off-resonance resiliency for different pulse shapes. Further research could also perform MRI measurements for different pulse parameters, to verify that the solutions found by the algorithm are also optimally resistant to off-resonance in real life.

Interestingly, the optimal pulse parameters for the $\tau_c = 0.01$ and 0.1 ns case were identical. Perhaps the pulse parameters approach a limit for rapid correlation times. Further research could investigate the whether optimization results for $\tau_c = 0.001$ and 0.0001 ns also give these same optimal parameters.

The experimental validation of the off-resonance behaviour was hindered by artefacts. The scan of the jar shows “ripples” of high and low signal values, while the homogeneous liquid should give the same signal everywhere. These artefacts could have been caused by the difference in susceptibility between the bottle and the surrounding air. This difference causes variations in the B_0 and B_1 field amplitude, which in turn cause artefacts.

One method by which this occurs is dephasing. In dephasing, differences in B_0 inside the sample leads the magnetizations to precess at different rates. This causes them to acquire a phase difference, which eventually causes T_2 decay of the magnetization. A solution to this problem would be to change the pulse shape to have a refocusing pulse. The simplest option would be to invert the latter half of the prepulse shown in figure 2.3. This would change the direction of the precession in the latter half of the pulse. This causes an extra phase difference that compensates the difference due to dephasing. Another possibility is that the inhomogeneities in the B_0 and B_1 fields cause spurious precession, which leads to these artefacts [17].

Since the received signal is altered by the artefacts, the exponential fit often does not give correct results. This explains the outliers with unfeasibly high $T_{1\rho}$ values, and the high fit standard deviation values. Taking only the pixels were the standard deviation was less than 100 ensures that the exponential fit was accurate. However, from the theoretical results (such as figure 3.1) we would expect the $T_{1\rho}$ values to be between 1 second and $T_1 = 1.5$ s. In reality the values are in the 0 to 25 ms range. This suggests that even though the exponential functions fit the measured data closely, they do not correctly give the underlying $T_{1\rho}$ value. Alternatively, the theoretical derivation could be invalid for the relatively short pulses used in the experiment. The results appear to give the correct qualitative behaviour (increasing $T_{1\rho}$ for increasing off-resonance) but the actual values are not reliable.

The 0 Hz off-resonance measurements also did not follow this qualitative behaviour. Perhaps this is caused by the FM function being zero at the middle part of the pulse. Further research should try to compare the 0 Hz results with results for a similarly small off-resonance, such as 0.01 Hz.

Finally, the application of these methods to clinical practice requires further investigation. More realistic phantom studies (e.g. on body-shaped phantoms made out of ballistic gelatin) and patient studies are required to evaluate the practical gain in contrast caused by these optimized pulses. If these give positive results, further research could investigate if this contrast gain results in more accurate diagnoses.

5

Conclusion

The aim of this project was to use Redfield theory to create a pulse optimization framework that can take dispersion into account. The theoretical calculation for time-independent off-resonance agrees with limits found in the literature. In order to simulate amplitude- and frequency modulated pulses it is necessary to assume quasistatic relaxation. This approximation appears to be valid for adiabatic pulses, but further experiments should be carried out to validate this. All the calculations assumed that relaxation was only due to a randomly fluctuating field. More accurate models directly consider a dipole-dipole Hamiltonian, or consider chemical exchange as well. These would, however, be more complex computationally.

A joint optimization using Bloch and Redfield simulations performs better than using Bloch simulations only. These result in a 83%, 83%, 88% improved resilience to off-resonance for $\tau_c = 0.01$, 0.1, 1 ns correlation times. The absolute value of off-resonance effects is small, however, as it is at most 0.15% RMS deviation. Perhaps different pulse shapes would benefit more from this optimization algorithm.

Experimental validation of the off-resonance behaviour encountered serious difficulties due to artefacts in the images. Further research using refocusing pulses should be able to bypass these problems. As it stands, the measurements seem to confirm the qualitative behaviour. The actual relaxation times, however, do not match theoretical calculations.

Overall, the joint Bloch and Redfield optimization method is able to take dispersion into account. It is able to provide better off-resonance resiliency than methods that neglect dispersion, but further research is necessary to obtain results that can improve MR imaging in practice.

Appendix A: Derivation of the Fictitious Field in the First Rotating Frame

In this appendix, we will calculate the fictitious magnetic field term that appears in the first rotating frame due to an off-resonant RF pulse. First, we calculate the effect moving to the first rotating frame has on the Hamiltonian. Afterwards, we fill in the Hamiltonian term that is already present due to the main magnetic field, and finally recognize the effective magnetic field.

For this first step we move to a frame rotating by $\omega_{\mathrm{rf}}t$ around the $\hat{z}$-axis. This has two effects:

1. The Hamiltonian needs to be rewritten in terms of the new reference frame (analogous to rewriting $\hat{x}, \hat{y}, \hat{z}$ to $\hat{x}', \hat{y}', \hat{z}'$)
2. Extra fictitious terms appear in the Hamiltonian (analogous to the Coriolis force, or the extra magnetic field in the Bloch equations.)

In this derivation we use the *density operator formalism*. This makes use of a density matrix (or density operator) $\hat{\rho}$ as an analogue to the wavefunction $|\Psi\rangle$ used in quantum mechanics. Superoperators $\hat{\hat{A}}$ are analogous to operators. Density operators evolve according to the Liouville-von Neumann equation:

$$\frac{\partial}{\partial t}\hat{\rho} = -i\hat{\hat{H}}\hat{\rho} \tag{1}$$

Our rotation is given by:

$$\hat{\rho}' = e^{-i\omega_{\mathrm{rf}}t\hat{\hat{I}}_z}\hat{\rho} \tag{2}$$

This follows from the Taylor series of infinitesimal rotations. Branson derives it in two dimensions, but it is true in general [18].

Now we use this to see:

$$\begin{aligned}\frac{\partial}{\partial t}\hat{\rho}' &= \frac{\partial}{\partial t}\left(e^{-i\omega_{\mathrm{rf}}t\hat{\hat{I}}_z}\right)\hat{\rho} + e^{-i\omega_{\mathrm{rf}}t\hat{\hat{I}}_z}\frac{\partial}{\partial t}\hat{\rho} \\ &= -i\omega_{\mathrm{rf}}\hat{\hat{I}}_z e^{-i\omega_{\mathrm{rf}}t\hat{\hat{I}}_z}\hat{\rho} + e^{-i\omega_{\mathrm{rf}}t\hat{\hat{I}}_z}\frac{\partial}{\partial t}\hat{\rho}\end{aligned}$$

Recognising $\hat{\rho}'$, and filling in equation 6 gives:

$$\begin{aligned}\frac{\partial}{\partial t}\hat{\rho}' &= -i\omega_{\mathrm{rf}}\hat{\hat{I}}_z\hat{\rho}' + e^{-i\omega_{\mathrm{rf}}t\hat{\hat{I}}_z}\left(-i\hat{\hat{H}}\hat{\rho}\right) \\ &= -i\left(\omega_{\mathrm{rf}}\hat{\hat{I}}_z\hat{\rho}' + e^{-i\omega_{\mathrm{rf}}t\hat{\hat{I}}_z}\hat{\hat{H}}\hat{\rho}\right)\end{aligned}$$

Now since $\hat{\hat{I}}_z$ is Hermitian, $e^{+i\omega_{\mathrm{rf}}t\hat{\hat{I}}_z}e^{-i\omega_{\mathrm{rf}}t\hat{\hat{I}}_z} = 1$. This allows us to write:

$$\begin{aligned}\frac{\partial}{\partial t}\hat{\rho}' &= -i\left(\omega_{\mathrm{rf}}\hat{\hat{I}}_z\hat{\rho}' + e^{-i\omega_{\mathrm{rf}}t\hat{\hat{I}}_z}\hat{\hat{H}}e^{+i\omega_{\mathrm{rf}}t\hat{\hat{I}}_z}e^{-i\omega_{\mathrm{rf}}t\hat{\hat{I}}_z}\hat{\rho}\right) \\ &= -i\left(\omega_{\mathrm{rf}}\hat{\hat{I}}_z + e^{-i\omega_{\mathrm{rf}}t\hat{\hat{I}}_z}\hat{\hat{H}}e^{+i\omega_{\mathrm{rf}}t\hat{\hat{I}}_z}\right)\hat{\rho}'\end{aligned}$$

This is again in the form of equation 6, with an *effective Hamiltonian*:

$$\hat{\hat{H}}_{\mathrm{eff}} = \omega_{\mathrm{rf}}\hat{\hat{I}}_z + e^{-i\omega_{\mathrm{rf}}t\hat{\hat{I}}_z}\hat{\hat{H}}e^{+i\omega_{\mathrm{rf}}t\hat{\hat{I}}_z} \tag{3}$$

The first term here is the fictitious term due to the rotation.

The main magnetic field causes a term $-\gamma B_0 \hat{\hat{I}}_z = -\omega_0 \hat{\hat{I}}_z$ in the Hamiltonian. This gives a total Hamiltonian of:

$$\begin{aligned}\hat{\hat{H}}_{\text{eff}} &= \omega_{\text{rf}} \hat{\hat{I}}_z - \omega_0 e^{-i\omega_{\text{rf}} t \hat{\hat{I}}_z} \hat{\hat{I}}_z e^{+i\omega_{\text{rf}} t \hat{\hat{I}}_z} \\ &= \omega_{\text{rf}} \hat{\hat{I}}_{z'} - \omega_0 \hat{\hat{I}}_{z'} = -(\omega_0 - \omega_{\text{rf}}) \hat{\hat{I}}_{z'} \\ &= -\Omega \hat{\hat{I}}_{z'}\end{aligned}$$

And since the Hamiltonian due to a magnetic field $\boldsymbol{B}$ is given by $-\gamma \boldsymbol{B} \cdot \hat{\boldsymbol{I}}$, I see that the corresponding magnetic field is

$$\boldsymbol{B}_{\text{fict}} = \frac{\omega_0 - \omega_{\text{rf}}}{\gamma} \hat{z} = \frac{\Omega}{\gamma} \hat{z}$$

Indeed we also see here for an on-resonance excitation $\omega_0 = \omega_{\text{rf}}$ there will be no term due to B_0: all the movement of the magnetization will be due to the B_1 field.

Appendix B: Derivation of the Relaxation Times for On-Resonance Excitation

Introduction and Methods

The derivation of $T_{1\rho}$ consists of four steps:

1. Formulating the Hamiltonian
2. Transferring it to the doubly rotating frame
3. Calculating the relaxation superoperator
4. Taking the inner product to calculate the relaxation time

$T_{1\rho}$ is the result of relaxation in the presence of a radiofrequency field. In the presence of this rf-field, we must use the doubly rotating frame to align the effective magnetic field to the z-axis. This simplifies the final calculation of the relaxation rates.

We assume the relaxation is the result of a fluctuating magnetic field. The final relaxation time is given as a function of the power spectrum of these fluctuations. This gives us an idea of the dependence of $T_{1\rho}$ on molecular vibrations. A more accurate model replaces these fields by an actual dipole-dipole interaction.

Deriving the Hamiltonian

In order to calculate $T_{1\rho}$, we must find a model that describes the behaviour of protons in an MRI scanner. Since protons are spin-half particles, they behave as magnetic dipoles. In a magnetic field $\boldsymbol{B}$, they have potential energy given by:

$$E = -\boldsymbol{\mu} \cdot \boldsymbol{B}(t)$$

The dipole moment is given by the spin operators $\hat{I}_x$, $\hat{I}_y$, $\hat{I}_z$:

$$\hat{\mu}_{x,y,z} = \gamma\hbar\hat{I}_{x,y,z}$$

This leads to the following Hamiltonian:

$$\begin{aligned}\hat{H} = \frac{\hat{E}}{\hbar} &= \frac{-\hat{\mu}_x B_x(t) - \hat{\mu}_y B_y(t) - \hat{\mu}_z B_z(t)}{\hbar} \\ &= \frac{-\gamma\hbar\left(\hat{I}_x B_x(t) + \hat{I}_y B_y(t) + \hat{I}_z B_z(t)\right)}{\hbar} \\ &= -\gamma\left(\hat{I}_x B_x(t) + \hat{I}_y B_y(t) + \hat{I}_z B_z(t)\right)\end{aligned} \tag{4}$$

Now we consider three magnetic fields: the main magnetic field $\boldsymbol{B_0}$, a on-resonance spin-lock pulse $\boldsymbol{B_1}$ and random fluctuations $\boldsymbol{\Delta B}$ that cause the relaxation:

$$\begin{aligned}\boldsymbol{B_0} &= B_0\hat{z} \\ \boldsymbol{B_1} &= B_1\left(\cos(\omega_0 t)\hat{x} - \sin(\omega_0 t)\hat{y}\right) \\ \boldsymbol{\Delta B} &= \Delta B_x(t)\hat{x} + \Delta B_y(t)\hat{y} + \Delta B_z(t)\hat{z}\end{aligned}$$

We assume the fluctuations are small: $\Delta B \ll B_0$. Substituting these fields into equation 4 gives:

$$\hat{H} = -\gamma B_0\hat{I}_z - \gamma B_1\left(\cos(\omega_0 t)\hat{I}_x - \sin(\omega_0 t)\hat{I}_y\right) - \gamma\Delta B_z(t)\hat{I}_z - \gamma\Delta B_x(t)\hat{I}_x - \gamma\Delta B_y(t)\hat{I}_y$$

Rearranging terms, and using the Larmor frequencies $\omega_0 = \gamma B_0$, $\omega_1 = \gamma B_1$:

$$\hat{H} = -\omega_0\hat{I}_z - \omega_1\left(\cos(\omega_0 t)\hat{I}_x - \sin(\omega_0 t)\hat{I}_y\right) - \gamma\Delta B_z(t)\hat{I}_z - \gamma\Delta B_x(t)\hat{I}_x - \gamma\Delta B_y(t)\hat{I}_y \tag{5}$$

The First Rotating Frame

First, we move to a frame rotating by $\omega_0 t$ around the $\hat{z}$-axis. This has two effects:

1. The Hamiltonian needs to be rewritten in terms of the new reference frame (analogous to rewriting $\hat{x}, \hat{y}, \hat{z}$ to $\hat{x}', \hat{y}', \hat{z}'$)
2. Extra fictitious terms appear in the Hamiltonian (analogous to the Coriolis force, or the extra magnetic field in the Bloch equations.)

In this derivation we use the *density operator formalism*. This makes use of a density matrix (or density operator) $\hat{\rho}$ as an analogue to the wavefunction $|\Psi\rangle$. Superoperators $\hat{\hat{A}}$ are analogous to operators. Density operators evolve according to the Liouville-von Neumann equation:

$$\frac{\partial}{\partial t}\hat{\rho} = -i\hat{\hat{H}}\hat{\rho} \tag{6}$$

Our rotation is given by:

$$\hat{\rho}' = e^{-i\omega_0 t\hat{\hat{I}}_z}\hat{\rho} \tag{7}$$

This follows from the Taylor series of infinitesimal rotations. Branson derives it in two dimensions, but it is true in general [18].

Now we use this to see:

$$\begin{aligned}\frac{\partial}{\partial t}\hat{\rho}' &= \frac{\partial}{\partial t}\left(e^{-i\omega_0 t\hat{\hat{I}}_z}\right)\hat{\rho} + e^{-i\omega_0 t\hat{\hat{I}}_z}\frac{\partial}{\partial t}\hat{\rho} \\ &= -i\omega_0\hat{\hat{I}}_z e^{-i\omega_0 t\hat{\hat{I}}_z}\hat{\rho} + e^{-i\omega_0 t\hat{\hat{I}}_z}\frac{\partial}{\partial t}\hat{\rho}\end{aligned}$$

Recognising $\hat{\rho}'$, and filling in equation 6 gives:

$$\begin{aligned}\frac{\partial}{\partial t}\hat{\rho}' &= -i\omega_0\hat{\hat{I}}_z\hat{\rho}' + e^{-i\omega_0 t\hat{\hat{I}}_z}\left(-i\hat{\hat{H}}\hat{\rho}\right) \\ &= -i\left(\omega_0\hat{\hat{I}}_z\hat{\rho}' + e^{-i\omega_0 t\hat{\hat{I}}_z}\hat{\hat{H}}\hat{\rho}\right)\end{aligned}$$

Now since $\hat{\hat{I}}_z$ is Hermitian, $e^{+i\omega_0 t\hat{\hat{I}}_z}e^{-i\omega_0 t\hat{\hat{I}}_z} = 1$. This allows us to write:

$$\begin{aligned}\frac{\partial}{\partial t}\hat{\rho}' &= -i\left(\omega_0\hat{\hat{I}}_z\hat{\rho}' + e^{-i\omega_0 t\hat{\hat{I}}_z}\hat{\hat{H}}e^{+i\omega_0 t\hat{\hat{I}}_z}e^{-i\omega_0 t\hat{\hat{I}}_z}\hat{\rho}\right) \\ &= -i\left(\omega_0\hat{\hat{I}}_z + e^{-i\omega_0 t\hat{\hat{I}}_z}\hat{\hat{H}}e^{+i\omega_0 t\hat{\hat{I}}_z}\right)\hat{\rho}'\end{aligned}$$

This is again in the form of equation 6, with an *effective Hamiltonian*:

$$\hat{H}_{\text{eff}} = \omega_0\hat{I}_z + e^{-i\omega_0 t\hat{I}_z}\hat{H}e^{+i\omega_0 t\hat{I}_z} \tag{8}$$

The first term here is the fictitious term due to the rotation.

The second term changes the basis of the original Hamiltonian to the rotating frame. It is also written with the rotation superoperator: $\hat{\hat{R}}_{-\omega_0 t\hat{I}_z}\hat{H}$. Since this is a rotation around the $\hat{z}$-axis, we can see that:

$$\begin{aligned}\hat{\hat{R}}_{-\omega_0 t\hat{I}_z}\hat{I}_x &= e^{-i\omega_0 t\hat{I}_z}\hat{I}_x e^{i\omega_0 t\hat{I}_z} = \hat{I}_{x'}\cos(\omega_0 t) + \hat{I}_{y'}\sin(\omega_0 t) \\ \hat{\hat{R}}_{-\omega_0 t\hat{I}_z}\hat{I}_y &= e^{-i\omega_0 t\hat{I}_z}\hat{I}_y e^{i\omega_0 t\hat{I}_z} = \hat{I}_{y'}\cos(\omega_0 t) - \hat{I}_{x'}\sin(\omega_0 t) \\ \hat{\hat{R}}_{-\omega_0 t\hat{I}_z}\hat{I}_z &= e^{-i\omega_0 t\hat{I}_z}\hat{I}_z e^{i\omega_0 t\hat{I}_z} = \hat{I}_{z'}\end{aligned} \tag{9}$$

This can also formally be proven by using the Taylor series of the exponential, and the fact that the spin operators cyclically commute [19]. $\hat{I}_{x'}, \hat{I}_{y'}$ and $\hat{I}_{z'}$ are the spin operators in the rotating reference frame.

Using these expressions we can fill in equation 5 and get:

$$\begin{aligned}\hat{H}_{\text{rot}} &= \hat{\hat{R}}_{-\omega_0 t\hat{I}_z}\hat{H} = -\omega_0\hat{I}_{z'} - \gamma\Delta B_z(t)\hat{I}_{z'} - \omega_1\cos(\omega_0 t)\hat{\hat{R}}_{-\omega_0 t\hat{I}_z}\hat{I}_x \\ &\quad + \omega_1\sin(\omega_0 t)\hat{\hat{R}}_{-\omega_0 t\hat{I}_z}\hat{I}_y - \gamma\hat{\hat{R}}_{-\omega_0 t\hat{I}_z}\left(\Delta B_x(t)\hat{I}_x + \Delta B_y(t)\hat{I}_y\right) \\ &= -\omega_0\hat{I}_{z'} - \gamma\Delta B_z(t)\hat{I}_{z'} - \omega_1\cos(\omega_0 t)\left(\hat{I}_{x'}\cos(\omega_0 t) + \hat{I}_{y'}\sin(\omega_0 t)\right) \\ &\quad + \omega_1\sin(\omega_0 t)\left(\hat{I}_{y'}\cos(\omega_0 t) - \hat{I}_{x'}\sin(\omega_0 t)\right) - \gamma\hat{\hat{R}}_{-\omega_0 t\hat{I}_z}\left(\Delta B_x(t)\hat{I}_x + \Delta B_y(t)\hat{I}_y\right) \\ &= -\omega_0\hat{I}_{z'} - \gamma\Delta B_z(t)\hat{I}_{z'} + \hat{I}_{x'}\left(-\omega_1\cos^2(\omega_0 t) - \omega_1\sin^2(\omega_0 t)\right) \\ &\quad - \gamma\hat{\hat{R}}_{-\omega_0 t\hat{I}_z}\left(\Delta B_x(t)\hat{I}_x + \Delta B_y(t)\hat{I}_y\right) \\ &= -\omega_0\hat{I}_{z'} - \gamma\Delta B_z(t)\hat{I}_{z'} - \omega_1\hat{I}_{x'} - \gamma\hat{\hat{R}}_{-\omega_0 t\hat{I}_z}\left(\Delta B_x(t)\hat{I}_x + \Delta B_y(t)\hat{I}_y\right)\end{aligned}$$

Finally we must add the fictitious term derived in equation 8:

$$\begin{aligned}\hat{H}_{\text{eff}} &= \omega_0\hat{I}_z + \hat{H}_{\text{rot}} = \omega_0\hat{I}_{z'} + \hat{H}_{\text{rot}} \\ &= -\gamma\Delta B_z(t)\hat{I}_{z'} - \omega_1\hat{I}_{x'} - \gamma\hat{\hat{R}}_{-\omega_0 t\hat{I}_z}\left(\Delta B_x(t)\hat{I}_x + \Delta B_y(t)\hat{I}_y\right)\end{aligned}$$

In order to simplify the last term, we make use of the spin raising and lowering operators:

$$\hat{I}_+ = \hat{I}_x + i\hat{I}_y \quad \text{and} \quad \hat{I}_- = \hat{I}_x - i\hat{I}_y$$

These are the eigenoperators of this rotation (shown in the appendix):

$$\begin{aligned}\hat{\hat{R}}_{-\omega_0 t\hat{I}_z}\hat{I}_+ &= e^{-i\omega_0 t\hat{I}_z}\hat{I}_+ e^{i\omega_0 t\hat{I}_z} = e^{-i\omega_0 t}\hat{I}_+ \\ \hat{\hat{R}}_{-\omega_0 t\hat{I}_z}\hat{I}_- &= e^{-i\omega_0 t\hat{I}_z}\hat{I}_- e^{i\omega_0 t\hat{I}_z} = e^{i\omega_0 t}\hat{I}_-\end{aligned}$$

In other words, $\hat{I}'_\pm = I_\pm$, and we only get a prefactor. Now since:

$$\hat{I}_x = \frac{1}{2}\left(\hat{I}_+ + \hat{I}_-\right) \quad \text{and} \quad \hat{I}_y = \frac{1}{2i}\left(\hat{I}_+ - \hat{I}_-\right)$$

we can write:

$$\begin{aligned}\hat{H}_{\text{eff}} &= -\gamma\Delta B_z(t)\hat{I}_{z'} - \omega_1\hat{I}_{x'} - \frac{\gamma}{2}\hat{\hat{R}}_{-\omega_0 t\hat{I}_z}\left(\Delta B_x(t)\left(\hat{I}_+ + \hat{I}_-\right) - i\Delta B_y(t)\left(\hat{I}_+ - \hat{I}_-\right)\right) \\ &= -\gamma\Delta B_z(t)\hat{I}_{z'} - \omega_1\hat{I}_{x'} - \frac{\gamma}{2}\hat{\hat{R}}_{-\omega_0 t\hat{I}_z}\hat{I}_+\left(\Delta B_x(t) - i\Delta B_y(t)\right) \\ &\quad - \frac{\gamma}{2}\hat{\hat{R}}_{-\omega_0 t\hat{I}_z}\hat{I}_-\left(\Delta B_x(t) + i\Delta B_y(t)\right) \\ &= -\gamma\Delta B_z(t)\hat{I}_{z'} - \omega_1\hat{I}_{x'} - \frac{\gamma}{2}e^{-i\omega_0 t}\hat{I}_+\left(\Delta B_x(t) - i\Delta B_y(t)\right) - \frac{\gamma}{2}e^{i\omega_0 t}\hat{I}_-\left(\Delta B_x(t) + i\Delta B_y(t)\right)\end{aligned}$$

The Second Rotating Frame

We now have a situation that is very similar to relaxation in the lab frame: a large term $\hat{H}'_0 = -\omega_1\hat{I}_{x'}$ that is constant in time, and smaller terms that change in time. This motivates us to move to a second rotating frame, where we only retain the time-varying component.
This frame rotates with angular velocity $-\omega_1$ around the $\hat{x}'$ axis, and is also called the interaction frame. A similar derivation as equation 8 gives:

$$\begin{aligned}\hat{H}'_{\text{eff}} &= \omega_1\hat{I}_{x'} + e^{-i\omega_1 t\hat{I}_{x'}}\hat{H}_{\text{eff}}e^{+i\omega_1 t\hat{I}_{x'}} = \omega_1\hat{I}_{x'} + \hat{\hat{R}}_{-\omega_1 t\hat{I}_{x'}}\hat{H}_{\text{eff}} \\ &= \omega_1\hat{I}_{x'} + \hat{H}'_{\text{rot}}\end{aligned} \tag{10}$$

Now we can calculate $\hat{H}'_{\mathrm{rot}}$:

$$\hat{H}'_{\mathrm{rot}} = \hat{\hat{R}}_{-\omega_1 t\hat{I}_{x'}}\Big(-\gamma\Delta B_z(t)\hat{I}_{z'} - \omega_1\hat{\hat{R}}_{-\omega_1 t\hat{I}_{x'}}\hat{I}_{x'} - \frac{\gamma}{2}e^{-i\omega_0 t}\hat{I}_+\left(\Delta B_x(t) - i\Delta B_y(t)\right) - \frac{\gamma}{2}e^{i\omega_0 t}\hat{I}_-\left(\Delta B_x(t) + i\Delta B_y(t)\right)\Big)$$

To find these rotations, it is convenient to do a coordinate substitution:

$$\tilde{x} = y' \qquad \tilde{y} = z' \qquad \tilde{z} = x'$$

Then our rotation is now along the $\tilde{z}$-axis. Note that in general, if the rf-pulse is off-resonant, the static component is not along one of the (x', y', z') axes. Then the $(\tilde{x}, \tilde{y}, \tilde{z})$ coordinate system must be tilted with respect to the (x', y', z') system. Then there is no such simple substitution.

Continuing on, we can now use the raising and lowering operators:

$$\begin{aligned}\hat{I}_{\tilde{z}} &= \hat{I}_{x'}\\ \hat{I}_{\tilde{+}} &= \hat{I}_{\tilde{x}} + i\hat{I}_{\tilde{y}} = \hat{I}_{y'} + i\hat{I}_{z'}\\ \hat{I}_{\tilde{-}} &= \hat{I}_{\tilde{x}} - i\hat{I}_{\tilde{y}} = \hat{I}_{y'} - i\hat{I}_{z'}\end{aligned}$$

These are the eigenoperators of this rotation:

$$\begin{aligned}\hat{\hat{R}}_{-\omega_1 t\hat{I}_{\tilde{z}}}\hat{I}_{\tilde{z}} &= \hat{I}_{\tilde{z}}\\ \hat{\hat{R}}_{-\omega_1 t\hat{I}_{\tilde{z}}}\hat{I}_{\tilde{+}} &= e^{-i\omega_1 t}\hat{I}_{\tilde{+}}\\ \hat{\hat{R}}_{-\omega_1 t\hat{I}_{\tilde{z}}}\hat{I}_{\tilde{-}} &= e^{i\omega_1 t}\hat{I}_{\tilde{-}}\end{aligned} \tag{11}$$

And also of $\hat{\hat{H}}_0{}' = -\omega_1\hat{\hat{I}}_{x'} = -\omega_1\hat{\hat{I}}_{\tilde{z}}$:

$$\begin{aligned}\hat{\hat{H}}_0{}'\hat{I}_{\tilde{z}} &= 0\cdot\hat{I}_{\tilde{z}}\\ \hat{\hat{H}}_0{}'\hat{I}_{\tilde{+}} &= -\omega_1\hat{I}_{\tilde{+}}\\ \hat{\hat{H}}_0{}'\hat{I}_{\tilde{-}} &= \omega_1\hat{I}_{\tilde{-}}\end{aligned} \tag{12}$$

Now with a little rewriting we can get

$$\begin{aligned}\hat{I}_{x'} &= \hat{I}_{\tilde{z}} \qquad \hat{I}_{y'} = \frac{1}{2}\left(\hat{I}_{\tilde{+}} + \hat{I}_{\tilde{-}}\right) \qquad \hat{I}_{z'} = \frac{1}{2i}\left(\hat{I}_{\tilde{+}} - \hat{I}_{\tilde{-}}\right)\\ \hat{I}_+ &= \hat{I}_{x'} + i\hat{I}_{y'} = \hat{I}_{\tilde{z}} + \frac{i}{2}\left(\hat{I}_{\tilde{+}} + \hat{I}_{\tilde{-}}\right)\\ \hat{I}_- &= \hat{I}_{x'} - i\hat{I}_{y'} = \hat{I}_{\tilde{z}} - \frac{i}{2}\left(\hat{I}_{\tilde{+}} + \hat{I}_{\tilde{-}}\right)\end{aligned}$$

Filling this in, we get:

$$\hat{H}'_{\mathrm{rot}} = \hat{\hat{R}}_{-\omega_1 t\hat{I}_{\tilde{z}}}\Big(-\gamma\Delta B_z(t)\frac{1}{2i}\left(\hat{I}_{\tilde{+}} - \hat{I}_{\tilde{-}}\right) - \omega_1\hat{\hat{R}}_{-\omega_1 t\hat{I}_{\tilde{z}}}\hat{I}_{\tilde{z}} - \frac{\gamma}{2}e^{-i\omega_0 t}\left(\Delta B_x(t) - i\Delta B_y(t)\right)\left(\hat{I}_{\tilde{z}} + \frac{i}{2}\left(\hat{I}_{\tilde{+}} + \hat{I}_{\tilde{-}}\right)\right) - \frac{\gamma}{2}e^{i\omega_0 t}\left(\Delta B_x(t) + i\Delta B_y(t)\right)\left(\hat{I}_{\tilde{z}} - \frac{i}{2}\left(\hat{I}_{\tilde{+}} + \hat{I}_{\tilde{-}}\right)\right)\Big)$$

Adding the fictitious term (from equation 10) allows us to write:

$$\begin{aligned}\hat{H}'_{\text{rot}} = \hat{\hat{R}}_{-\omega_1 t\hat{I}_{\tilde{z}}}\Bigg(&-\gamma\Delta B_z(t)\frac{1}{2i}\left(\hat{I}_{\tilde{+}}-\hat{I}_{\tilde{-}}\right)\\&-\frac{\gamma}{2}e^{-i\omega_0 t}\left(\Delta B_x(t)-i\Delta B_y(t)\right)\left(\hat{I}_{\tilde{z}}+\frac{i}{2}\left(\hat{I}_{\tilde{+}}+\hat{I}_{\tilde{-}}\right)\right)\\&-\frac{\gamma}{2}e^{i\omega_0 t}\left(\Delta B_x(t)+i\Delta B_y(t)\right)\left(\hat{I}_{\tilde{z}}-\frac{i}{2}\left(\hat{I}_{\tilde{+}}+\hat{I}_{\tilde{-}}\right)\right)\Bigg)\end{aligned}$$

Taking $\hat{\hat{R}} = \hat{\hat{R}}_{-\omega_1 t\hat{I}_{\tilde{z}}}$ for conciseness, we can rewrite this to:

$$\begin{aligned}\hat{H}'_{\text{eff}} = &-\frac{\gamma}{2}\hat{\hat{R}}\hat{I}_{\tilde{z}}\left(e^{-i\omega_0 t}\left(\Delta B_x(t)-i\Delta B_y(t)\right)+e^{i\omega_0 t}\left(\Delta B_x(t)+i\Delta B_y(t)\right)\right)\\&+\frac{i\gamma}{2}\hat{\hat{R}}\hat{I}_{\tilde{+}}\left(\Delta B_z(t)-\frac{1}{2}e^{-i\omega_0 t}\left(\Delta B_x(t)-i\Delta B_y(t)\right)+\frac{1}{2}e^{i\omega_0 t}\left(\Delta B_x(t)+i\Delta B_y(t)\right)\right)\\&-\frac{i\gamma}{2}\hat{\hat{R}}\hat{I}_{\tilde{-}}\left(\Delta B_z(t)+\frac{1}{2}e^{-i\omega_0 t}\left(\Delta B_x(t)-i\Delta B_y(t)\right)-\frac{1}{2}e^{i\omega_0 t}\left(\Delta B_x(t)+i\Delta B_y(t)\right)\right)\end{aligned}$$

Now taking these rotations, using equation 11, we finally get:

$$\begin{aligned}\hat{H}'_{\text{eff}} = &-\frac{\gamma}{2}\hat{I}_{\tilde{z}}\left(\left(\Delta B_x(t)-i\Delta B_y(t)\right)e^{-i\omega_0 t}+\left(\Delta B_x(t)+i\Delta B_y(t)\right)e^{i\omega_0 t}\right)\\&+\frac{i\gamma}{2}\hat{I}_{\tilde{+}}\left(\Delta B_z(t)e^{-i\omega_1 t}-\frac{1}{2}\left(\Delta B_x(t)-i\Delta B_y(t)\right)e^{-i(\omega_0+\omega_1)t}+\frac{1}{2}\left(\Delta B_x(t)+i\Delta B_y(t)\right)e^{-i(-\omega_0+\omega_1)t}\right)\\&-\frac{i\gamma}{2}\hat{I}_{\tilde{-}}\left(\Delta B_z(t)e^{i\omega_1 t}+\frac{1}{2}\left(\Delta B_x(t)-i\Delta B_y(t)\right)e^{-i(\omega_0-\omega_1)t}-\frac{1}{2}\left(\Delta B_x(t)+i\Delta B_y(t)\right)e^{-i(-\omega_0-\omega_1)t}\right)\end{aligned}$$

This is now nicely in terms of the eigenoperators of $\hat{\hat{H}}_0'$

$$\hat{H}'_{\text{eff}} = F'_0(t)\hat{A}'_0 + F'_1(t)\hat{A}'_1 + F'_{-1}(t)\hat{A}'_{-1}$$

with (using equation 12):

$$\begin{aligned}\hat{A}'_0 &= \hat{I}_{\tilde{z}} \qquad \hat{A}'_1 = \hat{I}_{\tilde{+}} \qquad \hat{A}'_{-1} = \hat{I}_{\tilde{-}}\\ e_0 &= \hat{\hat{H}}_0'\hat{A}'_0 = 0 \qquad e_1 = \hat{\hat{H}}_0'\hat{A}'_1 = -\omega_1 \qquad e_{-1} = \hat{\hat{H}}_0'\hat{A}'_{-1} = \omega_1\\ F'_0(t) &= -\frac{\gamma}{2}\left(\left(\Delta B_x(t)-i\Delta B_y(t)\right)e^{-i\omega_0 t}+\left(\Delta B_x(t)+i\Delta B_y(t)\right)e^{i\omega_0 t}\right)\\ F'_1(t) &= \frac{i\gamma}{2}\left(\Delta B_z(t)e^{-i\omega_1 t}-\frac{1}{2}\left(\Delta B_x(t)-i\Delta B_y(t)\right)e^{-i(\omega_0+\omega_1)t}+\frac{1}{2}\left(\Delta B_x(t)+i\Delta B_y(t)\right)e^{-i(-\omega_0+\omega_1)t}\right)\\ F'_{-1}(t) &= -\frac{i\gamma}{2}\left(\Delta B_z(t)e^{i\omega_1 t}+\frac{1}{2}\left(\Delta B_x(t)-i\Delta B_y(t)\right)e^{-i(\omega_0-\omega_1)t}-\frac{1}{2}\left(\Delta B_x(t)+i\Delta B_y(t)\right)e^{-i(-\omega_0-\omega_1)t}\right)\end{aligned} \tag{13}$$

Relaxation Superoperator

The relaxation times can be found from the relaxation superoperator $\hat{\hat{\Gamma}}$, which we define as:

$$\hat{\hat{\Gamma}} = \sum_q J_q \hat{\hat{A}}_{-q}\hat{\hat{A}}_q$$

with J_q defined by:

$$J_q = \int_0^\infty G_q(\tau)d\tau = \int_0^\infty \overline{F_{-q}(t')F_q(t'-\tau)}d\tau$$

Some methods add an additional $e^{-ie_q t}$ factor to J_q. This factor is a result of applying the transformations to the relaxation superoperator. Since we have already transformed the Hamiltonian, we do not need to add this factor.

Starting with $q = 0$:

$$G_0(\tau) = \overline{F_0'(t)F_0'(t-\tau)} = \frac{\gamma^2}{4}\left(\left(\Delta B_x(t) - i\Delta B_y(t)\right)e^{-i\omega_0 t} + \left(\Delta B_x(t) + i\Delta B_y(t)\right)e^{i\omega_0 t}\right)$$
$$\cdot\left(\left(\Delta B_x(t-\tau) - i\Delta B_y(t-\tau)\right)e^{-i\omega_0(t-\tau)} + \left(\Delta B_x(t-\tau) + i\Delta B_y(t-\tau)\right)e^{i\omega_0(t-\tau)}\right)$$

The overline is omitted in the last part, but we still average this expression over time.
Rewriting this gives:

$$\begin{aligned} G_0(\tau) = \frac{\gamma^2}{4}\Big(& \left(\Delta B_x(t) - i\Delta B_y(t)\right)\left(\Delta B_x(t-\tau) - i\Delta B_y(t-\tau)\right)e^{-i\omega_0(2t-\tau)} \\ & + \left(\Delta B_x(t) - i\Delta B_y(t)\right)\left(\Delta B_x(t-\tau) + i\Delta B_y(t-\tau)\right)e^{-i\omega_0\tau} \\ & + \left(\Delta B_x(t) + i\Delta B_y(t)\right)\left(\Delta B_x(t-\tau) - i\Delta B_y(t-\tau)\right)e^{i\omega_0\tau} \\ & + \left(\Delta B_x(t) + i\Delta B_y(t)\right)\left(\Delta B_x(t-\tau) + i\Delta B_y(t-\tau)\right)e^{i\omega_0(2t-\tau)}\Big) \end{aligned}$$

Now we assume our fluctuating magnetic field follows:

$$\left\langle \Delta B_p(t)\Delta B_q(t-\tau)\right\rangle = \begin{cases} 0 & p \neq q \\ G(\tau) = \left\langle B^2\right\rangle e^{-|\tau|/\tau_c} & p = q \end{cases} \tag{14}$$

This corresponds to a power spectrum:

$$J(\omega) = \frac{1}{\langle B^2\rangle}\int_0^\infty G(\tau)e^{-i\omega\tau}d\tau = \int_0^\infty e^{-|\tau|/\tau_c}e^{-i\omega\tau}d\tau = \frac{\tau_c}{1+\omega^2\tau_c^2} \tag{15}$$

We can therefore neglect all the cross-terms (like $\Delta B_x(t)\Delta B_y(t-\tau)$) and find:

$$\begin{aligned} G_0(\tau) = & \frac{\gamma^2}{4}\left(\left\langle B_x^2\right\rangle e^{-|\tau|/\tau_c} - \left\langle B_y^2\right\rangle e^{-|\tau|/\tau_c}\right)\left(e^{-i\omega_0(2t-\tau)} + e^{i\omega_0(2t-\tau)}\right) \\ & + \frac{\gamma^2}{4}\left(\left\langle B_x^2\right\rangle e^{-|\tau|/\tau_c} + \left\langle B_y^2\right\rangle e^{-|\tau|/\tau_c}\right)\left(e^{-i\omega_0\tau} + e^{i\omega_0\tau}\right) \end{aligned} \tag{16}$$

Now this gives

$$\begin{aligned} J_0 = \int_0^\infty G_0(\tau)d\tau = & \frac{\gamma^2}{4}\int_0^\infty \left(\left\langle B_x^2\right\rangle - \left\langle B_y^2\right\rangle\right)e^{-|\tau|/\tau_c}\left(e^{-i\omega_0(2t-\tau)} + e^{i\omega_0(2t-\tau)}\right) \\ & + \left(\left\langle B_x^2\right\rangle + \left\langle B_y^2\right\rangle\right)e^{-|\tau|/\tau_c}\left(e^{-i\omega_0\tau} + e^{i\omega_0\tau}\right)d\tau \\ = & \frac{\gamma^2}{4}\left(\left\langle B_x^2\right\rangle - \left\langle B_y^2\right\rangle\right)\left(\int_0^\infty e^{-|\tau|/\tau_c}e^{-i\omega_0(2t-\tau)}d\tau + \int_0^\infty e^{-|\tau|/\tau_c}e^{i\omega_0(2t-\tau)}d\tau\right) \\ & + \frac{\gamma^2}{4}\left(\left\langle B_x^2\right\rangle + \left\langle B_y^2\right\rangle\right)\left(\int_0^\infty e^{-|\tau|/\tau_c}e^{-i\omega_0\tau}d\tau + \int_0^\infty e^{-|\tau|/\tau_c}e^{i\omega_0\tau}d\tau\right) \end{aligned}$$

We can recognize the power spectrum of ΔB (equation 25), to see:

$$\begin{aligned} J_0 = & \frac{\gamma^2}{4}\left(\left\langle B_x^2\right\rangle - \left\langle B_y^2\right\rangle\right)\left(e^{-i\omega_0 2t}J(-\omega_0) + e^{i\omega_0 2t}J(\omega_0)\right) \\ & + \frac{\gamma^2}{4}\left(\left\langle B_x^2\right\rangle + \left\langle B_y^2\right\rangle\right)\left(J(\omega_0) + J(-\omega_0)\right) \end{aligned}$$

Now we can see from the definition (equation 25) that $J(-\omega) = J(\omega)$, which allows us to write:

$$J_0 = \frac{\gamma^2}{4}\left(\left\langle B_x^2\right\rangle - \left\langle B_y^2\right\rangle\right)2\cos(\omega_0 2t)J(\omega_0) + \frac{\gamma^2}{4}\left(\left\langle B_x^2\right\rangle + \left\langle B_y^2\right\rangle\right)2J(\omega_0)$$

The former term averages to zero over time, giving the final result:

$$J_0 = \frac{\gamma^2}{2}\left(\langle B_x^2\rangle + \langle B_y^2\rangle\right) J(\omega_0) = \gamma^2 \langle B^2\rangle J(\omega_0)$$

This almost agrees with the slides, but is still a factor 2 too large

For $q = 1$ we see

$$\begin{aligned}
&F_{-1}(t)F_1(t-\tau) = \\
&\quad \frac{\gamma^2}{4}\left(\Delta B_z(t)e^{i\omega_1 t} + \frac{1}{2}\left(\Delta B_x(t) - i\Delta B_y(t)\right)e^{-i(\omega_0-\omega_1)t} - \frac{1}{2}\left(\Delta B_x(t) + i\Delta B_y(t)\right)e^{-i(-\omega_0-\omega_1)t}\right) \\
&\quad \cdot\left(\Delta B_z(t-\tau)e^{-i\omega_1(t-\tau)} - \frac{1}{2}\left(\Delta B_x(t-\tau) - i\Delta B_y(t-\tau)\right)e^{-i(\omega_0+\omega_1)(t-\tau)}\right. \\
&\quad \left. + \frac{1}{2}\left(\Delta B_x(t-\tau) + i\Delta B_y(t-\tau)\right)e^{-i(-\omega_0+\omega_1)(t-\tau)}\right)
\end{aligned}$$

Rewriting this, separating the ΔB components:

$$\begin{aligned}
F_{-1}(t)F_1(t-\tau) = \frac{\gamma^2}{4}\Bigg(&\Delta B_z(t)e^{i\omega_1 t} + \frac{1}{2}\Delta B_x(t)\left(e^{-i(\omega_0-\omega_1)t} - e^{-i(-\omega_0-\omega_1)t}\right) \\
&- \frac{i}{2}\Delta B_y(t)\left(e^{-i(\omega_0-\omega_1)t} + e^{-i(-\omega_0-\omega_1)t}\right)\Bigg) \\
&\cdot\Bigg(\Delta B_z(t-\tau)e^{-i\omega_1(t-\tau)} + \frac{1}{2}\Delta B_x(t-\tau)\left(-e^{-i(\omega_0+\omega_1)(t-\tau)} + e^{-i(-\omega_0+\omega_1)(t-\tau)}\right) \\
&+ \frac{i}{2}\Delta B_y(t-\tau)\left(e^{-i(\omega_0+\omega_1)(t-\tau)} + e^{-i(-\omega_0+\omega_1)(t-\tau)}\right)\Bigg)
\end{aligned}$$

From equation 24, we see that eventually the ΔB-crossterms (like $\Delta B_x \Delta B_y$) will disappear. In the next step we thus neglect them:

$$\begin{aligned}
F_{-1}(t)F_1(t-\tau) = \frac{\gamma^2}{4}\Bigg(&\Delta B_z(t)\Delta B_z(t-\tau)e^{i\omega_1\tau} \\
&+ \frac{1}{4}\Delta B_x(t)\Delta B_x(t-\tau)\left(e^{-i(\omega_0-\omega_1)t} - e^{-i(-\omega_0-\omega_1)t}\right)\cdot\left(e^{-i(-\omega_0+\omega_1)(t-\tau)} - e^{-i(\omega_0+\omega_1)(t-\tau)}\right) \\
&+ \frac{1}{4}\Delta B_y(t)\Delta B_y(t-\tau)\left(e^{-i(\omega_0-\omega_1)t} + e^{-i(-\omega_0-\omega_1)t}\right)\cdot\left(e^{-i(\omega_0+\omega_1)(t-\tau)} + e^{-i(-\omega_0+\omega_1)(t-\tau)}\right)\Bigg) \\
= \frac{\gamma^2}{4}\Bigg(&\Delta B_z(t)\Delta B_z(t-\tau)e^{i\omega_1\tau} + \frac{1}{4}\Delta B_x(t)\Delta B_x(t-\tau)\cdot \mathrm{I} + \frac{1}{4}\Delta B_y(t)\Delta B_y(t-\tau)\cdot \mathrm{II}\Bigg)
\end{aligned}$$

The last expression defines I and II, so that we can calculate these separately:

$$\begin{aligned}
\mathrm{I} &= \left(e^{-i(\omega_0-\omega_1)t} - e^{-i(-\omega_0-\omega_1)t}\right)\cdot\left(e^{-i(-\omega_0+\omega_1)(t-\tau)} - e^{-i(\omega_0+\omega_1)(t-\tau)}\right) \\
&= e^{-i(\omega_0-\omega_1)t}e^{-i(-\omega_0+\omega_1)(t-\tau)} - e^{-i(\omega_0-\omega_1)t}e^{-i(\omega_0+\omega_1)(t-\tau)} \\
&\quad - e^{-i(-\omega_0-\omega_1)t}e^{-i(-\omega_0+\omega_1)(t-\tau)} + e^{-i(-\omega_0-\omega_1)t}e^{-i(\omega_0+\omega_1)(t-\tau)} \\
&= e^{i(-\omega_0+\omega_1)\tau} - e^{-i2\omega_0 t}e^{i(\omega_0+\omega_1)\tau} - e^{-i(-2\omega_0)t}e^{i(-\omega_0+\omega_1)\tau} \\
&\quad + e^{i(\omega_0+\omega_1)\tau}
\end{aligned}$$

We neglect the terms that oscillate in time, as these should average out to zero. We thus have:

$$\mathrm{I} = e^{i(-\omega_0+\omega_1)\tau} + e^{i(\omega_0+\omega_1)\tau}$$

For II we see:

$$\begin{aligned}\mathrm{II} &= \left(e^{-i(\omega_0-\omega_1)t} + e^{-i(-\omega_0-\omega_1)t}\right)\cdot\left(e^{-i(\omega_0+\omega_1)(t-\tau)} + e^{-i(-\omega_0+\omega_1)(t-\tau)}\right)\\ &= e^{-i(\omega_0-\omega_1)t}e^{-i(\omega_0+\omega_1)(t-\tau)} + e^{-i(\omega_0-\omega_1)t}e^{-i(-\omega_0+\omega_1)(t-\tau)}\\ &\quad + e^{-i(-\omega_0-\omega_1)t}e^{-i(\omega_0+\omega_1)(t-\tau)} + e^{-i(-\omega_0-\omega_1)t}e^{-i(-\omega_0+\omega_1)(t-\tau)}\\ &= e^{-i2\omega_0 t}e^{i(\omega_0+\omega_1)\tau} + e^{i(-\omega_0+\omega_1)\tau} + e^{i(\omega_0+\omega_1)\tau}\\ &\quad + e^{-i(-2\omega_0)t}e^{i(-\omega_0+\omega_1)\tau}\end{aligned}$$

Here the first and last term oscillate, giving:

$$\mathrm{II} = e^{i(-\omega_0+\omega_1)\tau} + e^{i(\omega_0+\omega_1)\tau} = \mathrm{I}$$

Filling this in gives:

$$\begin{aligned}G_1(\tau) = \frac{\gamma^2}{4}\Bigg(&\overline{\Delta B_z(t)\Delta B_z(t-\tau)}e^{i\omega_1\tau} + \frac{1}{4}\overline{\Delta B_x(t)\Delta B_x(t-\tau)}\left(e^{i(-\omega_0+\omega_1)\tau} + e^{i(\omega_0+\omega_1)\tau}\right)\\ &+ \frac{1}{4}\overline{\Delta B_y(t)\Delta B_y(t-\tau)}\left(e^{i(-\omega_0+\omega_1)\tau} + e^{i(\omega_0+\omega_1)\tau}\right)\Bigg)\end{aligned}$$

Using equation 24, we see:

$$\begin{aligned}G_1(\tau) = \frac{\gamma^2}{4}\Bigg(&\left\langle B_z^2\right\rangle e^{-|\tau|/\tau_c}e^{i\omega_1\tau} + \frac{1}{4}\left\langle B_x^2\right\rangle e^{-|\tau|/\tau_c}\left(e^{i(-\omega_0+\omega_1)\tau} + e^{i(\omega_0+\omega_1)\tau}\right)\\ &+ \frac{1}{4}\left\langle B_y^2\right\rangle e^{-|\tau|/\tau_c}\left(e^{i(-\omega_0+\omega_1)\tau} + e^{i(\omega_0+\omega_1)\tau}\right)\Bigg)\end{aligned}$$

Integrating this equation:

$$\begin{aligned}J_1 = &\frac{\gamma^2}{4}\left\langle B_z^2\right\rangle\int_0^\infty e^{-|\tau|/\tau_c}e^{i\omega_1\tau}d\tau + \frac{\gamma^2}{16}\left\langle B_x^2\right\rangle\int_0^\infty e^{-|\tau|/\tau_c}\left(e^{i(-\omega_0+\omega_1)\tau} + e^{i(\omega_0+\omega_1)\tau}\right)d\tau\\ &+ \frac{\gamma^2}{16}\left\langle B_y^2\right\rangle\int_0^\infty e^{-|\tau|/\tau_c}\left(e^{i(-\omega_0+\omega_1)\tau} + e^{i(\omega_0+\omega_1)\tau}\right)d\tau\end{aligned}$$

Recognizing the power spectrum of the fluctuations (equation 25):

$$J_1 = \frac{\gamma^2}{4}\left\langle B_z^2\right\rangle J(-\omega_1) + \frac{\gamma^2}{16}\left\langle B_x^2\right\rangle\left(J(\omega_0-\omega_1) + J(-\omega_0-\omega_1)\right) + \frac{\gamma^2}{16}\left\langle B_y^2\right\rangle\left(J(\omega_0-\omega_1) + J(-\omega_0-\omega_1)\right)$$

Assuming $J(-\omega) = J(\omega)$, and $\omega_0 \geq \omega_1 \geq 0$, we can rewrite this to only positive frequencies:

$$J_1 = \frac{\gamma^2}{4}\left\langle B_z^2\right\rangle J(\omega_1) + \frac{\gamma^2}{16}\left\langle B_x^2\right\rangle\left(J(\omega_0-\omega_1) + J(\omega_0+\omega_1)\right) + \frac{\gamma^2}{16}\left\langle B_y^2\right\rangle\left(J(\omega_0-\omega_1) + J(\omega_0+\omega_1)\right)$$

Which agrees with the $\hat{\hat{I}}_{\simeq}\hat{\hat{I}}_{\mp}$ term in $\hat{\hat{\Gamma}}$ in the Spielman lectures.
If we further assume that $\left\langle B_{x,y,z}^2\right\rangle = \left\langle B^2\right\rangle$.

$$J_1 = \frac{\gamma^2}{4}\left\langle B^2\right\rangle J(\omega_1) + \frac{\gamma^2}{8}\left\langle B^2\right\rangle\left(J(\omega_0-\omega_1) + J(\omega_0+\omega_1)\right)$$

and that $\omega_0 \gg \omega_1$:

$$J_1 = \frac{\gamma^2}{4}\left\langle B^2\right\rangle J(\omega_1) + \frac{\gamma^2}{4}\left\langle B^2\right\rangle J(\omega_0) = \frac{\gamma^2}{4}\left\langle B^2\right\rangle\left(J(\omega_1) + J(\omega_0)\right)$$

Note that this also agrees with the Spielman lectures, as there they rewrite:

$$\hat{\hat{I}}_{\simeq}\hat{\hat{I}}_{\mp} = \hat{\hat{I}}_{\mp}\hat{\hat{I}}_{\simeq} = \hat{\hat{I}}_{\tilde{x}}\hat{\hat{I}}_{\tilde{x}} + \hat{\hat{I}}_{\tilde{y}}\hat{\hat{I}}_{\tilde{y}}$$

and thus get an extra factor 2.

Finally, for $q = -1$, we see:

$$F_1(t)F_{-1}(t-\tau) = \frac{\gamma^2}{4}\Bigg(\Delta B_z(t)e^{-i\omega_1 t} - \frac{1}{2}\left(\Delta B_x(t) - i\Delta B_y(t)\right)e^{-i(\omega_0+\omega_1)t} + \frac{1}{2}\left(\Delta B_x(t) + i\Delta B_y(t)\right)e^{-i(-\omega_0+\omega_1)t}\Bigg)\cdot\Bigg(\Delta B_z(t-\tau)e^{i\omega_1(t-\tau)} + \frac{1}{2}\left(\Delta B_x(t-\tau) - i\Delta B_y(t-\tau)\right)e^{-i(\omega_0-\omega_1)(t-\tau)} - \frac{1}{2}\left(\Delta B_x(t-\tau) + i\Delta B_y(t-\tau)\right)e^{-i(-\omega_0-\omega_1)(t-\tau)}\Bigg)$$

Grouping by the ΔB terms gives:

$$F_1(t)F_{-1}(t-\tau) = \frac{\gamma^2}{4}\Bigg(\Delta B_z(t)e^{-i\omega_1 t} + \frac{1}{2}\Delta B_x(t)\left(e^{-i(-\omega_0+\omega_1)t} - e^{-i(\omega_0+\omega_1)t}\right) + \frac{i}{2}\Delta B_y(t)\left(e^{-i(-\omega_0+\omega_1)t} + e^{-i(\omega_0+\omega_1)t}\right)\Bigg)\cdot\Bigg(\Delta B_z(t-\tau)e^{i\omega_1(t-\tau)} + \frac{1}{2}\Delta B_x(t-\tau)\left(e^{-i(\omega_0-\omega_1)(t-\tau)} - e^{-i(-\omega_0-\omega_1)(t-\tau)}\right) - \frac{i}{2}\Delta B_y(t-\tau)\left(e^{-i(\omega_0-\omega_1)(t-\tau)} + e^{-i(-\omega_0-\omega_1)(t-\tau)}\right)\Bigg)$$

Multiplying this out, once again neglecting the cross-terms gives:

$$\begin{aligned}F_1(t)F_{-1}(t-\tau) &= \frac{\gamma^2}{4}\Delta B_z(t)\Delta B_z(t-\tau)e^{-i\omega_1\tau} + \frac{\gamma^2}{16}\Delta B_x(t)\Delta B_x(t-\tau)\left(e^{-i(-\omega_0+\omega_1)t} - e^{-i(\omega_0+\omega_1)t}\right)\cdot\left(e^{-i(\omega_0-\omega_1)(t-\tau)} - e^{-i(-\omega_0-\omega_1)(t-\tau)}\right)\\ &+ \frac{\gamma^2}{16}\Delta B_y(t)\Delta B_y(t-\tau)\left(e^{-i(-\omega_0+\omega_1)t} + e^{-i(\omega_0+\omega_1)t}\right)\cdot\left(e^{-i(\omega_0-\omega_1)(t-\tau)} + e^{-i(-\omega_0-\omega_1)(t-\tau)}\right)\\ &= \frac{\gamma^2}{4}\Delta B_z(t)\Delta B_z(t-\tau)e^{-i\omega_1\tau} + \frac{\gamma^2}{16}\Delta B_x(t)\Delta B_x(t-\tau)\cdot \mathrm{I} + \frac{\gamma^2}{16}\Delta B_y(t)\Delta B_y(t-\tau)\cdot \mathrm{II}\end{aligned}$$

With

$$\begin{aligned}\mathrm{I} &= \left(e^{-i(-\omega_0+\omega_1)t} - e^{-i(\omega_0+\omega_1)t}\right)\cdot\left(e^{-i(\omega_0-\omega_1)(t-\tau)} - e^{-i(-\omega_0-\omega_1)(t-\tau)}\right)\\ &= e^{-i0t}e^{i(\omega_0-\omega_1)\tau} - e^{-i(-2\omega_0)t}e^{i(-\omega_0-\omega_1)\tau} - e^{-i2\omega_0 t}e^{i(\omega_0-\omega_1)\tau} + e^{i(-\omega_0-\omega_1)\tau}\end{aligned}$$

Neglecting rapidly fluctuating terms:

$$\mathrm{I} = e^{i(\omega_0-\omega_1)\tau} + e^{i(-\omega_0-\omega_1)\tau}$$

and, similarly

$$\begin{aligned}\mathrm{II} &= \left(e^{-i(-\omega_0+\omega_1)t} + e^{-i(\omega_0+\omega_1)t}\right)\cdot\left(e^{-i(\omega_0-\omega_1)(t-\tau)} + e^{-i(-\omega_0-\omega_1)(t-\tau)}\right)\\ &= e^{-i(0)t}e^{i(\omega_0-\omega_1)\tau} + e^{-i(-2\omega_0)t}e^{i(-\omega_0-\omega_1)\tau} + e^{-i2\omega_0 t}e^{i(\omega_0-\omega_1)\tau} + e^{i(-\omega_0-\omega_1)\tau} \Rightarrow\\ \mathrm{II} &= e^{i(\omega_0-\omega_1)\tau} + e^{i(-\omega_0-\omega_1)\tau}\end{aligned}$$

Filling this in:

$$G_{-1}(\tau) = \overline{F_1(t)F_{-1}(t-\tau)} = \frac{\gamma^2}{4}\overline{\Delta B_z(t)\Delta B_z(t-\tau)}e^{-i\omega_1\tau} + \frac{\gamma^2}{16}\overline{\Delta B_x(t)\Delta B_x(t-\tau)}\left(e^{i(\omega_0-\omega_1)\tau} + e^{i(-\omega_0-\omega_1)\tau}\right) + \frac{\gamma^2}{16}\overline{\Delta B_y(t)\Delta B_y(t-\tau)}\left(e^{i(\omega_0-\omega_1)\tau} + e^{i(-\omega_0-\omega_1)\tau}\right)$$

Filling in the correlation of ΔB then gives:

$$\begin{aligned}G_{-1}(\tau) = \overline{F_1(t)F_{-1}(t-\tau)} &= \frac{\gamma^2}{4}\langle B_z^2\rangle e^{-|\tau|/\tau_c}e^{-i\omega_1\tau} \\ &+ \frac{\gamma^2}{16}\langle B_x^2\rangle e^{-|\tau|/\tau_c}\left(e^{i(\omega_0-\omega_1)\tau} + e^{i(-\omega_0-\omega_1)\tau}\right) \\ &+ \frac{\gamma^2}{16}\langle B_y^2\rangle e^{-|\tau|/\tau_c}\left(e^{i(\omega_0-\omega_1)\tau} + e^{i(-\omega_0-\omega_1)\tau}\right) \\ &= \frac{\gamma^2}{4}\langle B_z^2\rangle e^{-|\tau|/\tau_c}e^{-i\omega_1\tau} + \frac{\gamma^2}{16}\left(\langle B_x^2\rangle + \langle B_y^2\rangle\right)e^{-|\tau|/\tau_c}\left(e^{i(\omega_0-\omega_1)\tau} + e^{i(-\omega_0-\omega_1)\tau}\right)\end{aligned}$$

Again integrating and recognizing the fluctuating power spectrum gives:

$$J_{-1} = \frac{\gamma^2}{4}\langle B_z^2\rangle J(\omega_1) + \frac{\gamma^2}{16}\left(\langle B_x^2\rangle + \langle B_y^2\rangle\right)(J(\omega_1-\omega_0) + J(\omega_1+\omega_0))$$

Using $J(-\omega) = J(\omega)$ we see:

$$J_{-1} = \frac{\gamma^2}{4}\langle B_z^2\rangle J(\omega_1) + \frac{\gamma^2}{16}\left(\langle B_x^2\rangle + \langle B_y^2\rangle\right)(J(\omega_0-\omega_1) + J(\omega_1+\omega_0)) = J_1$$

And thus the $\hat{\tilde{I}}_{\mp}\hat{\tilde{I}}_{\simeq}$ term is exactly the same as the $\hat{\tilde{I}}_{\simeq}\hat{\tilde{I}}_{\mp}$ term in $\hat{\tilde{\Gamma}}$. This also agrees with the Spielman lectures.

Putting it all together, we obtain:

$$\begin{aligned}\hat{\tilde{\Gamma}} &= J_0\hat{\tilde{I}}_{\tilde{z}}\hat{\tilde{I}}_{\tilde{z}} + J_1\hat{\tilde{I}}_{\simeq}\hat{\tilde{I}}_{\mp} + J_{-1}\hat{\tilde{I}}_{\mp}\hat{\tilde{I}}_{\simeq} \\ &= \gamma^2\langle B^2\rangle J(\omega_0)\hat{\tilde{I}}_{\tilde{z}}\hat{\tilde{I}}_{\tilde{z}} + \frac{\gamma^2}{4}\langle B^2\rangle(J(\omega_1)+J(\omega_0))\left(\hat{\tilde{I}}_{\simeq}\hat{\tilde{I}}_{\mp} + \hat{\tilde{I}}_{\mp}\hat{\tilde{I}}_{\simeq}\right)\end{aligned}$$

Relaxation Times

The relaxation times can be found by inner products of the relaxation operator:

$$\begin{aligned}\frac{1}{T_{1\rho}} &= \langle\hat{I}_{\tilde{z}}|\,\hat{\tilde{\Gamma}}\,|\hat{I}_{\tilde{z}}\rangle = J_{-1}\langle\hat{I}_{\tilde{z}}|\,\hat{\tilde{I}}_{\mp}\hat{\tilde{I}}_{\simeq}\,|\hat{I}_{\tilde{z}}\rangle + J_1\langle\hat{I}_{\tilde{z}}|\,\hat{\tilde{I}}_{\simeq}\hat{\tilde{I}}_{\mp}\,|\hat{I}_{\tilde{z}}\rangle + J_0\langle\hat{I}_{\tilde{z}}|\,\hat{\tilde{I}}_{\tilde{z}}\hat{\tilde{I}}_{\tilde{z}}\,|\hat{I}_{\tilde{z}}\rangle \\ &= J_{-1}\,\mathrm{Tr}\left(\hat{I}_{\tilde{z}}\hat{\tilde{I}}_{\mp}\hat{\tilde{I}}_{\simeq}\hat{I}_{\tilde{z}}\right) + J_1\,\mathrm{Tr}\left(\hat{I}_{\tilde{z}}\hat{\tilde{I}}_{\simeq}\hat{\tilde{I}}_{\mp}\hat{I}_{\tilde{z}}\right) + J_0\,\mathrm{Tr}\left(\hat{I}_{\tilde{z}}\hat{\tilde{I}}_{\tilde{z}}\hat{\tilde{I}}_{\tilde{z}}\hat{I}_{\tilde{z}}\right)\end{aligned}$$

Calculating these commutators we get:

$$\frac{1}{T_{1\rho}} = 2J_{-1}\,\mathrm{Tr}\left(\hat{I}_{\tilde{z}}\hat{I}_{\tilde{z}}\right) + 2J_1\,\mathrm{Tr}\left(\hat{I}_{\tilde{z}}\hat{I}_{\tilde{z}}\right) = 2(J_{-1}+J_1)$$

Where we assumed the trace of these operators was normalized. Filling in J_1 and J_{-1} gives:

$$\begin{aligned}\frac{1}{T_{1\rho}} &= 2\left(\frac{\gamma^2}{4}\langle B^2\rangle(J(\omega_1)+J(\omega_0)) + \frac{\gamma^2}{4}\langle B^2\rangle(J(\omega_1)+J(\omega_0))\right) \\ &= \gamma^2\langle B^2\rangle(J(\omega_1)+J(\omega_0))\end{aligned}$$

Which matches the result from the Spielman lectures.

For $T_{2\rho}$, we can use many different expressions:

$$\frac{1}{T_{2\rho}} = \langle\hat{I}_{\tilde{x}}|\,\hat{\tilde{\Gamma}}\,|\hat{I}_{\tilde{x}}\rangle = \langle\hat{I}_{\tilde{y}}|\,\hat{\tilde{\Gamma}}\,|\hat{I}_{\tilde{y}}\rangle = \langle\hat{I}_{\mp}|\,\hat{\tilde{\Gamma}}\,|\hat{I}_{\mp}\rangle = \langle\hat{I}_{\simeq}|\,\hat{\tilde{\Gamma}}\,|\hat{I}_{\simeq}\rangle$$

For us, the $\hat{I}_{\tilde{x}}$ expression is simplest. We can see this after a little simplification. First we see $J_1 = J_{-1}$:

$$\begin{aligned}\hat{\hat{\Gamma}} &= J_0\hat{\hat{I}}_{\tilde{z}}\hat{\hat{I}}_{\tilde{z}} + J_1\hat{\hat{I}}_{\simeq}\hat{\hat{I}}_{\mp} + J_{-1}\hat{\hat{I}}_{\mp}\hat{\hat{I}}_{\simeq} \\ &= J_0\hat{\hat{I}}_{\tilde{z}}\hat{\hat{I}}_{\tilde{z}} + J_1\left(\hat{\hat{I}}_{\simeq}\hat{\hat{I}}_{\mp} + \hat{\hat{I}}_{\mp}\hat{\hat{I}}_{\simeq}\right)\end{aligned}$$

Now by working out the product, we can see:

$$\hat{\hat{I}}_{\simeq}\hat{\hat{I}}_{\mp} + \hat{\hat{I}}_{\mp}\hat{\hat{I}}_{\simeq} = 2\hat{\hat{I}}_{\tilde{x}}\hat{\hat{I}}_{\tilde{x}} + 2\hat{\hat{I}}_{\tilde{y}}\hat{\hat{I}}_{\tilde{y}}$$

This gives:

$$\hat{\hat{\Gamma}} = J_0\hat{\hat{I}}_{\tilde{z}}\hat{\hat{I}}_{\tilde{z}} + 2J_1\left(\hat{\hat{I}}_{\tilde{x}}\hat{\hat{I}}_{\tilde{x}} + \hat{\hat{I}}_{\tilde{y}}\hat{\hat{I}}_{\tilde{y}}\right)$$

This allows us to find $T_{2\rho}$:

$$\frac{1}{T_{2\rho}} = \langle\hat{I}_{\tilde{x}}|\,\hat{\hat{\Gamma}}\,|\hat{I}_{\tilde{x}}\rangle = J_0\,\mathrm{Tr}\left(\hat{I}_{\tilde{x}}\hat{\hat{I}}_{\tilde{z}}\hat{\hat{I}}_{\tilde{z}}\hat{I}_{\tilde{x}}\right) + 2J_1\left(\mathrm{Tr}\left(\hat{I}_{\tilde{x}}\hat{\hat{I}}_{\tilde{x}}\hat{\hat{I}}_{\tilde{x}}\hat{I}_{\tilde{x}}\right) + \mathrm{Tr}\left(\hat{I}_{\tilde{x}}\hat{\hat{I}}_{\tilde{y}}\hat{\hat{I}}_{\tilde{y}}\hat{I}_{\tilde{x}}\right)\right)$$

Calculating these commutators gives (assuming the traces are normalized):

$$\begin{aligned}\mathrm{Tr}\left(\hat{I}_{\tilde{x}}\hat{\hat{I}}_{\tilde{z}}\hat{\hat{I}}_{\tilde{z}}\hat{I}_{\tilde{x}}\right) &= \mathrm{Tr}\left(\hat{I}_{\tilde{x}}\hat{\hat{I}}_{\tilde{z}}i\hat{I}_{\tilde{y}}\right) = \mathrm{Tr}\left(\hat{I}_{\tilde{x}}i\left(-i\hat{I}_{\tilde{x}}\right)\right) = \mathrm{Tr}\left(\hat{I}_{\tilde{x}}\hat{I}_{\tilde{x}}\right) = 1 \\ \mathrm{Tr}\left(\hat{I}_{\tilde{x}}\hat{\hat{I}}_{\tilde{x}}\hat{\hat{I}}_{\tilde{x}}\hat{I}_{\tilde{x}}\right) &= \mathrm{Tr}\left(\hat{I}_{\tilde{x}}\hat{\hat{I}}_{\tilde{x}}0\right) = \mathrm{Tr}\,(0) = 0 \\ \mathrm{Tr}\left(\hat{I}_{\tilde{x}}\hat{\hat{I}}_{\tilde{y}}\hat{\hat{I}}_{\tilde{y}}\hat{I}_{\tilde{x}}\right) &= \mathrm{Tr}\left(\hat{I}_{\tilde{x}}\hat{\hat{I}}_{\tilde{y}}\left(-i\hat{I}_{\tilde{z}}\right)\right) = \mathrm{Tr}\left(\hat{I}_{\tilde{x}}\,(-i)\,i\hat{I}_{\tilde{x}}\right) = \mathrm{Tr}\left(\hat{I}_{\tilde{x}}\hat{I}_{\tilde{x}}\right) = 1\end{aligned}$$

And therefore:

$$\frac{1}{T_{2\rho}} = J_0 + 2J_1 \tag{17}$$

Filling in J_0 and J_1:

$$\begin{aligned}\frac{1}{T_{2\rho}} &= \gamma^2\left\langle B^2\right\rangle J(\omega_0) + \frac{\gamma^2}{2}\left\langle B^2\right\rangle (J(\omega_1) + J(\omega_0)) \\ &= \frac{\gamma^2}{2}\left\langle B^2\right\rangle (J(\omega_1) + 3J(\omega_0))\end{aligned}$$

To check this, I calculated $\langle\hat{I}_{\tilde{y}}|\,\hat{\hat{\Gamma}}\,|\hat{I}_{\tilde{y}}\rangle = J_0 + 2J_1$ as well.

Appendix C: Derivation of the Relaxation Times for Time-Independent Off-Resonance

In this appendix, we provide the detailed calculation of the relaxation times while an RF-pulse is transmitted at a frequency $\omega_{\mathrm{rf}} \neq \omega_0$, independent of time. This can, for instance, happen when B_0 inhomogeneity causes different ω_0 for different spins. The derivation is mostly the same as in the on-resonance case, (given in appendix A) until the second rotating frame.

Deriving the Hamiltonian

We once again take as a starting point

$$\hat{H} = -\gamma\left(\hat{I}_x B_x(t) + \hat{I}_y B_y(t) + \hat{I}_z B_z(t)\right)$$

The main magnetic field $\boldsymbol{B_0}$ and the fluctuations $\boldsymbol{\Delta B}$ remain the same. The spin-lock pulse now rotates at ω_{rf} instead:

$$\begin{aligned}\boldsymbol{B_0} &= B_0\hat{z}\\ \boldsymbol{B_1} &= B_1\left(\cos(\omega_{\mathrm{rf}}t)\hat{x} - \sin(\omega_{\mathrm{rf}}t)\hat{y}\right)\\ \boldsymbol{\Delta B} &= \Delta B_x(t)\hat{x} + \Delta B_y(t)\hat{y} + \Delta B_z(t)\hat{z}\end{aligned}$$

With still the assumption $\Delta B \ll B_0$.

Filling in these fields gives:

$$\hat{H} = -\gamma B_0\hat{I}_z - \gamma B_1\left(\cos(\omega_{\mathrm{rf}}t)\hat{I}_x - \sin(\omega_{\mathrm{rf}}t)\hat{I}_y\right) - \gamma\Delta B_z(t)\hat{I}_z - \gamma\Delta B_x(t)\hat{I}_x - \gamma\Delta B_y(t)\hat{I}_y$$

Rearranging terms, and using the Larmor frequencies $\omega_0 = \gamma B_0$, $\omega_1 = \gamma B_1$:

$$\hat{H} = -\omega_0\hat{I}_z - \omega_1\left(\cos(\omega_{\mathrm{rf}}t)\hat{I}_x - \sin(\omega_{\mathrm{rf}}t)\hat{I}_y\right) - \gamma\Delta B_z(t)\hat{I}_z - \gamma\Delta B_x(t)\hat{I}_x - \gamma\Delta B_y(t)\hat{I}_y \tag{18}$$

The First Rotating Frame

In this case, we rotate our frame by $\omega_{\mathrm{rf}}t$ around the $\hat{z}$-axis. This gives a fictitious term (derived in appendix A):

$$\hat{H}_{\mathrm{eff}} = \omega_{\mathrm{rf}}\hat{I}_z + e^{-i\omega_{\mathrm{rf}}t\hat{I}_z}\hat{H}e^{+i\omega_{\mathrm{rf}}t\hat{I}_z} \tag{19}$$

We again get a new basis:

$$\begin{aligned}\hat{\hat{R}}_{-\omega_{\mathrm{rf}}t\hat{I}_z}\hat{I}_x &= e^{-i\omega_{\mathrm{rf}}t\hat{I}_z}\hat{I}_x e^{i\omega_{\mathrm{rf}}t\hat{I}_z} = \hat{I}_{x'}\cos(\omega_{\mathrm{rf}}t) + \hat{I}_{y'}\sin(\omega_{\mathrm{rf}}t)\\ \hat{\hat{R}}_{-\omega_{\mathrm{rf}}t\hat{I}_z}\hat{I}_y &= e^{-i\omega_{\mathrm{rf}}t\hat{I}_z}\hat{I}_y e^{i\omega_{\mathrm{rf}}t\hat{I}_z} = \hat{I}_{y'}\cos(\omega_{\mathrm{rf}}t) - \hat{I}_{x'}\sin(\omega_{\mathrm{rf}}t)\\ \hat{\hat{R}}_{-\omega_{\mathrm{rf}}t\hat{I}_z}\hat{I}_z &= e^{-i\omega_{\mathrm{rf}}t\hat{I}_z}\hat{I}_z e^{i\omega_{\mathrm{rf}}t\hat{I}_z} = \hat{I}_{z'}\end{aligned}$$

Which allows us to write:

$$\hat{H}_{\mathrm{rot}} = -\omega_0\hat{I}_{z'} - \gamma\Delta B_z(t)\hat{I}_{z'} - \omega_1\hat{I}_{x'} - \gamma\hat{\hat{R}}_{-\omega_{\mathrm{rf}}t\hat{I}_z}\left(\Delta B_x(t)\hat{I}_x + \Delta B_y(t)\hat{I}_y\right)$$

Finally we must add the fictitious term derived in equation 19:

$$\begin{aligned}\hat{H}_{\text{eff}} &= \omega_{\text{rf}}\hat{I}_z + \hat{H}_{\text{rot}} = \omega_{\text{rf}}\hat{I}_{z'} + \hat{H}_{\text{rot}} \\ &= -(\omega_0 - \omega_{\text{rf}})\hat{I}_{z'} - \gamma\Delta B_z(t)\hat{I}_{z'} - \omega_1\hat{I}_{x'} - \gamma\hat{\hat{R}}_{-\omega_{\text{rf}}t\hat{I}_z}\left(\Delta B_x(t)\hat{I}_x + \Delta B_y(t)\hat{I}_y\right) \\ &= -\Omega\hat{I}_{z'} - \gamma\Delta B_z(t)\hat{I}_{z'} - \omega_1\hat{I}_{x'} - \gamma\hat{\hat{R}}_{-\omega_{\text{rf}}t\hat{I}_z}\left(\Delta B_x(t)\hat{I}_x + \Delta B_y(t)\hat{I}_y\right)\end{aligned}$$

Where we defined $\Omega = \omega_0 - \omega_{\text{rf}}$ the off-resonance.

We still have:

$$\hat{\hat{R}}_{-\omega_{\text{rf}}t\hat{I}_z}\hat{I}_+ = e^{-i\omega_{\text{rf}}t}\hat{I}_+$$
$$\hat{\hat{R}}_{-\omega_{\text{rf}}t\hat{I}_z}\hat{I}_- = e^{i\omega_{\text{rf}}t}\hat{I}_-$$

So we can rewrite:

$$\hat{I}_x = \frac{1}{2}\left(\hat{I}_+ + \hat{I}_-\right) \quad \text{and} \quad \hat{I}_y = \frac{1}{2i}\left(\hat{I}_+ - \hat{I}_-\right)$$

To get:

$$\begin{aligned}\hat{H}_{\text{eff}} &= -\Omega\hat{I}_{z'} - \gamma\Delta B_z(t)\hat{I}_{z'} - \omega_1\hat{I}_{x'} - \frac{\gamma}{2}\hat{\hat{R}}_{-\omega_{\text{rf}}t\hat{I}_z}\left(\Delta B_x(t)\left(\hat{I}_+ + \hat{I}_-\right) - i\Delta B_y(t)\left(\hat{I}_+ - \hat{I}_-\right)\right) \\ &= -\Omega\hat{I}_{z'} - \gamma\Delta B_z(t)\hat{I}_{z'} - \omega_1\hat{I}_{x'} - \frac{\gamma}{2}e^{-i\omega_{\text{rf}}t}\hat{I}_+\left(\Delta B_x(t) - i\Delta B_y(t)\right) - \frac{\gamma}{2}e^{i\omega_{\text{rf}}t}\hat{I}_-\left(\Delta B_x(t) + i\Delta B_y(t)\right)\end{aligned} \tag{20}$$

The Second Rotating Frame

The static component of our Hamiltonian is now:

$$\hat{H}_0' = -\Omega\hat{I}_{z'} - \omega_1\hat{I}_{x'}$$

The magnetic field corresponding to this static component is called the *effective magnetic field* $\boldsymbol{B}'_{\text{eff}}$.

We now wish to align this effective field with the z-axis in a new frame. Since the static component is no longer aligned to one of the axes, we can't just interchange the axis labels. Instead, we must create a new frame (x'', y'', z'') that is tilted with respect to (x', y', z').

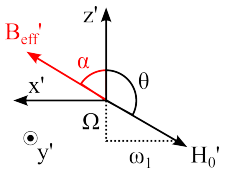

Figure 1: $\boldsymbol{B}'_{\text{eff}}$ in the first rotating frame

From figure 1 we see that we must tilt our frame by an angle α around the y'-axis. We can also see in this figure that:

$$\tan(\alpha) = \frac{\omega_1}{\Omega}$$

Using the fact that:

$$\begin{aligned}\sin(\arctan(x)) &= \frac{x}{\sqrt{1+x^2}} \\ \cos(\arctan(x)) &= \frac{1}{\sqrt{1+x^2}}\end{aligned} \tag{21}$$

We can see

$$\cos(\alpha) = \frac{1}{\sqrt{1+\left(\frac{\omega_1}{\Omega}\right)^2}} = \frac{\Omega}{\sqrt{\omega_1^2+\Omega^2}}$$
$$\sin(\alpha) = \frac{\left(\frac{\omega_1}{\Omega}\right)}{\sqrt{1+\left(\frac{\omega_1}{\Omega}\right)^2}} = \frac{\omega_1}{\sqrt{\omega_1^2+\Omega^2}}$$

These equations allow us to rewrite the spin operators in the new basis:

$$\hat{\hat{R}}_{\alpha\hat{I}_{y'}}\hat{I}_{x'} = \hat{I}_{x''}\cos(\alpha) + \hat{I}_{z''}\sin(\alpha) = \frac{1}{\sqrt{\omega_1^2+\Omega^2}}\left(\Omega\hat{I}_{x''} + \omega_1\hat{I}_{z''}\right) = \frac{1}{\omega_{\text{eff}}}\left(\Omega\hat{I}_{x''} + \omega_1\hat{I}_{z''}\right)$$
$$\hat{\hat{R}}_{\alpha\hat{I}_{y'}}\hat{I}_{y'} = \hat{I}_{y''}$$
$$\hat{\hat{R}}_{\alpha\hat{I}_{y'}}\hat{I}_{z'} = \hat{I}_{z''}\cos(\alpha) - \hat{I}_{x''}\sin(\alpha) = \frac{1}{\sqrt{\omega_1^2+\Omega^2}}\left(\Omega\hat{I}_{z''} - \omega_1\hat{I}_{x''}\right) = \frac{1}{\omega_{\text{eff}}}\left(\Omega\hat{I}_{z''} - \omega_1\hat{I}_{x''}\right)$$
$$\Rightarrow \hat{\hat{R}}_{\alpha\hat{I}_{y'}}\hat{I}_{+} = \hat{\hat{R}}_{\alpha\hat{I}_{y'}}\hat{I}_{x'} + i\hat{\hat{R}}_{\alpha\hat{I}_{y'}}\hat{I}_{y'} = \frac{1}{\omega_{\text{eff}}}\left(\Omega\hat{I}_{x''} + \omega_1\hat{I}_{z''}\right) + i\hat{I}_{y''} \tag{22}$$
$$= \frac{1}{\omega_{\text{eff}}}\left(\Omega\hat{I}_{x''} + \omega_1\hat{I}_{z''} + i\omega_{\text{eff}}\hat{I}_{y''}\right)$$
$$\Rightarrow \hat{\hat{R}}_{\alpha\hat{I}_{y'}}\hat{I}_{-} = \hat{\hat{R}}_{\alpha\hat{I}_{y'}}\hat{I}_{x'} - i\hat{\hat{R}}_{\alpha\hat{I}_{y'}}\hat{I}_{y'} = \frac{1}{\omega_{\text{eff}}}\left(\Omega\hat{I}_{x''} + \omega_1\hat{I}_{z''}\right) - i\hat{I}_{y''}$$
$$= \frac{1}{\omega_{\text{eff}}}\left(\Omega\hat{I}_{x''} + \omega_1\hat{I}_{z''} - i\omega_{\text{eff}}\hat{I}_{y''}\right)$$

Where we set $\omega_{\text{eff}} = \sqrt{\omega_1^2+\Omega^2}$, as this is the frequency corresponding to the effective field.

We can now write the effective Hamiltonian (equation 20) in this new basis:

$$\hat{H}_{\text{eff}} = -\Omega\hat{\hat{R}}_{\alpha\hat{I}_{y'}}\hat{I}_{z'} - \gamma\Delta B_z(t)\hat{\hat{R}}_{\alpha\hat{I}_{y'}}\hat{I}_{z'} - \omega_1\hat{\hat{R}}_{\alpha\hat{I}_{y'}}\hat{I}_{x'}$$
$$- \frac{\gamma}{2}e^{-i\omega_{\text{rf}}t}\left(\Delta B_x(t) - i\Delta B_y(t)\right)\hat{\hat{R}}_{\alpha\hat{I}_{y'}}\hat{I}_{+} - \frac{\gamma}{2}e^{i\omega_{\text{rf}}t}\left(\Delta B_x(t) + i\Delta B_y(t)\right)\hat{\hat{R}}_{\alpha\hat{I}_{y'}}\hat{I}_{-}$$
$$= -\Omega\frac{1}{\omega_{\text{eff}}}\left(\Omega\hat{I}_{z''} - \omega_1\hat{I}_{x''}\right) - \gamma\Delta B_z(t)\frac{1}{\omega_{\text{eff}}}\left(\Omega\hat{I}_{z''} - \omega_1\hat{I}_{x''}\right) - \omega_1\frac{1}{\omega_{\text{eff}}}\left(\Omega\hat{I}_{x''} + \omega_1\hat{I}_{z''}\right)$$
$$- \frac{\gamma}{2}e^{-i\omega_{\text{rf}}t}\left(\Delta B_x(t) - i\Delta B_y(t)\right)\frac{1}{\omega_{\text{eff}}}\left(\Omega\hat{I}_{x''} + \omega_1\hat{I}_{z''} + i\omega_{\text{eff}}\hat{I}_{y''}\right)$$
$$- \frac{\gamma}{2}e^{i\omega_{\text{rf}}t}\left(\Delta B_x(t) + i\Delta B_y(t)\right)\frac{1}{\omega_{\text{eff}}}\left(\Omega\hat{I}_{x''} + \omega_1\hat{I}_{z''} - i\omega_{\text{eff}}\hat{I}_{y''}\right)$$

Multiplying both sides by ω_{eff}, and simplifying, gives:

$$\hat{H}_{\text{eff}}\omega_{\text{eff}} = \left(-\Omega - \gamma\Delta B_z(t)\right)\left(\Omega\hat{I}_{z''} - \omega_1\hat{I}_{x''}\right) - \omega_1\left(\Omega\hat{I}_{x''} + \omega_1\hat{I}_{z''}\right)$$
$$- \frac{\gamma}{2}e^{-i\omega_{\text{rf}}t}\left(\Delta B_x(t) - i\Delta B_y(t)\right)\left(\Omega\hat{I}_{x''} + \omega_1\hat{I}_{z''} + i\omega_{\text{eff}}\hat{I}_{y''}\right)$$
$$- \frac{\gamma}{2}e^{i\omega_{\text{rf}}t}\left(\Delta B_x(t) + i\Delta B_y(t)\right)\left(\Omega\hat{I}_{x''} + \omega_1\hat{I}_{z''} - i\omega_{\text{eff}}\hat{I}_{y''}\right)$$

In the next step we will rotate this Hamiltonian by $\omega_{\text{eff}}t$ around the z'' axis. This is easier if we rewrite this in terms of the eigenoperators of this rotation:

$$\hat{I}_{z''} = \hat{I}_{z''}$$
$$\hat{I}_{+''} = \hat{I}_{x''} + i\hat{I}_{y''} \Rightarrow \hat{I}_{x''} = \left(\frac{1}{2}\hat{I}_{+''} + \frac{1}{2}\hat{I}_{-''}\right)$$
$$\hat{I}_{-''} = \hat{I}_{x''} - i\hat{I}_{y''} \Rightarrow \hat{I}_{y''} = \left(\frac{1}{2i}\hat{I}_{+''} - \frac{1}{2i}\hat{I}_{-''}\right)$$

Rewriting to these operators gives:

$$\begin{aligned}\hat{H}_{\text{eff}}\omega_{\text{eff}} &= (-\Omega-\gamma\Delta B_z(t))\left(\Omega\hat{I}_{z''}-\omega_1\left(\frac{1}{2}\hat{I}_{+''}+\frac{1}{2}\hat{I}_{-''}\right)\right)-\omega_1\left(\Omega\left(\frac{1}{2}\hat{I}_{+''}+\frac{1}{2}\hat{I}_{-''}\right)+\omega_1\hat{I}_{z''}\right)\\ &-\frac{\gamma}{2}e^{-i\omega_{\text{rf}}t}\left(\Delta B_x(t)-i\Delta B_y(t)\right)\left(\Omega\left(\frac{1}{2}\hat{I}_{+''}+\frac{1}{2}\hat{I}_{-''}\right)+\omega_1\hat{I}_{z''}+i\omega_{\text{eff}}\left(\frac{1}{2i}\hat{I}_{+''}-\frac{1}{2i}\hat{I}_{-''}\right)\right)\\ &-\frac{\gamma}{2}e^{i\omega_{\text{rf}}t}\left(\Delta B_x(t)+i\Delta B_y(t)\right)\left(\Omega\left(\frac{1}{2}\hat{I}_{+''}+\frac{1}{2}\hat{I}_{-''}\right)+\omega_1\hat{I}_{z''}-i\omega_{\text{eff}}\left(\frac{1}{2i}\hat{I}_{+''}-\frac{1}{2i}\hat{I}_{-''}\right)\right)\\ &=\hat{I}_{z''}\left(-\Omega^2-\omega_1^2-\Omega\gamma\Delta B_z(t)-\frac{\omega_1\gamma}{2}\Delta B_-(t)e^{-i\omega_{\text{rf}}t}-\frac{\omega_1\gamma}{2}\Delta B_+(t)e^{i\omega_{\text{rf}}t}\right)\\ &+\frac{1}{2}\hat{I}_{+''}\left(\omega_1\gamma\Delta B_z(t)-\frac{\gamma}{2}(\Omega+\omega_{\text{eff}})\Delta B_-(t)e^{-i\omega_{\text{rf}}t}-\frac{\gamma}{2}(\Omega-\omega_{\text{eff}})\Delta B_+(t)e^{i\omega_{\text{rf}}t}\right)\\ &+\frac{1}{2}\hat{I}_{-''}\left(\omega_1\gamma\Delta B_z(t)-\frac{\gamma}{2}(\Omega-\omega_{\text{eff}})\Delta B_-(t)e^{-i\omega_{\text{rf}}t}-\frac{\gamma}{2}(\Omega+\omega_{\text{eff}})\Delta B_+(t)e^{i\omega_{\text{rf}}t}\right)\end{aligned}$$

Where we substitute $\Delta B_+(t)=\Delta B_x(t)+i\Delta B_y(t)$ and $\Delta B_-(t)=\Delta B_x(t)-i\Delta B_y(t)$ to shorten the equations somewhat.

We rotate by an angle $\omega_{\text{eff}}t$, to finally get rid of the static component. These spin operators rotate as:

$$\begin{aligned}\hat{\hat{R}}_{-\omega_{\text{eff}}t\hat{I}_{z''}}\hat{I}_{z''} &= \hat{I}_{z''}\\ \hat{\hat{R}}_{-\omega_{\text{eff}}t\hat{I}_{z''}}\hat{I}_{+''} &= e^{-i\omega_{\text{eff}}t}\hat{I}_{+''}\\ \hat{\hat{R}}_{-\omega_{\text{eff}}t\hat{I}_{z''}}\hat{I}_{-''} &= e^{i\omega_{\text{eff}}t}\hat{I}_{-''}\end{aligned}$$

We also get an additional fictitious term (given by equation 8):

$$\begin{aligned}\hat{H}''_{\text{eff}}=\omega_{\text{eff}}\hat{I}_{z''}+\hat{H}''_{\text{rot}} &\Rightarrow \hat{H}''_{\text{eff}}\omega_{\text{eff}}=\omega_{\text{eff}}^2\hat{I}_{z''}+\omega_{\text{eff}}\hat{H}''_{\text{rot}}\\ &\Rightarrow \hat{H}''_{\text{eff}}\omega_{\text{eff}}=\left(\Omega^2+\omega_1^2\right)\hat{I}_{z''}+\omega_{\text{eff}}\hat{H}''_{\text{rot}}\end{aligned}$$

Filling this in gives the effective Hamiltonian in the second rotating frame:

$$\begin{aligned}\hat{H}''_{\text{eff}}\omega_{\text{eff}} &= \hat{I}_{z''}\left(-\Omega\gamma\Delta B_z(t)-\frac{\omega_1\gamma}{2}\Delta B_-(t)e^{-i\omega_{\text{rf}}t}-\frac{\omega_1\gamma}{2}\Delta B_+(t)e^{i\omega_{\text{rf}}t}\right)\\ &+\frac{1}{2}\hat{I}_{+''}\left(\omega_1\gamma\Delta B_z(t)e^{-i\omega_{\text{eff}}t}-\frac{\gamma}{2}(\Omega+\omega_{\text{eff}})\Delta B_-(t)e^{-i(\omega_{\text{rf}}+\omega_{\text{eff}})t}-\frac{\gamma}{2}(\Omega-\omega_{\text{eff}})\Delta B_+(t)e^{i(\omega_{\text{rf}}-\omega_{\text{eff}})t}\right)\\ &+\frac{1}{2}\hat{I}_{-''}\left(\omega_1\gamma\Delta B_z(t)e^{i\omega_{\text{eff}}t}-\frac{\gamma}{2}(\Omega-\omega_{\text{eff}})\Delta B_-(t)e^{-i(\omega_{\text{rf}}-\omega_{\text{eff}})t}-\frac{\gamma}{2}(\Omega+\omega_{\text{eff}})\Delta B_+(t)e^{i(\omega_{\text{rf}}+\omega_{\text{eff}})t}\right)\end{aligned}$$

This is now nicely in terms of the eigenoperators of $\hat{\hat{H}}_0{}'$:

$$\hat{H}'_{\text{eff}}=F'_0(t)\hat{A}'_0+F'_1(t)\hat{A}'_1+F'_{-1}(t)\hat{A}'_{-1}$$

with:

$$\begin{aligned}\hat{A}'_0=\hat{I}_{z''} \qquad \hat{A}'_1=\hat{I}_{+''} \qquad \hat{A}'_{-1}=\hat{I}_{-''}\\ F'_0(t)=\frac{-\gamma}{2\omega_{\text{eff}}}\left(2\Omega\Delta B_z(t)+\omega_1\Delta B_-(t)e^{-i\omega_{\text{rf}}t}+\omega_1\Delta B_+(t)e^{i\omega_{\text{rf}}t}\right)\\ F'_1(t)=\frac{\gamma}{4\omega_{\text{eff}}}\left(2\omega_1\Delta B_z(t)e^{-i\omega_{\text{eff}}t}-(\Omega+\omega_{\text{eff}})\Delta B_-(t)e^{-i(\omega_{\text{rf}}+\omega_{\text{eff}})t}-(\Omega-\omega_{\text{eff}})\Delta B_+(t)e^{i(\omega_{\text{rf}}-\omega_{\text{eff}})t}\right)\\ F'_{-1}(t)=\frac{\gamma}{4\omega_{\text{eff}}}\left(2\omega_1\Delta B_z(t)e^{i\omega_{\text{eff}}t}-(\Omega-\omega_{\text{eff}})\Delta B_-(t)e^{-i(\omega_{\text{rf}}-\omega_{\text{eff}})t}-(\Omega+\omega_{\text{eff}})\Delta B_+(t)e^{i(\omega_{\text{rf}}+\omega_{\text{eff}})t}\right)\end{aligned} \tag{23}$$

As a check, we calculate the limit with no off-resonance:

$$\Omega \to 0 \text{ so } \omega_{\text{rf}} \to \omega_0 \text{ and } \omega_{\text{eff}} \to \omega_1$$

$$\begin{aligned}
\hat{A}'_0 &= \hat{I}_{z''} \qquad \hat{A}'_1 = \hat{I}_{+''} \qquad \hat{A}'_{-1} = \hat{I}_{-''} \\
F'_0(t) &= -\frac{\gamma}{2}\left(\Delta B_-(t)e^{-i\omega_0 t} + \Delta B_+(t)e^{i\omega_0 t}\right) \\
F'_1(t) &= \frac{\gamma}{2}\left(\Delta B_z(t)e^{-i\omega_1 t} - \frac{1}{2}\Delta B_-(t)e^{-i(\omega_0+\omega_1)t} + \frac{1}{2}\Delta B_+(t)e^{i(\omega_0-\omega_1)t}\right) \\
F'_{-1}(t) &= \frac{\gamma}{2}\left(\Delta B_z(t)e^{i\omega_1 t} + \frac{1}{2}\Delta B_-(t)e^{-i(\omega_0-\omega_1)t} - \frac{1}{2}\Delta B_+(t)e^{i(\omega_0+\omega_1)t}\right)
\end{aligned}$$

And indeed (up to a phase difference in the transverse plane, due to different orientation of the axes) this agrees with the on-resonance result.

Relaxation Superoperator

Once again the relaxation matrix is defined by:

$$\hat{\hat{\Gamma}} = \sum_q J_q \hat{\hat{A}}_{-q}\hat{\hat{A}}_q$$

with:

$$J_q = \int_0^\infty G_q(\tau)d\tau = \int_0^\infty \overline{F_{-q}(t)F_q(t-\tau)}d\tau$$

We once again assume our fluctuations follow:

$$\left\langle \Delta B_p(t)\Delta B_q(t-\tau)\right\rangle = \begin{cases} 0 & p \neq q \\ G(\tau) = \left\langle B^2\right\rangle e^{-|\tau|/\tau_c} & p = q \end{cases} \tag{24}$$

With a power spectrum:

$$J(\omega) = \frac{1}{\langle B^2\rangle}\int_0^\infty G(\tau)e^{-i\omega\tau}d\tau = \int_0^\infty e^{-|\tau|/\tau_c}e^{-i\omega\tau}d\tau = \frac{\tau_c}{1+\omega^2\tau_c^2} \tag{25}$$

As for our $\Delta B_+(t)$ and $\Delta B_-(t)$, we can see that (neglecting crossterms, which must all be zero):

$$\begin{aligned}
\Delta B_\pm(t)\Delta B_+(t-\tau) &= \Delta B_x(t)\Delta B_x(t-\tau) \mp \Delta B_y(t)\Delta B_y(t-\tau) \\
\Delta B_\pm(t)\Delta B_-(t-\tau) &= \Delta B_x(t)\Delta B_x(t-\tau) \pm \Delta B_y(t)\Delta B_y(t-\tau)
\end{aligned} \tag{26}$$

Of course, all the combinations with ΔB_z consist entirely of cross-terms and are thus zero.

Starting with $q = 0$, we see:

$$\begin{aligned}
G_0(\tau) = \overline{F'_0(t)F'_0(t-\tau)} = \frac{\gamma^2}{4\omega_{\text{eff}}^2}&\left(2\Omega\Delta B_z(t) + \omega_1\Delta B_-(t)e^{-i\omega_{\text{rf}}t} + \omega_1\Delta B_+(t)e^{i\omega_{\text{rf}}t}\right) \\
&\cdot\left(2\Omega\Delta B_z(t-\tau) + \omega_1\Delta B_-(t-\tau)e^{-i\omega_{\text{rf}}(t-\tau)} + \omega_1\Delta B_+(t-\tau)e^{i\omega_{\text{rf}}(t-\tau)}\right)
\end{aligned}$$

Multiplying this out, neglecting the $\Delta B_{x,y,z}$ cross-terms:

$$\begin{aligned}
G_0(\tau) = \frac{\gamma^2}{4\omega_{\text{eff}}^2}\Big(&4\Omega^2\Delta B_z(t)\Delta B_z(t-\tau) + \omega_1^2\Delta B_+(t)\Delta B_+(t-\tau)e^{i\omega_{\text{rf}}(2t-\tau)} \\
&+ \omega_1^2\Delta B_+(t)\Delta B_-(t-\tau)e^{i\omega_{\text{rf}}\tau} + \omega_1^2\Delta B_-(t)\Delta B_+(t-\tau)e^{-i\omega_{\text{rf}}\tau} \\
&+ \omega_1^2\Delta B_-(t)\Delta B_-(t-\tau)e^{-i\omega_{\text{rf}}(2t-\tau)}\Big)
\end{aligned}$$

The second and the last term have an complex exponential in t and thus average out to zero. We can simplify the remaining terms by noting that:

$$\Delta B_+(t)\Delta B_-(t-\tau) = \Delta B_-(t)\Delta B_+(t-\tau) = \Delta B_x(t)\Delta B_x(t-\tau) + \Delta B_y(t)\Delta B_y(t-\tau)$$

So that:

$$G_0(\tau) = \frac{\gamma^2}{4\omega_{\text{eff}}^2}\left(4\Omega^2\Delta B_z(t)\Delta B_z(t-\tau) + \omega_1^2\left(\Delta B_x(t)\Delta B_x(t-\tau) + \Delta B_y(t)\Delta B_y(t-\tau)\right)\cdot\left(e^{i\omega_{\text{rf}}t} + e^{-i\omega_{\text{rf}}t}\right)\right)$$

Filling in the correlation of the fluctuations (equation 24):

$$G_0(\tau) = \frac{\gamma^2}{4\omega_{\text{eff}}^2}\left(4\Omega^2\left\langle B_z^2\right\rangle e^{-|\tau|/\tau_c} + \omega_1^2\left(\left\langle B_x^2\right\rangle + \left\langle B_y^2\right\rangle\right)e^{-|\tau|/\tau_c}\cdot\left(e^{i\omega_{\text{rf}}t} + e^{-i\omega_{\text{rf}}t}\right)\right)$$

We can now calculate the power spectrum:

$$J_0 = \int_0^\infty G_0(\tau)d\tau = \frac{\gamma^2}{4\omega_{\text{eff}}^2}\left(4\Omega^2\left\langle B_z^2\right\rangle\int_0^\infty e^{-|\tau|/\tau_c}d\tau + \omega_1^2\left(\left\langle B_x^2\right\rangle + \left\langle B_y^2\right\rangle\right)\int_0^\infty e^{-|\tau|/\tau_c}\cdot\left(e^{i\omega_{\text{rf}}t} + e^{-i\omega_{\text{rf}}t}\right)d\tau\right)$$

We can now recognize the power spectrum of the fluctuations (equation 25) to get:

$$J_0 = \int_0^\infty G_0(\tau)d\tau = \frac{\gamma^2}{4\omega_{\text{eff}}^2}\left(4\Omega^2\left\langle B_z^2\right\rangle J(0) + \omega_1^2\left(\left\langle B_x^2\right\rangle + \left\langle B_y^2\right\rangle\right)\left(J(-\omega_{\text{rf}}) + J(\omega_{\text{rf}})\right)\right)$$
$$= \frac{\gamma^2\Omega^2}{\omega_{\text{eff}}^2}\left\langle B_z^2\right\rangle J(0) + \frac{\gamma^2\omega_1^2}{2\omega_{\text{eff}}^2}\left(\left\langle B_x^2\right\rangle + \left\langle B_y^2\right\rangle\right)J(\omega_{\text{rf}})$$

If we assume $\left\langle B_{x,y,z}^2\right\rangle = \left\langle B^2\right\rangle$ (equal fluctuation size in all directions):

$$J_0 = \frac{\gamma^2\Omega^2}{\omega_{\text{eff}}^2}\left\langle B^2\right\rangle J(0) + \frac{\gamma^2\omega_1^2}{\omega_{\text{eff}}^2}\left\langle B^2\right\rangle J(\omega_{\text{rf}})$$
$$= \frac{\gamma^2\Omega^2}{\omega_1^2+\Omega^2}\left\langle B^2\right\rangle J(0) + \frac{\gamma^2\omega_1^2}{\omega_1^2+\Omega^2}\left\langle B^2\right\rangle J(\omega_{\text{rf}})$$

And taking the on-resonance limit gives:

$$J_0 = \gamma^2\left\langle B^2\right\rangle J(\omega_0)$$

Which is equal to our earlier result.

Continuing with $q = 1$, we get:

$$G_1(\tau) = \overline{F_{-1}(t)F_1(t-\tau)} = \frac{\gamma^2}{16\omega_{\text{eff}}^2}\left(2\omega_1\Delta B_z(t)e^{i\omega_{\text{eff}}t} - (\Omega-\omega_{\text{eff}})\Delta B_-(t)e^{-i(\omega_{\text{rf}}-\omega_{\text{eff}})t} - (\Omega+\omega_{\text{eff}})\Delta B_+(t)e^{i(\omega_{\text{rf}}+\omega_{\text{eff}})t}\right)\cdot\left(2\omega_1\Delta B_z(t-\tau)e^{-i\omega_{\text{eff}}(t-\tau)} - (\Omega+\omega_{\text{eff}})\Delta B_-(t-\tau)e^{-i(\omega_{\text{rf}}+\omega_{\text{eff}})(t-\tau)} - (\Omega-\omega_{\text{eff}})\Delta B_+(t-\tau)e^{i(\omega_{\text{rf}}-\omega_{\text{eff}})(t-\tau)}\right)$$

Multiplying this out:

$$G_1(\tau) = \frac{\gamma^2}{16\omega_{\text{eff}}^2}\left(4\omega_1^2\Delta B_z(t)\Delta B_z(t-\tau)e^{i\omega_{\text{eff}}\tau} + (\Omega+\omega_{\text{eff}})(\Omega-\omega_{\text{eff}})\Delta B_+(t)\Delta B_+(t-\tau)e^{i2\omega_{\text{rf}}t}e^{-i(\omega_{\text{rf}}-\omega_{\text{eff}})\tau} + (\Omega+\omega_{\text{eff}})^2\Delta B_+(t)\Delta B_-(t-\tau)e^{i(\omega_{\text{rf}}+\omega_{\text{eff}})\tau} + (\Omega-\omega_{\text{eff}})^2\Delta B_-(t)\Delta B_+(t-\tau)e^{-i(\omega_{\text{rf}}-\omega_{\text{eff}})\tau} + (\Omega-\omega_{\text{eff}})(\Omega+\omega_{\text{eff}})\Delta B_-(t)\Delta B_-(t-\tau)e^{-i2\omega_{\text{rf}}t}e^{i(\omega_{\text{rf}}+\omega_{\text{eff}})\tau}\right)$$

Neglecting the terms that oscillate in t:

$$G_1(\tau) = \frac{\gamma^2}{16\omega_{\text{eff}}^2}\Big(4\omega_1^2\Delta B_z(t)\Delta B_z(t-\tau)e^{i\omega_{\text{eff}}\tau} + (\Omega+\omega_{\text{eff}})^2\Delta B_+(t)\Delta B_-(t-\tau)e^{i(\omega_{\text{rf}}+\omega_{\text{eff}})\tau} + (\Omega-\omega_{\text{eff}})^2\Delta B_-(t)\Delta B_+(t-\tau)e^{-i(\omega_{\text{rf}}-\omega_{\text{eff}})\tau}\Big)$$

Filling in equation 26 to get rid of $B_\pm$:

$$G_1(\tau) = \frac{\gamma^2}{16\omega_{\text{eff}}^2}\Big(4\omega_1^2\Delta B_z(t)\Delta B_z(t-\tau)e^{i\omega_{\text{eff}}\tau} + \big(\Delta B_x(t)\Delta B_x(t-\tau)+\Delta B_y(t)\Delta B_y(t-\tau)\big)\cdot\big((\Omega+\omega_{\text{eff}})^2e^{i(\omega_{\text{rf}}+\omega_{\text{eff}})\tau}+(\Omega-\omega_{\text{eff}})^2e^{-i(\omega_{\text{rf}}-\omega_{\text{eff}})\tau}\big)\Big)$$

We can now fill in the correlation of the fluctuating fields:

$$G_1(\tau) = \frac{\gamma^2}{16\omega_{\text{eff}}^2}\Big(4\omega_1^2\left\langle B_z^2\right\rangle e^{-|\tau|/\tau_c}e^{i\omega_{\text{eff}}\tau} + \left(\left\langle B_x^2\right\rangle+\left\langle B_y^2\right\rangle\right)e^{-|\tau|/\tau_c}\left((\Omega+\omega_{\text{eff}})^2e^{i(\omega_{\text{rf}}+\omega_{\text{eff}})\tau}+(\Omega-\omega_{\text{eff}})^2e^{-i(\omega_{\text{rf}}-\omega_{\text{eff}})\tau}\right)\Big)$$

Integrating, and recognizing the power spectrum of the fluctuations, gives:

$$\begin{aligned}J_1 &= \frac{\gamma^2}{16\omega_{\text{eff}}^2}\Big(4\omega_1^2\left\langle B_z^2\right\rangle J(-\omega_{\text{eff}}) + \left(\left\langle B_x^2\right\rangle+\left\langle B_y^2\right\rangle\right)\cdot\left((\Omega+\omega_{\text{eff}})^2J(-\omega_{\text{rf}}-\omega_{\text{eff}})+(\Omega-\omega_{\text{eff}})^2J(\omega_{\text{rf}}-\omega_{\text{eff}})\right)\Big)\\ &= \frac{\gamma^2\omega_1^2}{4\omega_{\text{eff}}^2}\left\langle B_z^2\right\rangle J(\omega_{\text{eff}}) + \frac{\gamma^2(\Omega+\omega_{\text{eff}})^2}{16\omega_{\text{eff}}^2}\left(\left\langle B_x^2\right\rangle+\left\langle B_y^2\right\rangle\right)J(\omega_{\text{rf}}+\omega_{\text{eff}})\\ &\quad+\frac{\gamma^2(\Omega-\omega_{\text{eff}})^2}{16\omega_{\text{eff}}^2}\left(\left\langle B_x^2\right\rangle+\left\langle B_y^2\right\rangle\right)J(\omega_{\text{rf}}-\omega_{\text{eff}})\end{aligned}$$

Assuming equal fluctuation size in all directions:

$$\begin{aligned}J_1 &= \frac{\gamma^2\omega_1^2}{4\omega_{\text{eff}}^2}\left\langle B^2\right\rangle J(\omega_{\text{eff}}) + \frac{\gamma^2(\Omega+\omega_{\text{eff}})^2}{8\omega_{\text{eff}}^2}\left\langle B^2\right\rangle J(\omega_{\text{rf}}+\omega_{\text{eff}})\\ &\quad+\frac{\gamma^2(\Omega-\omega_{\text{eff}})^2}{8\omega_{\text{eff}}^2}\left\langle B^2\right\rangle J(\omega_{\text{rf}}-\omega_{\text{eff}})\end{aligned}$$

Taking the on-resonance limit:

$$\begin{aligned}J_1 &= \frac{\gamma^2}{4}\left\langle B^2\right\rangle J(\omega_1) + \frac{\gamma^2}{8}\left\langle B^2\right\rangle J(\omega_0+\omega_1) + \frac{\gamma^2}{8}\left\langle B^2\right\rangle J(\omega_0-\omega_1)\\ &= \frac{\gamma^2}{4}\left\langle B^2\right\rangle J(\omega_1) + \frac{\gamma^2}{8}\left\langle B^2\right\rangle\left(J(\omega_0-\omega_1)+J(\omega_0+\omega_1)\right)\end{aligned}$$

Again agrees with our earlier result.

Finally taking $q=-1$ gives:

$$G_{-1}(\tau) = \overline{F_1(t)F_{-1}(t-\tau)} = \frac{\gamma^2}{16\omega_{\text{eff}}^2}\Big(2\omega_1\Delta B_z(t)e^{-i\omega_{\text{eff}}t} - (\Omega+\omega_{\text{eff}})\,\Delta B_-(t)e^{-i(\omega_{\text{rf}}+\omega_{\text{eff}})t} - (\Omega-\omega_{\text{eff}})\,\Delta B_+(t)e^{i(\omega_{\text{rf}}-\omega_{\text{eff}})t}\Big)\cdot\Big(2\omega_1\Delta B_z(t-\tau)e^{i\omega_{\text{eff}}(t-\tau)} - (\Omega-\omega_{\text{eff}})\,\Delta B_-(t-\tau)e^{-i(\omega_{\text{rf}}-\omega_{\text{eff}})(t-\tau)} - (\Omega+\omega_{\text{eff}})\,\Delta B_+(t-\tau)e^{i(\omega_{\text{rf}}+\omega_{\text{eff}})(t-\tau)}\Big)$$

Rearranging the non-zero terms gives:

$$\begin{aligned}G_{-1}(\tau) = \frac{\gamma^2}{16\omega_{\text{eff}}^2}\Big(&4\omega_1^2\Delta B_z(t)\Delta B_z(t-\tau)e^{-i\omega_{\text{eff}}\tau}\\&+(\Omega-\omega_{\text{eff}})(\Omega+\omega_{\text{eff}})\Delta B_+(t)\Delta B_+(t-\tau)e^{i2\omega_{\text{rf}}t}e^{-i(\omega_{\text{rf}}+\omega_{\text{eff}})\tau}\\&+(\Omega-\omega_{\text{eff}})^2\Delta B_+(t)\Delta B_-(t-\tau)e^{i(\omega_{\text{rf}}-\omega_{\text{eff}})\tau}\\&+(\Omega+\omega_{\text{eff}})^2\Delta B_-(t)\Delta B_+(t-\tau)e^{-i(\omega_{\text{rf}}+\omega_{\text{eff}})\tau}\\&+(\Omega+\omega_{\text{eff}})(\Omega-\omega_{\text{eff}})\Delta B_-(t)\Delta B_-(t-\tau)e^{-i2\omega_{\text{rf}}t}e^{i(\omega_{\text{rf}}-\omega_{\text{eff}})\tau}\Big)\end{aligned}$$

Neglecting the time-oscillating terms, and filling in $\Delta B_\pm$ gives:

$$\begin{aligned}G_{-1}(\tau) = \frac{\gamma^2}{16\omega_{\text{eff}}^2}\Big(&4\omega_1^2\Delta B_z(t)\Delta B_z(t-\tau)e^{-i\omega_{\text{eff}}\tau} + \big(\Delta B_x(t)\Delta B_x(t-\tau)+\Delta B_y(t)\Delta B_y(t-\tau)\big)\\&\cdot\big((\Omega-\omega_{\text{eff}})^2e^{i(\omega_{\text{rf}}-\omega_{\text{eff}})\tau}+(\Omega+\omega_{\text{eff}})^2e^{-i(\omega_{\text{rf}}+\omega_{\text{eff}})\tau}\big)\Big)\end{aligned}$$

Filling in the correlation of the fluctuations:

$$\begin{aligned}G_{-1}(\tau) = \frac{\gamma^2}{16\omega_{\text{eff}}^2}\Big(&4\omega_1^2\left\langle B_z^2\right\rangle e^{-|\tau|/\tau_c}e^{-i\omega_{\text{eff}}\tau}\\&+\left(\left\langle B_x^2\right\rangle+\left\langle B_y^2\right\rangle\right)e^{-|\tau|/\tau_c}\cdot\big((\Omega-\omega_{\text{eff}})^2e^{i(\omega_{\text{rf}}-\omega_{\text{eff}})\tau}+(\Omega+\omega_{\text{eff}})^2e^{-i(\omega_{\text{rf}}+\omega_{\text{eff}})\tau}\big)\Big)\end{aligned}$$

Integrating this, and recognizing the power spectrum of the fluctuations, and that $J(\omega) = J(-\omega)$:

$$J_{-1} = \frac{\gamma^2\omega_1^2}{4\omega_{\text{eff}}^2}\left\langle B_z^2\right\rangle J(\omega_{\text{eff}}) + \frac{\gamma^2}{16\omega_{\text{eff}}^2}\left(\left\langle B_x^2\right\rangle+\left\langle B_y^2\right\rangle\right)\big((\Omega-\omega_{\text{eff}})^2J(\omega_{\text{rf}}-\omega_{\text{eff}})+(\Omega+\omega_{\text{eff}})^2J(\omega_{\text{rf}}+\omega_{\text{eff}})\big)\Big)$$

And we see now that this is equal to the J_1 we derived in this section. We thus also see that in the limit this agrees with the J_{-1} for the on-resonance case, as in that case $J_{-1} = J_1$ as well, and we already showed this limit for J_1.

Relaxation Times

The relaxation times can be found by inner products of the relaxation operator:

$$\begin{aligned}\frac{1}{T_{1\rho}} &= \langle\hat{I}_{\tilde{z}}|\,\hat{\hat{\Gamma}}\,|\hat{I}_{\tilde{z}}\rangle = J_{-1}\langle\hat{I}_{\tilde{z}}|\,\hat{\hat{I}}_{\mp}\hat{\hat{I}}_{\simeq}\,|\hat{I}_{\tilde{z}}\rangle + J_1\langle\hat{I}_{\tilde{z}}|\,\hat{\hat{I}}_{\simeq}\hat{\hat{I}}_{\mp}\,|\hat{I}_{\tilde{z}}\rangle + J_0\langle\hat{I}_{\tilde{z}}|\,\hat{\hat{I}}_{\tilde{z}}\hat{\hat{I}}_{\tilde{z}}\,|\hat{I}_{\tilde{z}}\rangle\\&= J_{-1}\,\text{Tr}\left(\hat{I}_{\tilde{z}}\hat{\hat{I}}_{\mp}\hat{\hat{I}}_{\simeq}\hat{I}_{\tilde{z}}\right) + J_1\,\text{Tr}\left(\hat{I}_{\tilde{z}}\hat{\hat{I}}_{\simeq}\hat{\hat{I}}_{\mp}\hat{I}_{\tilde{z}}\right) + J_0\,\text{Tr}\left(\hat{I}_{\tilde{z}}\hat{\hat{I}}_{\tilde{z}}\hat{\hat{I}}_{\tilde{z}}\hat{I}_{\tilde{z}}\right)\end{aligned}$$

Calculating these commutators we get:

$$\frac{1}{T_{1\rho}} = 2J_{-1}\,\text{Tr}\left(\hat{I}_{\tilde{z}}\hat{I}_{\tilde{z}}\right) + 2J_1\,\text{Tr}\left(\hat{I}_{\tilde{z}}\hat{I}_{\tilde{z}}\right) = 2(J_{-1}+J_1)$$

We once again have $J_{-1} = J_1$, and fill this in to get:

$$\begin{aligned}\frac{1}{T_{1\rho}} &= 4J_1\\&= \frac{\gamma^2\omega_1^2}{\omega_{\text{eff}}^2}\left\langle B_z^2\right\rangle J(\omega_{\text{eff}}) + \frac{\gamma^2(\Omega+\omega_{\text{eff}})^2}{4\omega_{\text{eff}}^2}\left(\left\langle B_x^2\right\rangle+\left\langle B_y^2\right\rangle\right)J(\omega_{\text{rf}}+\omega_{\text{eff}})\\&\quad+\frac{\gamma^2(\Omega-\omega_{\text{eff}})^2}{4\omega_{\text{eff}}^2}\left(\left\langle B_x^2\right\rangle+\left\langle B_y^2\right\rangle\right)J(\omega_{\text{rf}}-\omega_{\text{eff}})\\&= \frac{\gamma^2\omega_1^2}{\omega_{\text{eff}}^2}\left\langle B_z^2\right\rangle J(\omega_{\text{eff}}) + \frac{\gamma^2}{4\omega_{\text{eff}}^2}\left(\left\langle B_x^2\right\rangle+\left\langle B_y^2\right\rangle\right)\big((\Omega+\omega_{\text{eff}})^2J(\omega_{\text{rf}}+\omega_{\text{eff}})+(\Omega-\omega_{\text{eff}})^2J(\omega_{\text{rf}}-\omega_{\text{eff}})\big)\end{aligned} \tag{27}$$

For $\langle B_{x,y,z}^2 \rangle = \langle B^2 \rangle$:

$$\frac{1}{T_{1\rho}} = \frac{\gamma^2 \omega_1^2}{\omega_{\text{eff}}^2} \langle B^2 \rangle J(\omega_{\text{eff}}) + \frac{\gamma^2}{2\omega_{\text{eff}}^2} \langle B^2 \rangle \left((\Omega + \omega_{\text{eff}})^2 J(\omega_{\text{rf}} + \omega_{\text{eff}}) + (\Omega - \omega_{\text{eff}})^2 J(\omega_{\text{rf}} - \omega_{\text{eff}}) \right)$$

To find $T_{2\rho}$, we take an inner product in the transverse plane (we could have also used the inner product with $\hat{I}_y$, or a combination of the two):

$$\frac{1}{T_{2\rho}} = \langle \hat{I}_{\tilde{x}} | \hat{\hat{\Gamma}} | \hat{I}_{\tilde{x}} \rangle = J_0 \operatorname{Tr} \left(\hat{I}_{\tilde{x}} \hat{\hat{I}}_{\tilde{z}} \hat{\hat{I}}_{\tilde{z}} \hat{I}_{\tilde{x}} \right) + 2J_1 \left(\operatorname{Tr} \left(\hat{I}_{\tilde{x}} \hat{\hat{I}}_{\tilde{x}} \hat{\hat{I}}_{\tilde{x}} \hat{I}_{\tilde{x}} \right) + \operatorname{Tr} \left(\hat{I}_{\tilde{x}} \hat{\hat{I}}_{\tilde{y}} \hat{\hat{I}}_{\tilde{y}} \hat{I}_{\tilde{x}} \right) \right)$$

Calculating these commutators gives (assuming the traces are normalized):

$$\begin{aligned}
&\operatorname{Tr} \left(\hat{I}_{\tilde{x}} \hat{\hat{I}}_{\tilde{z}} \hat{\hat{I}}_{\tilde{z}} \hat{I}_{\tilde{x}} \right) = \operatorname{Tr} \left(\hat{I}_{\tilde{x}} \hat{\hat{I}}_{\tilde{z}} i \hat{I}_{\tilde{y}} \right) = \operatorname{Tr} \left(\hat{I}_{\tilde{x}} i \left(-i \hat{I}_{\tilde{x}} \right) \right) = \operatorname{Tr} \left(\hat{I}_{\tilde{x}} \hat{I}_{\tilde{x}} \right) = 1 \\
&\operatorname{Tr} \left(\hat{I}_{\tilde{x}} \hat{\hat{I}}_{\tilde{x}} \hat{\hat{I}}_{\tilde{x}} \hat{I}_{\tilde{x}} \right) = \operatorname{Tr} \left(\hat{I}_{\tilde{x}} \hat{\hat{I}}_{\tilde{x}} 0 \right) = \operatorname{Tr} (0) = 0 \\
&\operatorname{Tr} \left(\hat{I}_{\tilde{x}} \hat{\hat{I}}_{\tilde{y}} \hat{\hat{I}}_{\tilde{y}} \hat{I}_{\tilde{x}} \right) = \operatorname{Tr} \left(\hat{I}_{\tilde{x}} \hat{\hat{I}}_{\tilde{y}} \left(-i \hat{I}_{\tilde{z}} \right) \right) = \operatorname{Tr} \left(\hat{I}_{\tilde{x}} (-i)\, i \hat{I}_{\tilde{x}} \right) = \operatorname{Tr} \left(\hat{I}_{\tilde{x}} \hat{I}_{\tilde{x}} \right) = 1
\end{aligned}$$

And therefore:

$$\begin{aligned}
\frac{1}{T_{2\rho}} = J_0 + 2J_1 = {} & \frac{\gamma^2 \Omega^2}{\omega_{\text{eff}}^2} \langle B_z^2 \rangle J(0) + \frac{\gamma^2 \omega_1^2}{2\omega_{\text{eff}}^2} \left(\langle B_x^2 \rangle + \langle B_y^2 \rangle \right) J(\omega_{\text{rf}}) + \frac{\gamma^2 \omega_1^2}{2\omega_{\text{eff}}^2} \langle B_z^2 \rangle J(\omega_{\text{eff}}) \\
& + \frac{\gamma^2 (\Omega + \omega_{\text{eff}})^2}{8\omega_{\text{eff}}^2} \left(\langle B_x^2 \rangle + \langle B_y^2 \rangle \right) J(\omega_{\text{rf}} + \omega_{\text{eff}}) + \frac{\gamma^2 (\Omega - \omega_{\text{eff}})^2}{8\omega_{\text{eff}}^2} \left(\langle B_x^2 \rangle + \langle B_y^2 \rangle \right) J(\omega_{\text{rf}} - \omega_{\text{eff}})
\end{aligned} \tag{28}$$

For $\langle B_{x,y,z}^2 \rangle = \langle B^2 \rangle$:

$$\begin{aligned}
\frac{1}{T_{2\rho}} = {} & \frac{\gamma^2 \Omega^2}{\omega_{\text{eff}}^2} \langle B^2 \rangle J(0) + \frac{\gamma^2 \omega_1^2}{\omega_{\text{eff}}^2} \langle B^2 \rangle J(\omega_{\text{rf}}) + \frac{\gamma^2 \omega_1^2}{2\omega_{\text{eff}}^2} \langle B^2 \rangle J(\omega_{\text{eff}}) \\
& + \frac{\gamma^2 (\Omega + \omega_{\text{eff}})^2}{4\omega_{\text{eff}}^2} \langle B^2 \rangle J(\omega_{\text{rf}} + \omega_{\text{eff}}) + \frac{\gamma^2 (\Omega - \omega_{\text{eff}})^2}{4\omega_{\text{eff}}^2} \langle B^2 \rangle J(\omega_{\text{rf}} - \omega_{\text{eff}})
\end{aligned}$$

Bibliography

[1] J. L. Prince and J. M. Links, *Medical Imaging Signals and Systems*, Second edition. Prentice Hall, 2006, ISBN: 978-0-13-214518-3.

[2] J. Tourais, C. Coletti, and S. Weingärtner, *Brief Introduction to MRI Physics*. Elsevier, 2022, vol. 7, pp. 3–36. DOI: 10.1016/B978-0-12-822726-8.00010-5.

[3] J. Z. Bojorquez, S. Bricq, C. Acquitter, F. Brunotte, P. M. Walker, and A. Lalande, "What are normal relaxation times of tissues at 3 t?" *Magnetic Resonance Imaging*, vol. 35, pp. 69–80, Jan. 2017, ISSN: 0730-725X. DOI: 10.1016/J.MRI.2016.08.021.

[4] A. Borthakur, E. Mellon, S. Niyogi, W. Witschey, J. B. Kneeland, and R. Reddy, "Sodium and t1ρ mri for molecular and diagnostic imaging of articular cartilage," *NMR in Biomedicine*, vol. 19, pp. 781–821, 7 Nov. 2006, ISSN: 1099-1492. DOI: 10.1002/NBM.1102.

[5] C. Coletti, A. Fotaki, J. Tourais, *et al.*, "Robust cardiac t1ρ mapping at 3t using adiabatic spin-lock preparations," *Magnetic Resonance in Medicine*, 2023, ISSN: 1522-2594. DOI: 10.1002/MRM.29713.

[6] M. A. Cloos, F. Knoll, T. Zhao, *et al.*, "Multiparametric imaging with heterogeneous radiofrequency fields," *Nature Communications*, vol. 7, Aug. 2016, ISSN: 20411723. DOI: 10.1038/ncomms12445.

[7] B. B. Mehta, S. Coppo, D. F. McGivney, *et al.*, "Magnetic resonance fingerprinting: A technical review," *Magnetic Resonance in Medicine*, vol. 81, pp. 25–46, 1 Jan. 2019, ISSN: 15222594. DOI: 10.1002/mrm.27403.

[8] M. Garwood and L. DelaBarre, "The return of the frequency sweep: Designing adiabatic pulses for contemporary nmr," *Journal of Magnetic Resonance*, vol. 153, pp. 155–177, 2 Dec. 2001, ISSN: 1090-7807. DOI: 10.1006/JMRE.2001.2340.

[9] D. J. Sorce, S. Michaeli, and M. Garwood, "Relaxation during adiabatic radiofrequency pulses," *Current Analytical Chemistry*, vol. 3, pp. 239–251, 3 Jun. 2007, ISSN: 15734110. DOI: 10.2174/157341107781023848.

[10] C. Juchem and R. A. de Graaf, "B0 magnetic field homogeneity and shimming for in vivo magnetic resonance spectroscopy," *Analytical Biochemistry*, vol. 529, pp. 17–29, Jul. 2017, ISSN: 10960309. DOI: 10.1016/j.ab.2016.06.003.

[11] A. D. Elster, "Rf energy - questions and answers in mri," Feb. 2024. [Online]. Available: https://www.mriquestions.com/release-of-rf-energy.html.

[12] L. G. Hanson, "Is quantum mechanics necessary for understanding magnetic resonance?" *Concepts in Magnetic Resonance Part A: Bridging Education and Research*, vol. 32, pp. 329–340, 5 Sep. 2008, ISSN: 15466086. DOI: 10.1002/cmr.a.20123.

[13] Y. V. Nazarov and J. Danon, *Advanced Quantum Mechanics*. Cambridge University Press, 2013, ISBN: 978-0-521-76150-5.

[14] J. Kowalewski and L. Mäler, *Nuclear spin relaxation in liquids: theory, experiments and applications*, Second edition. CRC Press, Taylor & Francis Group, 2018, ISBN: 978-0-367-89006-3.

[15] D. Spielman, *RAD226B/BIOE326B - In Vivo MR: Relaxation Theory and Contrast Mechanisms. Lecture 10*, 2019. [Online]. Available: https://web.stanford.edu/class/rad226b/Lectures.html.

[16] A. G. Palmer III, *NMR Relaxation Lecture 4: Rotating Frame Relaxation*, 2019. [Online]. Available: https://youtu.be/I8IX1BngLhs?si=DTMkRz4gYlRlhUMg.

[17] M. Gram, M. Seethaler, D. Gensler, *et al.*, “Balanced spin-lock preparation for b 1-insensitive and b 0-insensitive quantification of the rotating frame relaxation time t 1ρ,” *Magnetic Resonance in Medicine*, Aug. 2020. DOI: 10.1002/mrm.28585. [Online]. Available: https://onlinelibrary.wiley.com/doi/10.1002/mrm.28585.

[18] J. Branson, *Quantum physics 130: Derive the expression for the rotation operator R_z*, Apr. 2013. [Online]. Available: https://quantummechanics.ucsd.edu/ph130a/130_notes/node275.html#derive:Rexp.

[19] D. Spielman, *RAD226a/BIOE326a - In Vivo MR: Spin Physics and Spectroscopy. Lecture 4*, 2019. [Online]. Available: https://web.stanford.edu/class/rad226a/Lectures.html.